

Urban Policy and Spatial Exposure to Environmental Risk

Augusto Ospital*

April 24, 2023

[\[Link to the latest version\]](#)

Abstract

In the past two decades, about half of the new homes in the United States were built in environmentally risky areas. Why is new residential development being exposed to such risk? I posit that land-use regulations restricting development in safer areas contribute to this pattern. I study this question in the context of exposure to wildfire risk in the metropolitan area of San Diego, California, where areas unexposed to risk are highly regulated and built out. I estimate a quantitative urban model using detailed spatial data on zoning, density limits, lot size restrictions, wildfire risk, and insurance. In the model, the regulations benefit landowners and reallocate the population to unregulated at-risk areas. These effects depend on estimated disamenities from wildfire risk, insurance access, and the spatial correlations between regulations, wildfire risk, and location amenities. I find that land-use regulations raise city-level rents by an average 28% and explain 7% of the residents living in fire-prone areas. The estimated present-discounted cost of wildfire risk is \$14,149 per person, with existing regulations accounting for 10% of that cost. Over the next 40 years, as wildfire risk intensifies, the population grows, and the current land restrictions become more binding, the number of exposed residents will grow by 12%. The results show that institutions that restrain relocating out of harm's way, such as land-use regulations, can limit adaptation to climate change.

JEL Codes: O18, Q54, Q56, R23, R31, R52.

*University of California, Los Angeles, Department of Economics. Email: aospital@ucla.edu. I am indebted to Pablo Fajgelbaum, John Asker, and Jonathan Vogel for their guidance and support. I thank Will Rafey, Ariel Burstein, David Atkin, Treb Allen, Lorenzo Cattivelli, and participants in the Proseminar in International and Development at UCLA, the Proseminar in Industrial Organization at UCLA, and the Internal Trade Workshop at Dartmouth College for insightful comments and suggestions. Jiajun Ma provided excellent research assistance. The project was supported by the Lewis L. Clarke Fellowship Fund.

I Introduction

Assessing the natural hazard risks from climate change is among the most pressing policy concerns of our time. Central to this discussion is understanding people’s adaptation to natural hazard risk. Because the effects of climate change are local, natural hazard risk can be partly avoided by the population moving into safer areas. However, in the United States, adaptation through relocation appears limited: 47.6% of the 21.5 million homes added since the year 2000 were located in Census tracts prone to natural hazards such as flooding, drought, extreme weather, and wildfire.¹

Why do people choose to live in areas exposed to natural hazard risk? Multiple geographic, institutional, and economic factors are at work. In this paper, I posit that land-use regulations—such as single-family zoning laws or lot size restrictions—are an important factor that has been driving people to live in areas prone to natural hazards. Therefore, unless these regulations are relaxed, their role in increasing environmental risk exposure will intensify as population grows and climate change intensifies.

To motivate my point, I first show that in most U.S. cities there is a negative correlation between inelastic housing supply and natural hazard risk. In 105 out of 141 Combined Statistical Areas the tract-level elasticities of housing supply are positively correlated with natural hazard risk exposure. Moreover, regressions show that U.S. cities with a less elastic supply of housing in safe areas saw particularly high growth in at-risk areas: reducing the average housing supply elasticity of safe tracts by one standard deviation is associated with riskier tracts growing 5.7% more. Because the price elasticity of housing supply is a function of land-use regulations (Baum-Snow and Han, 2021), this pattern suggests that regulations have the potential to drive exposure to a wide range of natural hazard risks all across the United States. In this paper, I focus on one city and one hazard to quantify the extent to which land-use regulations explain the pattern.

To quantify the effect of land-use regulations alongside other determinants of risk exposure, I study the wildfire risk exposure of homes in the San Diego, California, metropolitan area. First, I use highly granular data on land-use regulations, fire risk, insurance, and economic activity to estimate a quantitative spatial equilibrium model. Then, based on the model, I run counterfactuals that demonstrate the effects of land-use regulations and wildfire risk on the spatial distributions of population, house prices, and welfare. My central results show that land-use regulations raise average rents by an average of 28%, leading to a 16% increase in the fraction, and 7% in the number, of people in at-risk areas. Land-use regulations account for 10% of the \$14.7 billion (\$14,149 per incumbent worker) present discounted cost of wildfire risk.² I also decompose the incidence on workers and landowners, and I examine the impact of increasing population pressure

¹The measure of risk is FEMA’s 2021 National Risk Index, which describes the current relative risk for 18 natural hazards across U.S. census tracts. Housing growth is the net change in the housing unit count from the Longitudinal Tract Data Base (LTDB). Of the new homes in the period 2000–2017, 47.6% were built in areas classified as having a relative risk that is “moderate”, “high”, or “very high.” The fraction of total homes with moderate risk or higher increased by 3.1%, from 40.2% to 41.5%, in this period.

²All present-discounted values are the accumulation of annual values over 65 years with a 5% discount rate.

and increasing wildfire risk due to climate change. I project a 12% increase in the number of exposed people by the year 2060.

San Diego is an ideal stage to study the interaction of urban policies and wildfire risk. In San Diego, wildfires threaten the urban periphery while land-use regulations limit housing availability in central areas. The left-hand panel of Figure 1 shows the distribution of wildfire risk in the study area, with darker shading representing higher risk. Wildfire risk grows eastward as we move from downtown San Diego and the coastline to the urban periphery. About 12% of the San Diego population lives in areas with at least 1% probability of a wildfire within the next 30 years, and 7% lives in areas with a probability of at least 20% of a wildfire within the same period.³ The right-hand panel of Figure 1 shows the distribution of housing built in San Diego as a fraction of the maximum allowed by current land-use regulations, with darker shading indicating a location close to capacity. A location becomes built-out by a combination of high demand and restrictive regulations. While areas in the periphery have plenty of spare capacity, central areas are closer to being built-out. Taken together, the two maps in Figure 1 show a positive correlation between built-out areas and safety from wildfire risk. This correlation motivates my hypothesis that land-use regulations are an important driver of population exposure to wildfire risk.

My analysis has several steps. First, I estimate people’s willingness to pay for safety from wildfire risk by estimating housing demand from observed location choices. I model workers who first choose whether to live in San Diego or in the rest of the country and then where to work and live within San Diego. As in standard urban frameworks, workers care about residential amenities, commuting costs, and wage opportunities. In addition, the workers here care about an expected amenity cost that captures the negative health and safety effects of being close to a wildfire burning. I quantify this location choice with tract-level data on commuting flows, parcel-level data on homes, and probabilistic measures of wildfire risk.⁴ I find that wildfire risk reduces the amenity value of a location, and also of locations within a 1-km radius. These estimates imply a willingness to pay equivalent to 4.8% of annual income to avoid a 20% likelihood of wildfire burning within 30 years.⁵

³Fires that spread from wildland make the urban periphery of San Diego one of the areas with the highest natural hazard risk in the United States. Wildfires increasingly threaten the health, safety, and comfort of people exposed to them. Of the top 20 deadliest wildfires in California’s history, 11 happened since 2003. Besides the wildfires’ direct threat to safety, they have been linked to harmful smoke exposure, deterioration of mental health, and reductions in the value of outdoor recreation. Moreover, wildfire damages to property have dramatically increased in recent years in the United States. Between 2015 and 2018 wildfires caused the same losses, \$53 billion, as in the prior 26 years combined. Please refer to Section III.A.2 for citations and data sources.

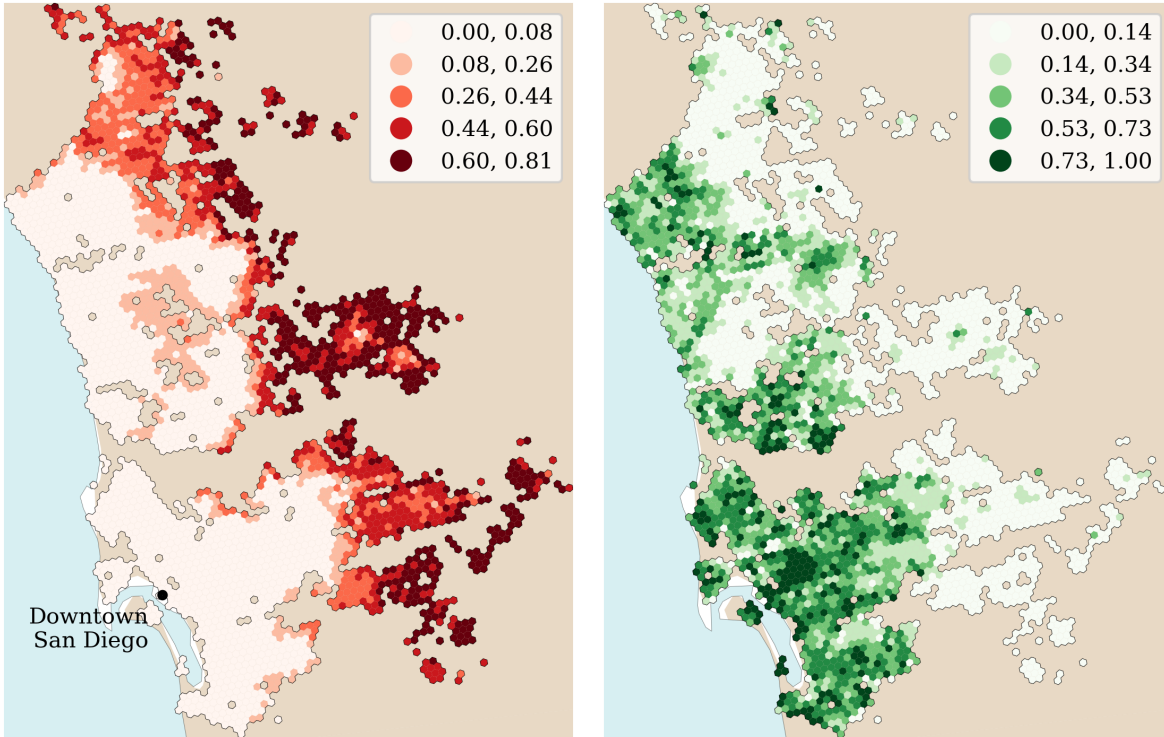
⁴My estimation strategy leverages the structure of the location choice model. The model yields a composite amenity that rationalizes housing choices and housing costs. I first invert the amenity composite from the quantified model, and then estimate the effect of the probabilities of burning on this amenity composite using variation in the number of homes over short distances that are located on land with a similar topography and are at a similar distance from wildland.

⁵Wildfire risk is influenced by human activity, but in this case, it is unlikely to be a significant factor. The study focuses on a highly urbanized metropolitan area, where changes in development density are not expected to increase accidental ignitions that could lead to an increased wildfire risk. Additionally, the rugged terrain surrounding the metropolitan area, as mapped in Figure A.3 in the appendix, features steep slopes unsuitable for residential construction (Saiz, 2010). Therefore, there is little potential for sprawling land-use changes that could fragment the natural vegetation and decrease wildfire risk. In ongoing work, I attempt to calculate bounds on how the endogeneity of wildfire risk to density impacts results.

Figure 1: Wildfire risk and land-use regulations in the San Diego metropolitan area

(a) Wildfire likelihood over 30 years

(b) Fraction built out of maximum allowed



Note: Choropleth maps of wildfire risk and spare building capacity within regular hexagons of side length 560 meters. Only populated hexagons are shown. The ranges of the bins in each map were chosen following Jenks' classification method. In panel (a) the areas with a wildfire likelihood of 0.08 or higher (i.e., the four darkest bins) hold 8% of the population. The areas with a wildfire likelihood of 0.26 or higher (i.e., the three darkest bins) hold 4.6% of the population.

Second, I combine the previous housing demand system with a housing supply model to determine a general equilibrium with endogenous distributions of population, housing, wages, house prices, and insurance premiums. I model immobile landowners that choose housing supply subject to expected property damages due to fire risk and mitigate this financial cost through buying insurance. Crucially, I model the land-use regulations observed in the data, which cap the number or sizes of homes that may be built in a location. My modeling of insurance premiums is consistent with the institutional reality of California, where regulations limit insurers' use of probabilistic risk models, the FAIR Plan mandates the provision of coverage to high-risk homes, and reinsurance expenses are not considered in the process of premiums approval, leading to cross-subsidization. Specifically, I assume that an insurer regulated to have zero profits offers two uniform premiums, one for riskier and one for safer locations. In addition, I explore alternative insurance mechanisms in counterfactuals.

A central aspect of the model's quantification is detailed land-use regulation data. These regu-

lations are hard to measure because they are complex, take many forms, and can vary considerably between municipalities.⁶ The model captures two key types of regulation: the maximum number of homes allowed and the amount of land zoned for single- and multi-family use. To measure these variables at a fine spatial resolution, I extracted the current land-use zoning designation for each parcel and the development regulations from the zoning maps of all jurisdictions in the San Diego area, and combined them with parcel-level data on all lots in the county.

In the spatial equilibrium of the model, binding regulatory limits increase housing costs in constrained places and residential demand in unconstrained places. To the extent that restrictive land-use regulations are positively correlated with amenity value, these regulations will lead to more people choosing to live in low-amenity locations.⁷ These are areas more likely to have a high wildfire risk, according to my estimation. However, binding regulations make competitive landowners of regulated areas better off, because the quantity restriction distorts the market solution towards the profit-maximizing solution that would be chosen by a monopolist landowner. Moreover, binding regulations in a location make landowners in other locations in the same metropolitan area better off, because their residual demand increases.

Using the estimated model, I first quantify the overall welfare cost of wildfire risk by simulating a wildfire-free city. I find that the present discounted welfare cost of wildfires is \$14.7 billion, split evenly between workers and landowners. For workers, the equivalent variation to removing wildfire risk is an annual \$353 per worker; this amount is similar to the average monthly health insurance premium per capita, \$378. Among landowners, removing wildfire risk increases total welfare but generates winners and losers. The owners of land in the periphery of the city are better off; they have 7.27% higher certainty equivalent profits, because the amenity value of their land is higher without risk, and their insurance costs are lower. In contrast, the owners of the land in central areas have 2.51% lower certainty equivalent profits, because they no longer benefit from wildfire risk pushing demand out of the periphery.

Second, I calculate the welfare gains of relaxing land-use regulations. I simulate a city where density limits are high enough so they never bind and where central areas are all zoned for multi-family residential use. This counterfactual results in rents falling by 28%, driven mostly by locations that were originally restricted. Wages fall 3.3% on average, coverage-weighted insurance premiums fall 0.7%, and the number of workers in San Diego increases 10.7%. In response, the number of residents in central areas increases and the number of residents in the periphery decreases. The population facing moderate to major wildfire risk (3%–14% likelihood over 30 years) decreases 4%, from 157,000 to 151,000. The population facing a severe to extreme wildfire risk (greater than 14%

⁶Land-use regulations restrict housing production both through prohibition and process (Monkkonen et al., 2020). The former means that municipal codes prohibit residential buildings in some areas, and even when they allow it, they may exclude developments other than detached single-family homes. In the San Diego metropolitan area, more than 80% of the residential land is reserved for low-density detached single-family homes. Moreover, process regulations can increase the cost of building through impact fees, a large number of hearings, architectural review board assessments, parking requirements, and more.

⁷To aid intuition, section G.1 offers a visual representation of the model’s equilibrium under certain simplifying assumptions.

over 30 years) decreases 6.9%, from 195,000 to 181,000; therefore, 13,500 fewer people are exposed to severe wildfire risk. This deregulation experiment leads to a welfare gain for workers of \$2.5 billion per year, which, when set against landowners' annual losses of \$1.7 billion, nets out at \$791 million per year.⁸

In a third set of simulations, I isolate the contribution of restrictive land-use regulations on the welfare costs of wildfire risk. Intuitively, if the gains from deregulation are lower in a wildfire-free city, then wildfire risk is contributing to the welfare cost of regulations. I test this hypothesis with a difference-in-differences approach between different simulated outcomes. I find that regulations hurt workers more when wildfire risk is present: workers enjoy a 2.47% higher welfare gain from deregulation. For landowners, the benefits of regulations when wildfire risk is present are 2.93% higher for owners of land in central areas and 4.30% lower for owners of peripheral land. Overall, regulations account for 10.1% of the total cost of wildfire risk. This cost is equivalent to a 13% increase in all burn probabilities, or 0.9 times the average increase in risk due to rising temperatures that I project by 2060.

Finally, I use the model to examine the evolution of wildfire risk and its interaction with land-use regulations, population growth, and climate change. Numerous studies predict increases in wildfire risk in the United States as a result of increasing temperatures, droughts, and lightning strikes.⁹ The number of homes in areas with wildfire risk will also increase if the wildland-urban interface growth trends continue (Radeloff et al., 2018). I find that if the current distribution of land-use regulations is kept, the growth of hazard-prone areas will be more than proportional to city growth. The reason is that an increasing number of central areas will stop growing as their density limits become binding. I estimate that the total welfare cost of wildfire risk will be 18.7% higher in 2060 than it is today, and workers' equivalent variation to no wildfire risk will increase by 28.5%, to reach \$473 per worker per year. Interestingly, my results also indicate that the predicted welfare costs of land-use regulations in 2060 will be 6% lower than they are today. This counter-intuitive result holds because because the benefits to landowners of increased demand due to population pressure will increase more than the welfare cost to workers.

⁸Simulating alternative land use policies is of interest beyond their interaction with wildfire risk. The total certainty equivalent profits of landowners would decrease by 20.9% if land-use regulations were removed, with losses concentrated in previously regulated areas. These results suggest that landowners have strong profit incentives to maintain the status quo land-use regulations. Moreover, the welfare loss can be interpreted as a lower bound on the unobserved value of regulations that results from a benevolent planner who maximizes worker surplus, landowner surplus, and some unobserved (non-negative) value of the regulations. I also show that a policy change similar to the California Senate Bill 10 passed in 2021 delivers 85.6% of the welfare gains of full deregulation.

⁹Westerling (2016) shows a strong association between warming temperatures and wildfire activity, and Littell et al. (2016) find a link between increased drought and increased fire risk. Lightning strikes are the primary trigger of wildfires in the western United States except in California (Short, 2017), and they result in unpredictable wildfires that are hard to contain before they grow (Cart, 2021). Romps et al. (2014) predict that lightning strikes in continental United States will increase by 12% for every degree Celsius of global warming. Combining these predictions with climate forecasts for the next century, wildfire risk is projected to increase. Stavros et al. (2014) project increases in very large fires (greater than 50,000 acres) across the western United States by mid-century. The National Research Council projects that each degree-Celsius increase in global temperature will quadruple the area burned (National Research Council, 2011). For more on the relationship between climate and forest fires in the United States, see Wehner et al. (2017).

The main contribution of this paper is to improve our understanding of how institutions mediate exposure to environmental risk in space. My paper is related to a recent literature that uses quantitative spatial models to evaluate the costs of climate risk. [Jia et al. \(2022\)](#), [Balboni \(2021\)](#), and [Desmet et al. \(2021\)](#) study the aggregate effects of floods. [Costinot et al. \(2016\)](#), [Cruz \(2021\)](#), [Cruz and Rossi-Hansberg \(2021\)](#), and [Nath \(2021\)](#) focus on the effects of rising temperatures. In these studies, reallocating goods and factors of production in space is key for adapting to climate change. My paper explicitly considers both the institutional constraints to the location of economic activity (such as land-use restrictions) and the potential for endogenous risk mitigation (such as insurance markets). Therefore, my results complement those in [Nath \(2021\)](#), where trade barriers limit adaptation to climate change through the reallocation of production. In [Jia et al. \(2022\)](#) location decisions depend on expectations about environmental risk, as they do in my model; however, their model does not include neither housing supply nor insurance in land development. Finally, compared to all these papers, I contribute a framework that accounts for the direct effects of environmental risk on housing supply within a detailed urban setup, thus highlighting the importance of highly granular urban policies.¹⁰

This paper also demonstrates a novel cost of land-use restrictions. An extensive literature in urban economics shows that land-use regulations can lead to higher housing costs, misallocation of production, and long commutes ([Gyourko and Molloy, 2015](#)). I show that regulations that constrain construction in environmentally safe places may displace new residential development to riskier areas. Underlying this mechanism is a more general idea that the welfare costs of land-use restrictions depend on their covariance with fundamental amenities in space.¹¹ However, environmental risks such as wildfires are different from other amenities because they also affect the supply of housing directly and depend on mitigation choices, such as insurance.

In particular, my paper is related to recent studies that use quantitative urban models to assess the general equilibrium consequences of land-use regulations within a city. [Acosta \(2021\)](#) focuses on the relative incidence of zoning and density restrictions on low- and high-skilled workers in Chicago, Illinois. [Martynov \(2021\)](#) studies the welfare effects of land-use regulations in New York City while accounting for heterogeneous spillovers across industries. [Anagol et al. \(2021\)](#) evaluate an actual zoning reform in São Paulo, Brazil, while accounting for the value of densification and a newer housing stock. [Favilukis et al. \(2022\)](#) use a dynamic two-region model to study the insurance value of housing affordability policies against the misallocation generated in labor and housing markets. My paper departs from these studies by modeling spatial heterogeneity in landowners' profits, which allows quantifying how environmental risk and land-use restrictions have different effects on more or less regulated areas, or areas with lower or higher environmental risk. Moreover, I focus on the aggregate effects within the city and study how the incidence of these regulations is

¹⁰More generally, my paper is part of a growing literature on adaptation to climate change. [Kahn \(2016\)](#) and [Masseti and Mendelsohn \(2018\)](#) review the climate adaptation literature. [Barreca et al. \(2016\)](#), [Heutel et al. \(2021\)](#), and [Carleton et al. \(2021\)](#) show that climate adaptation reduces the mortality effects of temperature. [Barwick et al. \(2021\)](#) study how transportation infrastructure allows adaptation to pollution and extreme temperatures. [Albert et al. \(2021\)](#) study the reallocation of workers and capital as a response to droughts in Brazil.

¹¹In Section G.2, I present a simple decomposition that illustrates this point with my model.

affected by population growth.

My paper is also related to a literature investigating the environmental impact of urban form. Glaeser and Kahn (2010) and Zheng et al. (2011) show that households who live in denser cities have lower carbon footprints in the US and China, and Blaudin de Thé et al. (2021) assess the effect of density and other features of city geometry on car usage and emissions in France. Glaeser and Kahn (2010) document a negative correlation between emissions and the level of land use controls across U.S. metropolitan areas. Colas and Morehouse (2022) use a spatial equilibrium model to quantify the effect of city-level land-use restrictions on national emissions. The focus of my paper is on local exposure to risk *from* the environment, rather than harm *to* the environment. Carozzi and Roth (2023) argue that the lower emissions associated with denser cities come at the cost of higher local pollution exposure. While my setting does not feature a direct externality such as carbon emissions, it does have an indirect pecuniary externality arising from insurance cross-subsidization. Another difference is the focus on within-city effects. My model captures the micro-geography of land-use regulations and wildfire risk in the San Diego metropolitan area at the resolution that these vary, and I measure regulations directly instead of using survey-based measures.

Finally, this paper expands a recent literature on the economic impacts of wildfires. Some of these papers focus on the mitigation of wildfire risk: Baylis and Boomhower (2019) estimate the implicit subsidy of federal suppression to development in harm’s way, Plantinga et al. (2020) study the effectiveness of suppression and how value at risk determines suppression effort, Wibbenmeyer et al. (2019) study the determinants of the provision of fuel management, Baylis and Boomhower (2021) measure the effects of building codes on structure survival, and Burke et al. (2021) and Heft-Neal et al. (2023) study behavioral responses to wildfire smoke. Other papers analyze the effects of wildfire risk on home prices (Garnache, 2020; McCoy and Walsh, 2018; Mueller et al., 2009), on mortgages (Issler et al., 2020), and on migration (McConnell et al., 2021; Sharygin, 2021; Winkler and Rouleau, 2021). My paper complements this literature by modeling how wildfire risk interacts with the housing and labor markets of a city, which allows running counterfactual simulations and quantifying the aggregate cost of wildfire risk.

The paper is structured as follows. Section II shows motivating evidence using data of environmental hazards all across the United States. Section III describes the setting, the San Diego metropolitan area. Section IV lays out the theoretical framework for location choices, and describes the estimation of the amenity costs of wildfire risk. Section V specifies how housing markets work in the model. Section VI completes the theoretical framework, laying out the general equilibrium, and describes its quantification. Section VII contains the counterfactual model simulations, and Section VIII concludes.

II Motivating Evidence: National Patterns of Urban Growth in Hazard-Prone Areas

In this section I investigate the relation between natural hazard risk and housing growth in the United States. I show that a disproportionate fraction of the growth in the housing stock is happening in areas with higher natural hazard risk. Moreover, the growth of these areas has been higher in cities with a low elasticity of housing supply in areas with low natural hazard risk. Motivated by these facts, in this paper I develop a model to quantify the costs of restrictive housing supply policies in terms of wildfire risk exposure in the San Diego, California, metropolitan area.

I show that increased exposure to natural hazards has happened both between and within cities. In principle, restrictive land-use regulations could either encourage or discourage exposure to environmental risk at different aggregation levels. For example, if cities that are on average exposed to higher environmental risk were more regulated, but within cities the areas with a lower environmental risk were more restricted, regulations would be driving people to safer cities but then to the parts of those cities with the highest environmental risk. However, in this paper, I focus only on the internal structure of cities and leave the related research avenue for future work.

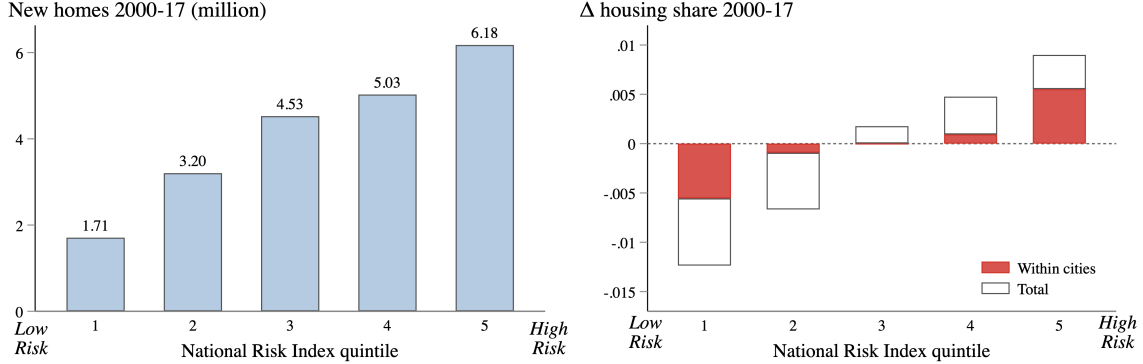
II.A Growth in At-risk Areas Within and Between Cities

Over the past decades, housing growth has disproportionately happened in areas of the United States with the highest natural hazard risk (henceforth “risky”). The left panel of Figure 2 shows that of the 21.5 million homes added since 2000, 6.1 million (28.3%) are in the 20% riskier census tracts in the country. A total of 11.2 million (52.1%) homes were added in the top 40% riskier census tracts. The measure of risk (on the x-axis) is quintiles of FEMA’s National Risk Index (NRI), which captures the current relative risk to 18 natural hazards.¹² Figure A.1 in the appendix shows that this growth pattern has been going on at least since 1970.

To show the recent growth of residential development in risky areas, I performed a decomposition of the change between 2000 and 2017 in the fraction of housing units in different risk quintiles (right panel of Figure 2). The black-outline bars depict the total change in the housing share, and the solid bars show the contribution of within-city growth. The figure shows that riskier places around the country received a higher share of total housing, both because there are more homes in riskier cities (the between-cities component of the decomposition) and more homes in the riskier parts of a city (the within-city component). Section E in the appendix provides details about the decomposition.

¹²FEMA’s 2021 National Risk Index (Zuzak et al., 2021) describes the current relative risk for 18 natural hazards across all U.S. Census tracts. The central component of the index is the expected annual losses in dollars, which is then scaled by measures of social vulnerability and resilience. A limitation of the index is that for all hazards except for earthquakes and wildfire, annualized frequencies instead of probabilistic models are used to estimate expected losses. Rare events (e.g., hurricanes, tsunamis, and volcanic activity) would benefit from probabilistic modeling. Another limitation is that the index is designed to provide a national baseline measure of risk, so particular regions or particular hazards may have varying levels of accuracy because of differing quality of source data and methodologies.

Figure 2: New and total fraction of housing against natural hazard risk from 2000 to 2017



Notes: The risk quintiles are computed over FEMA’s 2020 National Risk Index of natural hazard risk. The number of homes is the housing unit count from the Longitudinal Tract Data Base (LTDB).

II.B Housing Supply in the Safest Areas of Cities

The growth in risky areas was higher in cities whose areas with a lower natural hazard risk (henceforth “safe”) had a less elastic housing supply. I show this was the case by combining the relative natural hazard risk measure from FEMA with census tract–level estimates of housing supply elasticities from Baum-Snow and Han (2021).

I run regressions of the growth in number of homes between 2000 and 2017 on housing supply elasticities in the year 2000 and the current distribution of natural hazard risk. In particular, I estimate

$$\Delta \ln Homes_{it} = \alpha Risky_{it} + \beta Risky_{it} \cdot \overline{Elast}_{c(i)t-1}^{Safe} + \gamma Risky_{it} \cdot \overline{Elast}_{c(i)t-1} + \zeta Elast_{it-1} + \mu_{c(i)} + e_i, \quad (1)$$

where i indexes census tracts, and $c(i)$, the Combined Statistical Areas (CSA) where tracts i are located. The left-hand side of the equation is the tract-level log change in housing stock between 2000 ($t - 1$) and 2017 (t). The variable $Risky_i$ is a dummy indicating that the tract is among the top 50% riskiest in the CSA. I construct the relative risk rating from FEMA’s 2020 National Risk Index. The tract-level housing supply elasticities, $Elast_i$, are the estimates in Baum-Snow and Han (2021) for the year 2000, and $\overline{Elast}_{c(i)}$ is the average elasticity within a CSA.¹³ The variable $\overline{Elast}_{c(i)}^{Safe}$ is the average elasticity among the tracts in the CSA that are safe (i.e., $Risky_i = 0$). Finally, μ_c is a CSA fixed effect, and e_i is the residual. The coefficient α measures the growth in housing stock in at-risk places relative to safe places, and the CSA-level fixed effect means that the comparison is using only variation within cities. The coefficient β measures how housing stock growth changes if the price elasticity of housing supply in the safe parts of the city is increased. Adding the tract-level elasticity of housing supply as a control ensures that β is not driven by the riskier places having higher housing supply elasticities. Moreover, controlling for the city-average housing supply elasticity helps ruling out differential trends in the growth of risky places in cities

¹³I use their quadratic finite mixture model (FMM) estimates.

that are more or less elastic in terms of housing supply.

The estimates show that there is growth in risky areas ($\alpha > 0$), but that growth is lower in cities where the housing supply is more elastic in safe areas ($\beta < 0$). I run two versions of the regression, and both show the same pattern. In the first one, shown in column 1 of Table 1, I consider all hazards in the National Risk Index (NRI) across the United States. In the second one, I restrict the sample to the 11 western continental states and to wildfire risk alone, as measured by the fire-specific NRI component index.

Table 1: Housing supply elasticity in safe areas and growth in risky areas

	$\Delta\log(\text{Homes})$ 2000–2017	
	(1)	(2)
Region	U.S.	West U.S.
Hazard	All	Wildfire
<i>Risky</i>	0.0773*** (0.0157)	0.0559** (0.0257)
<i>Risky</i> \times \overline{Elast}^{Safe}	-0.5326*** (0.1685)	-0.3484*** (0.0706)
<i>Risky</i> \times \overline{Elast}	0.3574** (0.1578)	0.3378*** (0.0942)
<i>Elast</i>	0.4004*** (0.0264)	0.3068*** (0.0304)
CSA fixed effects	Yes	Yes
Observations	48,291	14,069
Mean \overline{Elast}	0.4039	0.4030
50% \overline{Elast}^{Safe}	0.3834	0.5573
90% \overline{Elast}^{Safe}	0.5115	0.7025

Notes: Ordinary least squares estimates of Equation 1. The standard errors, shown in parentheses, are one-way clustered at the level of the Combined Statistical Areas (CSA) by the risky-place indicator. Asterisks indicate 10% (*), 5% (**), and 1% (***) significance.

The estimates are statistically and economically significant. The value $\beta = -0.5326$ means that reducing the housing supply elasticity of safe places by one standard deviation while keeping the city average fixed leads to riskier tracts growing by 5.7% more than the safer ones. If I consider a city with an overall housing supply elasticity at the average value and a safe-area housing supply elasticity at the median value, the riskier areas are predicted to grow by 1.8% more. If the safe-area housing supply elasticity is reduced to the 10th percentile, the riskier areas are predicted to grow

by 9.8% more.

The results of the regressions with wildfire risk alone are similar to the results of the regressions with all natural hazard risks (column 2 of Table 1). Reducing the housing supply elasticity of safe places by one standard deviation while keeping the city average fixed leads to riskier tracts growing by 4.7% more than the safer ones. In a city with an overall housing supply elasticity at the average value and a safe-area housing supply elasticity at the median value, both riskier and safer areas grow at virtually the same rate (i.e., by 0.2% less). Reducing the housing supply elasticity of safe areas to the 10th percentile leads to risky areas growing by 6.2% more.

III Setting: The San Diego Metropolitan Area

In this section I describe two key features of the San Diego metropolitan area: wildfires threaten homes in the periphery, and land-use regulations restrict building homes in central areas that are unexposed to wildfire risk.

III.A Wildfires Threaten the Urban Periphery

This study focuses on the San Diego metropolitan area because it has both high exposure to natural hazard risk and a large dispersion in the degree of risk exposure. The main natural hazard threatening San Diego, as well as most of California, is wildfires. To the east, the metropolitan area limits with state and federal parks, areas of rugged terrain and wildland with a landscape dominated by fire-prone native shrubland (Figure A.2 in the appendix shows a detailed map). It is from this wildland that fires can spread to homes in the urban periphery of San Diego.

Wildfire risk is influenced by human activity, but in this setting, it is unlikely to be a significant factor. Empirically, there is a generally negative effect of human population on fire (Andela et al., 2017; Knorr et al., 2016a,b, 2014). In principle, the link is non-monotonic: development increases wildfire risk at low densities and reduces risk at high densities. Risk may increase at low densities because of accidental ignitions from power line failures, increased traffic, or increased recreational use. At high densities, risk may decrease because of mitigation (faster detection, higher firefighting effort) or vegetation changes (fragmentation of wild vegetation, e.g., roads contain spread preventing fires from becoming large). This paper focuses on a highly urbanized metropolitan area, where changes in development density are not expected to increase accidental ignitions. Additionally, the rugged terrain surrounding the metropolitan area, as mapped in Figure A.3 in the appendix, features steep slopes unsuitable for residential construction. Areas with slopes above 15% are deemed severely constrained for residential construction (Saiz, 2010). Therefore, there is little potential for sprawling land-use changes that could fragment the natural vegetation and decrease wildfire risk.

III.A.1 Exposure to wildfire risk

San Diego County is among the places in the United States with the highest natural hazard risk, both on average and in the dispersion of risk within the county. According to FEMA’s NRI index, 95.5% of U.S. counties and 91.3% of counties in California have a lower overall risk. This position in the overall ranking is driven mostly by wildfire risk. San Diego County ranks third in the country in wildfire risk, behind Riverside and Los Angeles County. Moreover, the variance of wildfire risk across census tracts in San Diego-Chula Vista-Carlsbad is a close second among all core-based statistical areas (CBSA) with more than one million people, being surpassed only by the Riverside-San Bernardino-Ontario CBSA. Considering all risks, its variance ranks third after Sacramento-Roseville-Folsom, California, and Houston-The Woodlands-Sugarland, Texas.

Whether wildfire risk is high or low in absolute terms will ultimately depend on landowners’ and residents’ risk preferences and on the magnitude of damages. Through my model and estimates I will show that these levels of risk effectively carry high costs in terms of property damage, safety, health, and comfort. But, as a first approach, I can consider how the probabilities of burning compare with the risk categories developed by the First Street Foundation, a nonprofit that develops measures of property-level climate risk. The organization uses a 1% cumulative burn probability over 30 years as a threshold separating places with no or minor wildfire risk from places with moderate or higher wildfire risk. In my study area, 358,000 people, or 12% of the population, live above that threshold. First Street considers as “extreme risk” its highest risk category, when the cumulative burn probability over a 30-year period exceeds 26%. In the San Diego metropolitan area, 139,000 people, or 4.6% of the total, live in such areas, based on data from several sources, which I describe in Section IV.B.

III.A.2 The dangers of wildfires to property, health, and comfort

When a wildfire burns, exposed people and buildings can suffer severe damages. Exposed people face a multitude of negative health outcomes, and experience discomfort and feelings of unsafety. I will later introduce a model where wildfires cause property damages and reductions in residential amenity values. The latter, which I estimate, capture the effects on exposed people’s health and comfort.

Wildfire damages to property have dramatically increased in recent years. In only four years, from 2015 to 2018, wildfires in the United States caused the same losses, \$53 billion, as in the previous 26 years (1990–2014).¹⁴ Of the top 20 most destructive wildfires in California history, 18 happened since 2003 and 15, since 2015.¹⁵

Wildfires carry increasing direct and indirect health risks. For people living near wildfires, direct health effects include death, burns, injuries, and mental health effects due to exposure to

¹⁴This is in terms of both insured and uninsured losses, based on Munich Re estimates, transformed to 2015 U.S. dollars using the Consumer Price Index.

¹⁵This figure comes from the California Department of Forestry and Fire Protection (CAL FIRE). CAL FIRE defines “destruction” by the number of structures destroyed, where structures include homes, outbuildings (barns, garages, sheds, etc.), and commercial properties.

flames or radiant heat (Xu et al., 2020). For example, the 2009 Black Saturday wildfires in Victoria, Australia, killed 173 people directly (Cameron et al., 2009). In California, of the top 20 deadliest wildfires in the state’s history, 11 have happened since 2003 and 7, since 2017. The 2018 Camp Fire, the deadliest wildfire in California history, resulted in 85 deaths (CAL FIRE).

Owing to traumatic experiences, property loss, and displacement, residents in areas affected by wildfires are at an increased risk for mental illness, including post-traumatic stress disorder, depression, and insomnia. For example, survivors of wildfires in Canada (Brown et al., 2019), Greece (Psarros et al., 2017), and Australia (Bryant et al., 2018) reported symptoms that include anxiety and trouble sleeping. Johnston et al. (2021) find a reduction in surveyed life satisfaction for individuals residing in close proximity to the 2009 Black Saturday bushfires valued at 80% of average annual income. The satisfaction domain most negatively affected is how safe the person feels.

An indirect risk that I cannot fully capture in this paper comes from exposure to wildfire smoke. Burke et al. (2020) estimate that wildfires contribute to up to 25% of fine particulate matter (PM_{2.5}) in the United States, and up to half in some of the western regions in the country. Burke et al. (2023) show that wildfire smoke has significantly slowed down the improvements in trends in particulate matter concentrations. Exposure to fine particulate matter can have adverse health effects in the short and long term (U.S. EPA, 2019; Deryugina et al., 2019; Anderson, 2019; Knittel et al., 2016; Zhou et al., 2021). My estimation strategy can only partially capture the effects of wildfire smoke, because I use variation over short distances to identify the impact of wildfire risk on the amenity value of a location. Therefore, any consequence that affects a large area at the same time cannot be identified.

Wildfires also reduce the value of outdoor recreation. Gellman et al. (2021) find a decline in campground use as a result of nearby fires and smoke exposure. Kim and Jakus (2019) find that burned area is associated with lower visits to Utah’s National Parks, and estimate negative regional economic impacts especially in rural, tourism-dependent counties. Survey evidence shows that a majority of people exposed to wildfire smoke from California’s Station Fire of 2009 stayed indoors more than usual and avoided normal outdoor recreation and exercise (Richardson et al., 2012).

III.A.3 Home insurance and risk mitigation

The extent to which the dangers described in the previous section affect the well-being of people (as well as affecting buildings) depends on the opportunities and costs of risk mitigation. In my model I include a key factor that can help mitigate the financial costs of natural hazards: insurance. Wildfires differ from other hazards, such as floods, in that standard homeowner policies typically include coverage against wildfire damage.

The homeowner insurance market in California has two important institutional features that I incorporate in my analysis. The first is the segmentation of the market into an admitted, or standard, market, and a residual market called the California Fair Access to Insurance Requirements (FAIR) Plan Association. Insurers in the admitted market are regulated by the California

Department of Insurance. Alternatively, people can obtain a basic policy with limited coverage (including wildfires) from the California FAIR Plan Association. The California FAIR Plan acts as an insurer of last resort, but it is not a state agency and is not backed by government funds. It was established by a state statute in 1968, and all insurers licensed in the admitted market participate in the gains and losses in proportion to their market share.

The second institutional feature is the regulated use of probabilistic models. Insurers in the admitted market are not allowed to use probabilistic models in setting premiums. They can use only their history of losses to support rate change requests. They are allowed, however, to use these tools to decide whether to write or renew a policy. The short available history may not be representative of events that happen only once in 250 years or once in 500 years, which could lead to both underpricing of the real risk and overpricing of regions where an event happens. The regulator has criticized the risk models for their omission of some inputs (e.g., mitigation efforts), and raised the concern that the modeled risk scores produced are not granular enough for use on particular properties (Cignarale et al., 2017).

There are other forms of risk mitigation, both private and carried out by governments, that do not appear explicitly in my analysis. Although I include them in my measurements and estimates of risk and damages, they remain fixed by assumption in the counterfactual experiments. Private mitigation methods include expenses paid by homeowners to protect their properties, such as the elimination of flammable materials inside a “defensible space” around a home, or the use of ignition-resistant roofing (Baylis and Boomhower, 2021). Another example is air filtration technology. Survey evidence shows that a majority of people exposed to wildfire smoke from California’s Station Fire of 2009 ran the air conditioner more than usual (Richardson et al., 2012).

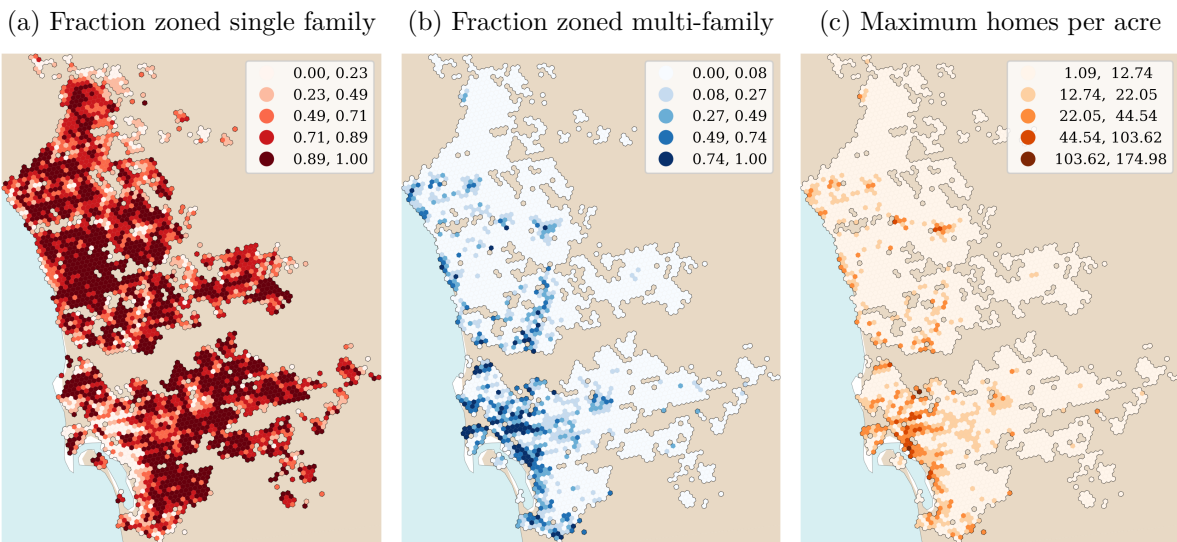
A notable way to mitigate wildfire risk is through suppression. The federal government and the state of California are in charge of suppressing the majority of fires because they start in land that these institutions own, and these expenditures have been growing over time. I chose to treat government suppression as given because looking at data from incident reports I found that the per capita cost of firefighting in the parks around the study area is small. Moreover, a recent paper, Baylis and Boomhower (2019), estimates the per-home implicit subsidy of federal firefighting and finds that the expected protection costs are low in Southern California. The reason is that firefighting costs are non-monotonic in density: beyond low levels of housing density, the marginal effect of additional homes on firefighting expenditures is small.

III.B Land-use Regulations

Strict land-use regulations in areas with high demand, such as San Diego, are credited with deteriorating housing affordability. The maps in Figure 1 suggest that this pattern is also present within cities, and that central areas tend to have higher demand and be more restricted.

California house prices and rents are at historic highs and housing production is at historic lows. San Diego is not an exception: median house values increased from 2.7 to 6.9 times the median income between 1970 and 2017, and median rents increased from 16.3% to 24% of median income

Figure 3: Zoning and maximum homes allowed



Notes: Choropleth maps of zoning and maximum density allowed within regular hexagons of side length 560 meters. Only populated hexagons are shown. Data from municipal codes and zoning maps of cities in San Diego County and the the San Diego Association of Governments. Refer to Section IV.B for details on data collection.

in the same period (LTDB, 2010). The region added an average of about 25,000 homes annually in the 1970s and 1980s but fewer than 7,000 homes per year since 2006 (SANDAG, 2019).

Restrictive land-use regulations are widely credited with originating the housing supply shortage (Molnar, 2022). Panels (a) and (b) of Figure 3 show the distribution of single- and multi-family zoning over a 560-meter-sided hexagonal grid, with a darker color indicating a larger fraction of a hexagon is zoned that way. In the San Diego metropolitan area, more than 80% of the residential land is reserved exclusively for low-density detached single-family homes. The multi-family zones are mostly concentrated close to Downtown San Diego and along the coastline.

Panel (c) plots the maximum number of homes (i.e., dwelling units) allowed per acre of land. The vast majority of the residential land is mandated to be under 12 dwelling units per acre, and these are typically single-family detached homes. Densities between 12 and 30 dwelling units per acre are typically achieved by duplexes or rowhouses. The areas that allow the most density are close to Downtown San Diego and along the coast. However, high-density areas are very limited, and even the densest are relatively sparse. Densities between 100 and 150 dwelling units per acre, similar to the higher bin in the map, are typically achieved with 5–7-story apartment buildings with underground parking.

IV The Effects of Wildfire Risk on Location Choice

I begin by examining how location decisions depend on wildfire risk. I first develop a model of location choice within the city, and then leverage the model’s structure to estimate the reduction in residential amenity values associated with wildfire risk. These amenity costs capture all the

negative outcomes related to health, safety, and comfort that arise from being close to a burning wildfire, as described in III.A.2.

In Section V, I focus on the effect of property damages on housing supply. In reality, decisions about location and housing development are not necessarily isolated. Owner-occupiers both own the land and live in the home on it, and landowners who do not live on their property can choose to sell and buy in different locations. My modeling choice is an abstraction that allows separating the welfare effects of environmental risk on the owners of immobile factors (land) and of mobile factors (labor).

IV.A Location Choice with Wildfire Risk

Workers choose where to live and work. In making these decisions they weigh the expected amenity costs of wildfire risk and the value of other residential amenities against housing costs, and weigh wages against commuting costs.

The model partitions the San Diego metropolitan area in two levels of geographies. The upper level is census tracts. Each tract is then partitioned into residential locations, which are a grid of 215-meter-sided regular hexagons. I use capital letters I and J to indicate the tracts, and lowercase letters i and r to indicate the hexagons. The notation $I(i)$ indicates the tract where hexagon i is located. I chose to use this fine resolution because wildfire risk varies over very short distances. The two levels are at a different resolution so that I can keep the model computationally tractable while allowing a commuting choice, a key feature of the value of locations that make the pattern of substitution more realistic.

There is a continuum of workers indexed by ω that first draw idiosyncratic values e_{IJ} for every tract pair $I-N$ to live and work in, and choose one of the pairs. Second, they draw idiosyncratic values for residential hexagons b_i and choose one within tract I to live in. I assume that the idiosyncratic values b_i and $e_{I(i)J}$ are i.i.d. type II extreme value with shape parameters $\varepsilon^B > 1$ and $\varepsilon^E > 1$ and means equal to 1. To live in hexagon i , workers need to rent a home there. They pay for rent with the income from a unit of labor supplied inelastically in their workplace tract, and spend the remaining income on a consumption good that is freely traded nationally. Wildfires happen after workers make all these choices except the consumption of the tradable good.¹⁶

The expected indirect utility of worker ω who lives in hexagon i and works in tract J is

$$V_{iJ}(\omega) = \underbrace{b_i(\omega)\mathbb{E}[B_i(n)]}_{\text{hexagon amenity}} \cdot \underbrace{e_{I(i)J}(\omega)E_{I(i)J}}_{\text{tract-tract amenity}} \cdot \underbrace{(W_J - \psi_i Q_i)^+}_{\text{disposable income}}.$$

The term $B_i(n)$ measures the vertically differentiated value of residential amenities. Amenities capture the need for compensating differentials in proportion to consumption. This term includes

¹⁶I make this timing choice because of two reasons: first, the focus of my paper is on long-term patterns of housing choices; second, making this choice allows introducing risk in the landowner's decision. Jia et al. (2022) model the timing in an alternative way where all markets clear after environmental shocks are realized, so there is one price per state of the world. They do so to separately capture the effects of risk and realizations. A way to interpret my framework is that workers make a commitment to stay in a location for a period of time, and this commitment captures the existing frictions to moving.

both the disamenity cost of the realization of wildfires, n_i , and the value of other amenities that are exogenous. The random variable n_i takes a value of 1 when a wildfire burns in hexagon i with probability δ_i , and 0 otherwise. I denote by n the vector of n_i across hexagons i . The variable E_{IJ} captures the vertically differentiated bilateral utility shifters, which include the disamenity of commuting distance. The price of housing space is Q_i , and W_J is the labor income. The scalar ψ_i is the housing space consumption per capita, which is assumed exogenous and can vary between hexagons because of regulation. Section IV.C specifies the link between land-use regulations and home sizes.

Given the assumptions about the timing of the choices and the distribution of the unobservable idiosyncratic values, the probability of choosing residence i after having chosen residence-workplace tracts I - J is

$$\pi_{i|J} = \left(\frac{V_{iJ}}{\bar{V}_{IJ}} \right)^{\varepsilon^B}, \quad (2)$$

and the probability of choosing the tract pair I - J is

$$\pi_{IJ} = \frac{\left(E_{IJ} \bar{V}_{IJ} \right)^{\varepsilon^E}}{\sum_{I'} \sum_{J'} \left(E_{I'J'} \bar{V}_{I'J'} \right)^{\varepsilon^E}}. \quad (3)$$

The term $V_{iJ} \equiv \mathbb{E}[B_i(n)] (W_J - \psi_i Q_i)^+$ is the relative value from choosing hexagon i and commuting to tract J that is common across workers, and $\bar{V}_{IJ} \equiv \left(\sum_{i \in I} V_{iJ} \varepsilon^B \right)^{\frac{1}{\varepsilon^B}}$ is a tract-pair-specific aggregate of those values. The notation C^+ is shorthand for $\max\{C, 0\}$. The expected utility from living in the city is

$$\mathcal{V}(\mathbf{B}, \mathbf{E}, \mathbf{W}, \mathbf{Q}) = \left[\sum_I \sum_J \left(E_{IJ} \bar{V}_{IJ} \right)^{\varepsilon^E} \right]^{\frac{1}{\varepsilon^E}}. \quad (4)$$

Finally, I assume that the mapping between wildfires and amenity values takes the form

$$\mathbb{E}[B_i(n)] = \bar{B}_i \cdot \exp \left(- \sum_{\ell} \varphi_{\ell}^B \cdot \bar{\delta}_{i\ell} \right), \quad (5)$$

where the first term, \bar{B}_i , is an exogenous amenity index, and the second term is the value of expected safety from wildfire risk. The variable $\bar{\delta}_{i\ell}$ is the mean burn probability at ring distance ℓ from i , and $\bar{\delta}_{i0} = \delta_i$. When all lags of risk are zero, the expected damages are zero and $\mathbb{E}[B_i(n)] = \bar{B}_i$. The maximum expected damages happen when the burn probability is 1: $1 - \exp \left(- \sum_{\ell} \varphi_{\ell}^B \right)$.

IV.B Data on Housing, Population, and Wildfire Risk in the San Diego Area

I quantify the model with detailed data on commuting flows, the distribution of homes in space, and probabilistic measures of wildfire risk. I adjust all nominal monetary variables described next to 2018 dollars using the California Consumer Price Index from the Department of Industrial Relations.

Geographic units. Throughout the analysis I use data at two geographic levels. The upper level is census tracts or tract pairs under the 2010 census geography. The lower level is a regular

hexagonal grid implemented with Uber’s H3 hierarchical geospatial indexing system. H3 supports 16 resolutions, where each finer resolution has cells with one-seventh of the area of the coarser resolution. I aggregate the parcel-level data described below to resolution-9 hexagons, which in my sample have an average side length of 215 meters (705 feet) and an area of 0.12 square kilometers (29 acres). The radius of the smallest circle that contains a regular hexagon of side 215 meters (circumcircle radius) is 215 meters as well. The radius of the largest circle contained within the hexagon (incircle radius) is 186 meters (611 feet).

Commuting flow data. The source for tract-to-tract commuting flow data is the LEHD Origin Destination Employment Statistics (LODES) data set. I use information on all types of jobs of workers whose workplace and residence are in California. I average the count of workers in each tract-tract pair across the three-year period 2017–2019 to reduce the influence of individual idiosyncrasies on estimation and counterfactuals (Dingel and Tintelnot, 2021).

Place-of-work data. Because LODES reports only a few income bins, I use the 2017 National Household Travel Survey (NHTS) to measure workplace income. With the geocoded detailed version of the data set I match respondents’ household incomes to workplace locations and then aggregate them to tracts using the provided weights to make the numbers representative of the total number of workers. Income is reported in 11 bins, and I take the midpoint of each bin except for the top one. When income is missing in a tract, I input the average in the ZIP code. If there are no other tracts in the same ZIP code with non-missing data, I input the average of the five nearest neighbors.

Residential housing data. To construct measures of the number of workers and the average rent in each hexagon, I combine 2019 parcel-level data with data from the U.S. Census American Community Survey (ACS) at block-group level. The parcel data is from the San Diego Association of Governments (SANDAG), the main planning and transportation agency in the region. These data sets have the number of housing units, square footage, and assessed value for each parcel on each plot of land in the County of San Diego. Section A in the appendix provides details about the parcel data. I overlay the plots on the hexagonal grid and count the number of housing units to compute the median assessed value per square feet in each hexagon. To make the housing counts consistent with the tract-level number of workers, I allocate the workers of each tract to hexagons according to the share of housing units. Finally, to obtain the yearly rents per square footage in each hexagon, I rescale the assessed value per square feet with the ratio of yearly rent to home values in the 2014–2018 ACS.

Wildfire risk. I measure wildfire risk using the Burn Probability (BP) data set from the United States Forest Service (Scott et al., 2020). I overlay the hexagonal grid with the original raster data sets at 270-meter spatial resolution and calculate the mean values within each cell. The burn probability represents the annual likelihood of burning in a given location, and I use it as a direct measure of the burn probability in the model, δ_i .

The United States Forest Service risk measures are the result of a model developed by Finney et al. (2011) that simulates the occurrence and spread of large wildfires under many hypothetical fire

seasons. It is important to use probabilistic measures derived from a model and not the distribution of historical burns because these are rare events. Although it may seem that wildfires are not that rare, because burned area and property damages are on an increasing trend at the state level, at fine resolution the realization of a fire burning is still a low-probability event.

Topography and current weather. I measure current weather as the “normal” in the most recent three decades (1991–2020) with data from the PRISM Climate Group (PRISM, 2020), which I also use to calculate the mean elevation in each hexagon. I measure the distance of each hexagon’s centroid to the closest wildland, as well as the fuel types in each hexagon, using the 2019 National Land Cover Database. Lastly, I calculate the mean terrain slope (in percentages) from the United States Geological Survey’s Digital Elevation Model raster files.

IV.C Calibrated Parameters

I use parameters from the literature to calibrate workers’ preferences, and I use the model to determine home sizes as a function of zoning.

Mobility. I use estimates from the literature to calibrate the standard elasticities of labor supply and mobility. I set the parameter ε^E , which controls the homogeneity in the values for tract pairs, equal to 4.61 following the results in Lee (2020). Additionally, I set the parameter ε^B , which controls the homogeneity in the values of hexagons, equal to 1.725 following the estimates in Martynov (2021).

Home sizes. I start by jointly calibrating the hexagon-level amenity values, B_i , and the home sizes, ψ_i , consistent with the observed commuting flows and distribution of housing across hexagons. Intuitively, if I set home sizes that are too large, then housing expenditures would be more likely to be larger than income, and then the model would contradict the data by predicting zero commuting flows. In that case, the model would not have a solution. Instead, If I set very small home sizes, the model would predict unrealistically high disposable incomes. The procedure that follows balances the two forces.

First, I impose some structure on home sizes, assuming they are a function of land-use zoning:

$$\psi_i = s_i^{SFR} \psi^{SFR} + s_i^{MFR} \psi^{MFR} + (1 - s_i^{SFR} - s_i^{MFR}) \psi^{Other}.$$

The variable s^{SFR} is the fraction of land in hexagon i that is zoned for single-family residential use, and s^{MFR} is the fraction zoned for multi-family residential use. The variables ψ^{SFR} , ψ^{MFR} , and ψ^{Other} are the mandated home sizes in single-family zones, multi-family zones, and other residential zones, respectively. Furthermore, I define ψ^{MFR} and ψ^{Other} as a constant fraction of the single-family size: $\psi^{MFR} = \alpha^{MFR} \psi^{SFR}$, and $\psi^{Other} = \alpha^{Other} \psi^{SFR}$. I set these parameters equal to the ratio of median unit sizes across zones in the data: $\alpha^{MFR} = 0.30$ and $\alpha^{Other} = 0.86$. Under these assumptions, I need to determine housing size only in single-family zones, ψ^{SFR} , to recover the housing size in every hexagon, ψ_i .

If the size of a single-family home was too large, then there would not be a solution to inverting the amenities B_i from residential choices. But for some value that is small enough, it must be that

all smaller values solve the amenities. Therefore, I find ψ^{SFR} using a bisection method where I select the upper subinterval when there is no solution for amenities, and the lower subinterval when there is a solution.

The resulting housing size for single-family zones is $\psi^{SFR} = 1,567 \text{ ft}^2$. That result implies $\psi^{MFR} = 472 \text{ ft}^2$ in multi-family zones and $\psi^{Other} = 1,350 \text{ ft}^2$ in the remaining zones. As a sanity check I compute the model-implied housing expenditure share for every hexagon-tract pair, $\psi_i Q_i / W_J$, for pairs i - J where disposable income is positive, $W_J - \psi_i Q_i > 0$. The mean and median housing shares are 18% and 16%, respectively. The bottom and top deciles are 8% and 31%, respectively. These results are comparable to an average share of annual rent to household income of 28% across block groups in the 2014–2018 ACS. The median is 27%, and the bottom and top deciles are 18% and 40%, respectively.

IV.D Estimation of the Amenity Cost of Wildfire Risk

The damages of wildfires to amenity values are difficult to measure directly because they include a multitude of negative effects on health and comfort. Thus, I estimate these effects using the model.

To quantify the welfare cost of wildfire risk and forecast how the residential amenity values of places at risk will evolve with climate change, I need to separate the effects of wildfire risk from other determinants of the amenity value of an area. This separation is important because wildfire-prone areas are bundled with positive amenities, such as natural beauty, that may dominate the negative risk effect.

I assume that the variable capturing other amenities that are not wildfire safety is $\bar{B}_i = \exp(\zeta_I + X_i^B \gamma^B + e_i)$, a function of observable variables X_i^B with parameters γ^B , a component that is fixed within a tract (or coarser-resolution hexagon) ζ_I , and an unobserved component e_i . Replacing in the amenity function in Equation 5 leads to the estimating equation

$$\ln(\mathbb{E}[B_i]) = - \sum_{\ell} \varphi_{\ell}^B \cdot \bar{\delta}_{i\ell} + \zeta_I + X_i^B \gamma^B + e_i. \quad (6)$$

As before, the variable $\bar{\delta}_{i\ell}$ is the mean burn probability at ring distance ℓ from hexagon i . The parameter φ_{ℓ}^B measures how much does wildfire risk at distance ℓ reduce the residential amenity value of a hexagon. I can directly use the optimal-hexagon-choice equation from the model to invert the values of the expected amenity composite $\mathbb{E}[B_i]$ from the data, given knowledge of ε^B and ψ_i . The controls included in X_i^B are distance to wildland, topographical variables, weather variables, and their squares. Therefore, this specification exploits variation between small hexagons within a tract that are at similar distance from wildland.

The fixed effects and controls help address threats to identification of the coefficients φ_{ℓ}^B . Controlling for topography and weather is important because these characteristics determine burn probabilities and have amenity value. Moreover, topography affects construction costs and therefore housing prices.

Another concern is reverse causation from density to wildfire risk through land-use, firefighting, or human-caused ignitions. The tract fixed effects help address this concern because these mecha-

nisms arguably operate at a larger scale. Having more traffic or recreational use of wildland would increase the likelihood of ignitions; however, that likelihood would be a function of the overall level of development in the area and not of variation between hexagons within a tract.

Additionally, recent wildfire realizations or incomplete information could also bias the estimates. A recent catastrophe could reduce population density only temporarily while homes are rebuilt, thus biasing the amenity damages. I address this concern by excluding from the estimation sample those locations that burned within the previous five years; this is the amount of time it has taken to rebuild destroyed buildings in the past in the United States (Alexandre et al., 2014). Incomplete information, if residents' perceptions of risk are different from objective risk, could also bias the results. This is less of a concern with wildfire risk because wildfires' recurrence in this area makes the risk salient. Moreover, myopia would bias the amenity costs towards zero, so my estimates would be conservative.

An important implicit assumption is that current prices reflect only the current risk, but do not anticipate the future changes in risk. Violations of this assumption could bias the estimated preferences and, as a consequence, put in question the use of the model on counterfactual risks from other environmental risks or projections of wildfire risk (Severen et al., 2018).

Willingness to pay for safety. The estimated amenity costs of wildfires are large but localized. Figure 4 plots the results of estimating Equation 6 by Poisson pseudo-likelihood. The effects are very local: wildfire risk in a residential hexagon and in the twice-removed neighbor reduces the amenity level, but the effect disappears at approximately 1-kilometer distance.

The units of the estimates of Equation 6 are hard to interpret, but allow constructing monetary measures of the willingness to pay for wildfire safety. The partial equilibrium willingness to pay to avoid the disamenity of wildfires, in terms of wage income, is

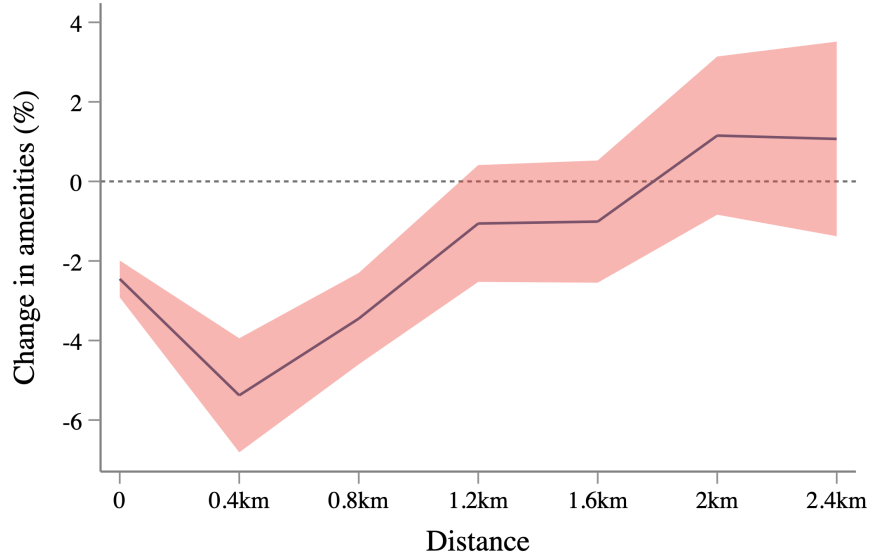
$$WTP_{iJ} = \frac{\partial V_{iJ} / \partial W}{V_{iJ}^{(\delta=0)} - V_{iJ}} = \frac{\mathbb{E}[\varphi^B(n, i)]}{1 - \mathbb{E}[\varphi^B(n, i)]} \frac{C_{iJ}}{W_J}$$

where, as defined before, V_{iJ} is the common indirect utility of workers that live in hexagon i and commute to tract J . The other variables are defined as before. The numerator subtracts the value at observed burn probabilities, V_{iJ} , from the one if all burn probabilities are zero, $V_{iJ}^{(\delta=0)}$.

The interpretation of this willingness-to-pay measure is the consumption equivalent, as a fraction of annual income, from avoiding risk altogether while keeping location choices and the prices in the economy fixed. This is, of course, an incomplete measure of the welfare effects of the wildfire disamenities because it ignores the general equilibrium effects that would arise from changing allocations and prices. I calculate more comprehensive equivalent variations to risk reductions in Section VII.

The implied willingness to pay is large, but it is also concentrated in the riskiest places. Evaluating it at a housing expenditure share of 30%, the willingness to pay to avoid moderate to major risk in the range 3%–14% likelihood of burning within 30 years is between 0.7% and 3.4% of income. The willingness to pay to avoid a 19% likelihood of burning within 30 years is 4.8% of income. Avoiding the likelihoods of burning within 30 years of 36%, 49%, and 66% is worth

Figure 4: Marginal Impact of Greater Burn Probability on Amenities, by Distance



Notes: Marginal effect of a one standard deviation (0.013) increase in annual burn probability at different distances from a resolution-9 hexagon. The dark line runs through the point estimates and the red shaded area indicates 95% confidence intervals. Estimated using the Poisson pseudo-likelihood estimator. The fixed effects are the parent hexagons with an average edge of 1,221 meters (H3 resolution 7). The standard errors are clustered at the level of the fixed effects. I only include in the sample parent hexagons with children in the wildland-urban interface and with at least one populated child. The sample also excludes children hexagons burned in the previous five years

10.6%, 16.5%, and 28% of income, respectively. To put these numbers in perspective, the average combined employee health insurance premium contribution and deductible in the United States in 2019 was 11.5% of median income, and 11.7% in California (Collins et al., 2022).

Robustness. The robustness of the findings is demonstrated in Table A.5, which can be found in the appendix. The table presents instrumental variable estimates that address the two main concerns regarding endogeneity. The first concern is reverse causation from human development to wildfire ignitions. To address this concern, I instrument burn probability with the non-anthropogenic wildfire risk measure from Parisien et al. (2012). This measure nets out the direct effects of human presence on the probability of wildfire. The results of this approach are shown in column 1. The second concern is that climate and topography have amenity value and affect risk. To address this concern, I use variation in expected risk driven by the salience of nearby burns. I construct an instrument that is the interaction of the topographic determinants of wildfire with the cumulative history of nearby burns. The results of this approach are shown in column 2. Despite these additional measures to address endogeneity, the estimates remain significant and larger than the baseline comparable estimate in column 0. This suggests that the baseline estimates may actually be conservative.

V Housing Markets with Wildfire Risk and Insurance

The workers' choices, discussed in the previous section, determine the demand for housing in each location in the city. I now examine how those choices interact with housing supply and land-use regulations. The risk of property damage will affect the supply of housing, and insurance markets will help mitigate the burden.

V.A Housing Supply with Wildfire Risk and Insurance

I develop a model of how immobile and risk-averse landowners choose housing supply. They consider wildfire risk and buy insurance coverage to mitigate the financial cost of property damages.

Landowners – supply of housing space and demand for insurance. In each hexagon i there is a continuum of landowners indexed by v that own the stock of land zoned for housing, L_i^H . Each owns a single unit of land, chooses how much housing space ($h > 0$) to build on it, and then rents it to workers at price Q_i . After building housing, landowners can purchase wildfire insurance at a price p_i per dollar of coverage. After wildfire realizations happen, landowners use their rental profits for consumption of the tradable good. I assume they have preferences with constant absolute risk aversion (i.e., invariance of risk aversion across the wealth distribution), characterized by utility function $u(C) = 1 - \exp(-\sigma C)$, where $\sigma > 0$ is the coefficient of absolute risk aversion.

The choices of housing development and insurance coverage are subject to the following budget constraint:

$$C_i(n_i) = \underbrace{Q_i h - P h^{\frac{1}{\mu}} D_i^{-\frac{1-\mu}{\mu}}}_{\text{rental profits}} - \underbrace{n_i \varphi_i^H Q_i h}_{\text{damages}} + \underbrace{I(n_i - p_i)}_{\text{insurance}}.$$

The left-hand side is consumption of the nationally traded good. As before, n_i is a random variable that takes a value of 1 with probability δ_i , and 0 otherwise, capturing the occurrence of a wildfire burn. On the right-hand side of the equation, the first term is the rental profits excluding wildfire damage and insurance costs. The landowners transform land into housing space with a cost function $P h^{\frac{1}{\mu}} D_i^{-\frac{1-\mu}{\mu}}$, where P is the price of materials that they buy from a national market, D_i is the development productivity of land that varies in space, and μ is the share of materials in production. The second term on the right-hand side is wildfire damages: a fraction φ_i^H of the value of the housing stock. One interpretation is that this parameter is repair costs that are the responsibility of the landowner. An alternative but related interpretation of the parameter φ_i^H is as the conditional probability of destruction when a wildfire happens. This probability reflects the fact that a structure (e.g., a home) that is within a wildfire-affected area may or may not burn down, depending on the spatial arrangement of vegetation and other buildings, topography, and firefighting effort (Alexandre et al., 2016). The last term on the right-hand side of the equation is the net payments from insurance, where I denotes the amount of coverage purchased (in U.S. dollars).

Starting from the second step, the insurance decision solves the problem of maximizing expected utility subject to the budget constraint while taking the housing space decision as given. The first-

order condition with respect to I yields the demand for insurance coverage:

$$I_i^D(p_i) = \varphi_i^H Q_i h + \underbrace{\frac{1}{\sigma} \ln \left(\frac{\delta_i}{1 - \delta_i} \frac{1 - p_i}{p_i} \right)}_{\text{market imperfections}}. \quad (7)$$

Equation 7 can be interpreted as explaining deviations from full insurance as a function of the imperfections in insurance markets. These imperfections will drive a wedge between premiums (p) and expected damages (δ). If these imperfections cause premiums to exceed expected damages, $p > \delta$, then the second term is negative and it leads to partial insurance. The degree of risk aversion, captured by the coefficient of absolute risk aversion σ , is inversely related to the importance of these distortions. In the extreme, if $\sigma \rightarrow \infty$, the landowner always insures fully.

In the first step, landowners decide how much space to build on their land. The constant absolute risk aversion (CARA) assumption means that the profits in the two states of the world are equal in every term that is a function of h . Solving the first-order condition leads to an expression for unconstrained housing supply per unit of land

$$h_i^S(Q_i) = \chi D_i Q_i^{\frac{\mu}{1-\mu}} \left(1 - \varphi_i^H p_i\right)^{\frac{\mu}{1-\mu}}, \quad (8)$$

where $\chi \equiv (\mu/P)^{\frac{\mu}{1-\mu}}$ is a constant. I characterize this supply function as unconstrained because, as it will be clear in Section V.B, the aggregation of this supply across landowners will equal the aggregate supply of housing in a hexagon only when density limits are not binding. Note that the degree of risk aversion does not affect housing supply; it depends only on the insurance premium p_i and the damages parameter φ_i^H . This fact is a consequence of the CARA assumption.

Insurance supply. I develop a tractable framework of insurance supply that still captures two key institutional features of the market: the regulatory restriction of pricing with probabilistic models and the existence of a high-risk residual market.

There is a regulated insurer that sells coverage to landowners in the city before the realization of wildfire shocks, and finances the payouts with the premiums earned. I assume there is a cutoff burn probability δ^F such that the hexagons below it are in the admitted market, and the remaining hexagons are in the FAIR Plan. The insurer is then restricted to choose two rates per dollar of coverage that are uniform within the two market segments. In each market segment, the premium will be determined by a revenue requirement condition where the total premium earned cannot exceed total expected payments plus an allowed return.

Specifically, all hexagons where $\delta_i < \delta^F$ are insured in the admitted market and pay a premium p^A that solves

$$\sum_i p^A I_i^D(p^A) = R \times \sum_i \delta_i I_i^D(p^A). \quad (9)$$

The left side of the equation is the total premiums earned in the city. The right side of the equation is the total expected payments (i.e., the total cost for a risk-neutral insurer) plus an allowed return of $R - 1$ that captures an allowed return on investment and surplus requirements. Similarly, all

hexagons where $\delta_i < \delta^F$ are insured in the FAIR Plan and pay an uniform premium p^F that solves

$$\sum_i p^F I_i^D(p^F) = R \times \sum_i \delta_i I_i^D(p^F). \quad (10)$$

The restriction to uniform premiums captures the regulatory restriction on the use of probabilistic models. This regulatory restriction will generate adverse selection because there is hexagon-specific information that cannot be priced; the insurer cannot distinguish between high- and low-risk hexagons. The segmentation of the high-risk areas captures that while insurers are allowed to drop policies in the admitted market, they are mandated to offer coverage through the residual market at higher premiums.

Finally, I assume that there is an upper bound to how much landowners can overinsure. In particular, I assume that insurance demand (7) is capped at $\iota^{max} Q_i h$, which is ι^{max} times the value of the home. This assumption is necessary because in its absence landowners that face premiums significantly below fair values would want to overinsure by a lot to arbitrage the policy distortion. This scenario would not be realistic because insurance agents would not agree to cover an amount that is many times the value of the home.

V.B Housing Market Clearing and Land-use Regulations

The interaction of location choices and housing supply constrained by land-use regulations determines rental prices.

I take regulations as given. In my framework, local landowners can benefit from local regulations that reduce the amount of housing. However, these regulations can have other benefits that shaped their current distribution. For example, landowners may have preferences for low density or direct preferences for regulations, but since landowners are immobile, their preferences would not affect the equilibrium. Any welfare statements will be up to landowner preferences.¹⁷ I treat these regulations as exogenous in the model because they typically do not change much over time.

Each hexagon has exogenous limits on the amount of housing space that can be built, denoted by \bar{H}_i . Without density limits, the supply of housing space in hexagon i is the product of the floorspace supply per unit of land (8) and the land area zoned for residential use, L_i^h . Therefore, the effective supply of floorspace will be the minimum of this amount and the density limit in the hexagon.

The demand for housing space by worker ω is ψ_i , so the total demand for housing space in i is

$$H_i^D(Q_i) = \psi_i N_i = \sum_J \tilde{\psi}_{iJ} (W_J - \psi_i Q_i)^{\varepsilon^B +}, \quad (11)$$

with $\tilde{\psi}_{iJ} \equiv \psi_i N_{IJ} (\mathbb{E}[B_i(n)] / \bar{V}_{IJ})^{\varepsilon^B}$. As before, the $+$ exponent is shorthand for the non-negative part, $\max\{x, 0\}$. The housing demand equation satisfies $dH_i^D(Q_i)/dQ < 0$ as long as for one workplace tract J , $W_J > \psi_i Q_i$, and it satisfies $d^2 H_i^D(Q_i)/dQ dQ < 0$ because $\varepsilon^B > 1$.

The rental prices in each hexagon will be determined by the intercept of the effective supply of

¹⁷While in exploratory regressions I found no evidence of diseconomies of density in the calibrated residential amenities, that measure comes from mobile workers' preferences. The preferences of landowners may be different.

floorspace and the demand for floorspace by workers:

$$H_i^D(Q_i) = \min\{h_i^S(Q_i)L_i^h, \bar{H}_i\}. \quad (12)$$

The left-hand side of Equation 12 shows that wildfires reduce partial equilibrium rents. This reduction happens because the left-hand side of the equation is decreasing both in rents Q_i and in amenity values inside $\tilde{\psi}_{i,J}$. However, when regulations are not binding, the overall effect of wildfire risk on rents is ambiguous because wildfires affect rents positively through supply. The supply effect appears because the unrestricted supply function on the right-hand side of the equation is increasing in rents Q_i but decreasing in insurance premiums p_i .

V.C Data on Land Use Regulations in the San Diego Metropolitan Area

To bring the model to the data, I need to measure land-use regulations and how wildfire burns map to property damages.

Land, zoning, and regulation data. I combine data from SANDAG with detailed data on zoning regulations from the jurisdictions in the study area, I extract the current land-use zoning for each parcel and the development regulations from zoning maps and municipal codes. The key regulatory variables I use are the minimum lot size allowed and the maximum number of dwelling units allowed per plot area. Combining these variables with the plot areas from SANDAG, I calculate the maximum number of homes allowed in each hexagon, the amount of land zoned for residential or commercial use, and within residential land, what fraction is zoned for single-family housing and for multi-family housing. Section A in the appendix provides further details about the zoning data.

Conditional damages. I measure wildfire risk and potential damages using the Burn Probability (BP) and Conditional Risk to Potential Structures (cRPS) data sets from the United States Forest Service (Scott et al., 2020). The conditional risk to potential structures represents the potential consequences of fire to a home at a given location if a fire occurs there and if a home were located at that location. It measures the relative effect of damage of wildfire on structures ranging from 0 (no loss) to 100 (complete loss). I divide this measure by 100 and interpret it as the conditional probability of destruction, φ_i^H . These measures represent weather conditions circa year 2015.

V.D Calibrated Parameters

I calibrate the landowners' degree of risk aversion and the land input share using estimates from the literature. I use auxiliary data on the distribution of FAIR Plan policies to set the admitted market cutoff.

Land input share. I set a value of 0.46 for the non-land input share in housing production, μ ; this value is based on the estimates in Severen (2019) for Los Angeles.

Risk aversion. I calibrate the coefficient of absolute risk aversion using estimates from the literature. Handel et al. (2015) estimate a mean coefficient of absolute risk aversion of 4.39×10^{-4} ,

with a range of 4.33×10^{-4} to 4.79×10^{-4} . These are preferences for financial risk estimated from health insurance contract choices. Closer to my setting, [Sydnor \(2010\)](#) estimates absolute risk aversion of between 1.7×10^{-3} and 1.6×10^{-2} using choices of deductibles for homeowners insurance, but argues that these estimates are implausibly high. Given this parameter uncertainty, I set $\sigma = 5 \times 10^{-4}$ as my preferred coefficient of absolute risk aversion and consider deviations around this number for robustness.

FAIR Plan cutoff. I set the value for the burn probability cutoff for the FAIR Plan, δ^F , using auxiliary data on insurance. The data on the count of policies by insurer and ZIP code are sourced from the California Department of Insurance; I use these data to compute the fraction of dwelling policies that are from the FAIR Plan (mapped in [Figure A.5](#) in the appendix). As expected, this fraction is increasing in burn probability δ_i . I set $\delta^F = 0.015$ because at that value the relation between burn probability and FAIR fraction crosses 50% and levels off ([Figure A.6](#)).

Finally, I set the maximum gross rate of return allowed for insurers R equal to 10%, and the maximum contractible insurance as a fraction of home value ι^{max} to 1.2. The value of R approximately reflects that the California Department of Insurance’s rate of return formula sets a maximum return of 8% as well as requiring insurers to hold extra surplus. I do not have a good reference for the maximum overinsurance possible, so I assume 1.2 and later check the sensitivity of the results to different values.

VI Location Choice and Housing Supply in Spatial Equilibrium

I combine location choices and housing supply decisions in a spatial equilibrium model, based on which I simulate changes in land-use regulations and wildfire risk (in [Section VII](#)).

I assumed that workers consume a single unit of housing ([Section IV.A](#)) and that the size of homes is fixed by zoning regulations ([Section V.B](#)). These assumptions imply that regulated places can become full. In the appendix I develop a model where workers choose the amount of floorspace they use and the main mechanism (i.e., density limits pushing people to unregulated places) is still operative in that model. However, it has the undesirable property that places where regulations bind will always grow as the city grows. This happens because extreme value preferences mean population densities never become zero no matter how high prices get, as people substitute by consuming less and less space. This pattern is undesirable because, on the demand side, there is a minimum amount of space that people need in order to live.¹⁸ On the supply side, regulations put a lower bound on how small housing units can get.

VI.A Aggregation and Spatial Equilibrium

I now formulate the market clearing conditions and define the general equilibrium of the full model. I allow workers to first choose between living in the San Diego metropolitan area and the

¹⁸[Couture et al. \(2020\)](#) model residential choices in a similar way to explore the effect of unequal income growth on sorting. An alternative way would be to have workers with Stone–Geary preferences, like in the extension in [Appendix D.5 of Tsivanidis \(2019\)](#).

rest of the country.

City choice. I incorporate migration in and out of the city in the model. Workers first choose whether to live in the city (i.e., the San Diego metropolitan area) and the rest of the country. The rest of the country is the outside option and offers mean utility \mathcal{U} . Living in the city offers expected indirect utility \mathcal{V} as defined in Equation 4. I also assume that workers have idiosyncratic preferences for the city given by $z^{city}(\omega)$ and $z^{out}(\omega)$, i.i.d. type II extreme value with shape $\varepsilon^C > 1$ and mean 1. Under these assumptions, the number of workers who choose to live in the city, N , solves

$$\frac{N}{N^* - N} = \left(\frac{\mathcal{V}}{\mathcal{U}} \right)^{\varepsilon^C}, \quad (13)$$

where N^* is the (exogenous) total population in the country.

Aggregation. The number of workers who commute from I to J is $N_{IJ} = \pi_{IJ}N$, where N is the total mass of workers in the city and π_{IJ} is the probability of choosing tract pair I - J as defined in Equation 3. Therefore, labor supply in tract J is $N_J^y = \sum_{I'} N_{I'J} = \sum_{I'} \pi_{I'J}N$. The number of residents in tract I is $N_I = \sum_{J'} N_{IJ'} = \sum_{J'} \pi_{IJ'}N$. The number of residents that live in hexagon i in tract $I(i)$ is $N_i = \sum_{J'} \pi_{i|J'} N_{I(i)J'}$, where $\pi_{i|J}$ is the conditional hexagon choice probability defined in Equation 2.

Production and labor market clearing. The final consumption good is tradable and produced under the conditions of perfect competition and constant returns to scale. The technology uses labor N^y and land L^y as inputs and is Cobb-Douglas $Y = A_J (N^y)^\alpha (L^y)^{1-\alpha}$ with Hicks-neutral productivity A_J and labor share given by α . Solving the cost minimization problem and replacing the market clearing condition results in the following equilibrium wage setting equation:

$$W_J = \alpha A_J \left(\frac{L_J^y}{\sum_{I'} \pi_{I'J} N} \right)^{1-\alpha}. \quad (14)$$

Equilibrium. An equilibrium of the model is a distribution of hexagon conditional choices $\pi_{i|J}$, choices of tract pairs π_{IJ} , the number of workers in the city N , rents Q_i , wages W_I , and insurance premiums p_i such that (i) workers optimally choose city, tract pairs, and hexagons according to Equations 13, 3, and 2; (ii) landowners optimize and housing markets clear such that rents are determined by Equation 12; (iii) insurance prices are given by balancing expected payments as in Equations 9 and 10; and (iv) firms optimize and labor markets clear such that wages are determined by Equation 14.

VI.B Measuring Welfare

I define monetary measures of workers' and landowners' surplus that I later use to measure the welfare impact of wildfire risk and land-use regulations.

I measure workers' expected (or average) welfare change between two equilibria using the equivalent variation for the change. Denote by $\mathbb{E}[B_i(n)]^{(0)}$, $E_{IJ}^{(0)}$, $W_I^{(0)}$, and $Q_i^{(0)}$ the fundamentals and endogenous variables in an initial equilibrium, and by $\mathbb{E}[B_i(n)]^{(1)}$, $E_{IJ}^{(1)}$, $W_I^{(1)}$, and $Q_i^{(1)}$ the new values. Then the equivalent variation is defined as the lump-sum uniform income transfer T that

would yield the new utility level with the old fundamentals and endogenous variables:

$$\mathcal{E}^{(1,0)} \equiv \left\{ T : \mathcal{V}(\mathbf{B}^{(1)}, \mathbf{E}^{(1)}, \mathbf{W}^{(1)}, \mathbf{Q}^{(1)}) = \mathcal{V}(\mathbf{B}^{(0)}, \mathbf{E}^{(0)}, \{W_J^{(0)} + T\}_J, \mathbf{Q}^{(0)}) \right\} \quad (15)$$

where the expected indirect utilities $\mathcal{V}(\cdot)$ are given by Equation 4.

I measure the well-being of landowners in hexagon i with the certainty equivalent profits to their expected utility. The certainty equivalent profits per unit of land in hexagon i as a function of equilibrium prices Q_i and total floorspace in the hexagon H_i are

$$\mathcal{C}_i = \left[Q_i - \varphi_i^H p_i - \mu \left(\frac{H_i}{\chi D_i L_i^h} \right)^{\frac{1-\mu}{\mu}} \right] \frac{H_i}{L_i^h} - \frac{1}{\sigma} \ln \left[(1 - \delta_i) \mathcal{O}_i^{p_i-1} + \delta_i \mathcal{O}_i^{p_i} \right], \quad (16)$$

where $\mathcal{O}_i \equiv \frac{\delta_i}{1-\delta_i} \frac{1-p_i}{p_i}$ is the ratio of the odds of wildfire relative to insurance premiums. I then define the welfare change of a landowner in hexagon i as $\mathcal{C}_i^{(1,0)} = \mathcal{C}_i^{(1)} - \mathcal{C}_i^{(0)}$, where $\mathcal{C}_i^{(0)}$ is the certainty equivalent profits in the initial equilibrium, and $\mathcal{C}_i^{(1)}$, the ones in the new equilibrium.

The first term in the certainty equivalent \mathcal{C}_i is the profits under full insurance with fair pricing. The second term is an adjustment due to risk aversion and distortions in insurance markets. If landowners are more risk averse, then the CARA coefficient σ is larger and the last term is smaller, making the certainty equivalent higher because being insured becomes more valuable. If the insurer prices fairly in every location, $p_i = \delta_i$, then $\mathcal{O}_i = 1$, so the certainty equivalent equals $\mathcal{C}_i = \Pi_i - p_i d_i$, the full insurance value without distortions.

VI.C Calibration of the Model Fundamentals

I invert the equilibrium to recover the model fundamentals: home sizes, hexagon-level residential amenities, values for tract pairs, workplace productivities, and housing development productivities.

Worker fundamentals. I first invert the hexagon-level amenities B_i from the hexagon choice equation (2). Then, I take the calibrated hexagon-level amenities, use them to compute \bar{V}_{IJ} , and calibrate the tract-tract values E_{IJ} by inverting the tract choice equation (3). Last, I use the city choice equation (13) to recover the reservation expected utility of living in the rest of the country, \mathcal{U} .

Workplace fundamentals. I directly invert the vector of workplace fundamentals A_I from the equilibrium condition for wages in Equation 14.

Insurance premiums and land development fundamentals. First, I use the revenue condition given by (9) and (10) to solve for equilibrium premiums p^A and p^F . Then, I proceed to calibrate the land development productivities D_i . To calibrate the land development productivities D_i , I leverage the fact that the housing market equilibrium conditions (12) imply a lower bound for the productivities,

$$\chi D_i \geq \frac{H_i^D(Q_i)}{L_i^h Q_i^{\frac{\mu}{1-\mu}} (1 - \varphi^H p_i^I)^{\frac{\mu}{1-\mu}}},$$

where floorspace demand is given by Equation 11, which is a function of the low-level amenities

B_i through the conditional residence choice probability. The other variables and parameters are defined as before. This inequality follows from constrained locations satisfying $h_i^S L_i^h = H_i^D$ and unconstrained locations satisfying $h_i^S L_i^h > H_i^D = \bar{H}_i$. For every residential location i where density limits do not bind (i.e., $H_i < \bar{H}_i$), the equation holds with equality, so I can invert construction productivities directly. For hexagons where the restrictions bind, the equation is a strict inequality, so the productivities are not exactly identified by the equilibrium condition. I then interpolate in space over the locations where the density limits bind and keep the maximum between the interpolated value and the lower bound, using the average value of the five nearest neighbors where the maximum allowed does not bind.

VI.D Estimating Future Wildfire Risk

To explore the effects of future increases in wildfire risk driven by climate change, I need estimates of future risk. Therefore, I estimate the historical relation between maximum temperatures and burn probabilities, and then use the estimates to predict future wildfire risk under forecast temperatures in the year 2060.

Historical wildfires and weather. To estimate the relation between temperature and wildfire risk, I use data on past wildfire burns and temperatures between 1981 and 2019 in California. I compute the average maximum summer temperature by year and resolution-7 hexagon using monthly data from [PRISM \(2020\)](#). I identify hexagons that burn each year from the maps of wildfire perimeters published by CAL FIRE ([FRAP, 2019](#)), considering as burned a resolution-9 hexagon that has more than 80% of its area within a wildfire perimeter.

Future weather. I obtain measures of future and current maximum temperatures from the Localized Climate Analogues (LOCA) Downscaled Climate Projections from Cal-Adapt ([Cal-Adapt, 2018](#); [Pierce et al., 2018](#)). There exist different projections with different future emissions scenarios and different climates. The RCP 4.5 scenario represents a medium emissions future where societies work to reduce greenhouse gas emissions. The RCP 8.5 scenario represents a “business as usual” future that is used to explore a higher emissions scenario. I use four global climate models that represent a range of possible futures for California ([Pierce et al., 2018](#)). First, I download the daily projections for maximum temperatures until the year 2100 and compute the average maximum temperature during the summer of each year. Then I map pixels to resolution-5 hexagons in Southern California using the closest distance between centroids. Last, I average the maximum temperatures over 30-year periods.

Estimation. I estimate the following regression:

$$Fire_{jt} = \exp [\alpha \ln(MaxTemp_{jt}) + \mu_j + \mu_t + e_{jt}],$$

where j identifies a resolution-7 hexagon, t is a year between 1981 and 2019, $Fire_{jt}$ is a dummy that indicates a wildfire burn, $MaxTemp_{jt}$ is the average summer maximum temperature in degrees Celsius; μ_j and μ_t are hexagon- and year-fixed effects, respectively; and e_{jt} is a residual. I mark a resolution-7 hexagon as burning during a given year if at least one of its children that are resolution-

9 hexagons burned. I estimate this regression with data for the entire state of California. Table A.4 in the appendix shows the estimates, where columns differ in the sets of included fixed effects. My preferred specification (column 4), with year and resolution-5 hexagon fixed effects, yields an estimate $\hat{\alpha} = 2.433$.

I then use the estimated elasticity of wildfire probability with respect to temperature together with climate projections to generate simple predictions of future wildfire risk driven by climate change. I assign the same resolution-7 temperature to all resolution-9 children and compute counterfactual wildfire risk as a function of current risks δ_i , the ratio of future to current temperatures, and the elasticity estimated above:

$$\delta_i^{CF} = \delta_i \times \left(\frac{MaxTemp_i^{CF}}{MaxTemp_i} \right)^\alpha.$$

VII Counterfactual Scenarios

In this section, I present the results of the simulated scenarios that quantify the current and future costs of wildfire risk and how land-use regulations contribute to that cost. Later, I consider the effects of a mandated relocation program, a policy that is increasingly featured in public discussions about adaptation to environmental risk. Finally, I explore the consequences of a realistic reform of housing regulations.

When measuring total welfare, I assume equal weighing of a dollar for workers and one for landowners. That is, total welfare change is simply the sum of the changes in the aggregate welfare of workers and of landowners:

$$\mathcal{W}(2, 1) = [\mathcal{E}^{(2,0)} - \mathcal{E}^{(1,0)}] N^{(1)} + \sum_i [\mathcal{C}_i^{(2)} - \mathcal{C}_i^{(1)}] L_i^h,$$

where the exponent (0) indicates the equilibrium observed in the data, (1) indicates an initial equilibrium and (2) indicates a new equilibrium. The first term on the right side is the total welfare change of incumbent workers, where \mathcal{E} is the expected equivalent variation defined in Equation 15 and $N^{(1)}$ is the number of workers in the city in the initial equilibrium. The second term is the aggregate welfare change of landowners, which is the sum of the change in certainty equivalent profits \mathcal{C}_i across hexagons, with \mathcal{C}_i as defined in Equation 16, multiplied by the stock of land zoned for housing, L_i^h .

VII.A The Welfare Cost of Wildfire Risk

To quantify the welfare cost of wildfire risk, I simulate a scenario where there is no risk; therefore, in the model, $\delta_i = 0$ in every hexagon i . Then the welfare cost of wildfire risk is the welfare change from a baseline equilibrium with risk to a new equilibrium without risk: $\mathcal{W}(\text{No Risk}, 0)$.

Removing wildfire risk increases welfare, rents, and population in the San Diego metropolitan area. Specifically, the population grows by 1.49%, to 3.03 million people, and the rents increase by 3.03%, as shown in Table 2. The third row of Table 3 shows the effects of removing wildfire

Table 2: Counterfactual prices and allocations

	(1)	(2)	(3)	(4)
	Baseline	No LUR	No risk	No LUR & No risk
Population	2.984M	3.302M	3.029M	3.345M
Workers	1.043M	1.155M	1.059M	1.170M
Workers (Center)	301.432K	466.117K	297.913K	460.140K
Workers (Periphery)	741.936K	688.454K	761.048K	709.444K
C.E. rent profits	8.040B	6.363B	8.436B	6.743B
C.E. rent profits (Center)	1.928B	1.119B	1.880B	1.094B
C.E. rent profits (Periphery)	6.112B	5.244B	6.556B	5.649B
£ property damage	10.859M	9.252M	0.000	0.000
Wages	89.217K	86.307K	88.867K	86.085K
Rents	14.200K	10.207K	14.653K	10.676K
Rents (Center)	11.738K	4.445K	11.591K	4.402K
Rents (Periphery)	15.201K	14.108K	15.852K	14.746K
Premiums	9.529	9.445	-	-

Notes: C.E. stands for certainty equivalent; LUR stands for land-use regulation. The unit M means million, and B means billion. Wages and rents are population-weighted averages. Premiums are coverage-weighted averages.

risk on welfare. In the last column, I present the aggregate effects, considering both workers and landowners. I find that welfare increases by \$764 million per year, or \$14.7 billion over a 65-year horizon with a 5% discount rate.

A worker’s expected equivalent variation to removing risk is \$7.4 billion, 48% of the total welfare gain. This aggregate gain arises from an expected equivalent variation of \$353 per worker per year, or 0.4% of the average wage income in the initial equilibrium. To put this number in context, the average monthly health insurance premium per person in Southern California in 2018 was \$378.¹⁹ Therefore, the model implies that the impact of wildfire risk on the health, safety, and comfort of workers is comparable to the cost of one month of health insurance.

The total certainty equivalent profits of landowners increase by \$8 billion, a 4.9% increase over the equilibrium with risk. As before, this figure is the present value over a 65-year horizon with a 5% discount rate. Alternatively, this number can be interpreted as wealth destruction. A way to accumulate the yearly effects of the static model consistent with the wealth interpretation is to multiply the rental profits by the price-to-rent ratio in the data. In the ACS, this ratio is 23, higher but very similar to the factor of 19.3 implied by a 5% discount rate over 65 years. I use the more conservative value of 19.3 in all my calculations.

¹⁹The number is adjusted for inflation to a 2018 equivalent from the \$394 reported by Covered California, 2020 Health Plan Rate Booklet: https://hbex.coveredca.com/insurance-companies/PDFs/2020_rate_booklet_final.pdf

Table 3: The welfare effects of removing risk or regulations

Scenario	(1)	(2)	(3)	(4)	(5)
	Workers (\$/worker)	Workers (\$M)	Landowners (\$M) Center	Landowners (\$M) Periphery	Total (\$M)
1. No LUR	2,365	2,468	-809	-868	791
2. No LUR in world w/o risk	2,307	2,407	-786	-907	714
3. No risk	353	368	-48	444	764
4. Cost of risk due to LUR (row 1 - row 2)	59	61	-23	39	77
5. Ratio of rows 4 and 3	16.6%	16.6%	48.1%	8.82%	10.1%

Notes: The units are 2018 U.S. dollars per year, and \$M stands for million dollars. The welfare measures are equivalent variation for the workers and the change in certainty equivalent profits for the landowners. The last column is the equally weighted sum of columns (2), (3), and (4). Landowners are partitioned into two groups: hexagons within 8 miles of downtown (the center) and the remaining hexagons (the periphery). The first scenario (row 1) considers a change from the observed equilibrium (with land-use regulations and wildfire risk) to an equilibrium without land-use regulations, as described in the main text. The second scenario (row 2) considers a change from an equilibrium without wildfire risk to an equilibrium with neither wildfire risk nor land-use regulations. The third scenario (row 3) considers a change from the observed equilibrium (with land-use regulations and wildfire risk) to an equilibrium without wildfire risk. LUR stands for land-use regulations.

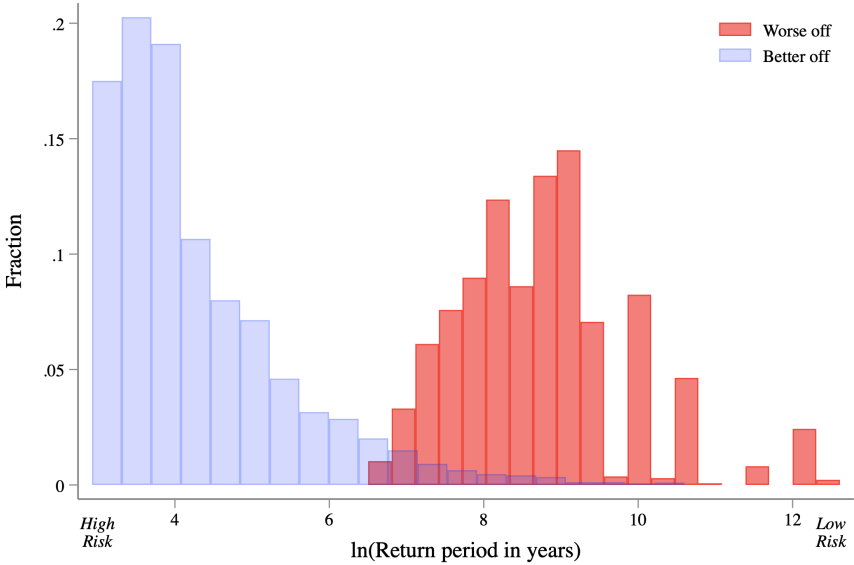
The aggregate gains for landowners hide heterogeneous effects. When wildfire risk is eliminated, the owners of the riskier land gain more, while the owners of the safest land lose. Specifically, landowners in 49.4% of the hexagons are worse off when risk is removed, suffering a total loss in certainty equivalent profits of \$2.8 billion. This loss results in an aggregate gain because the remaining 50.6% of hexagons gain a total of \$10.4 billion. The landowners who are better (resp., worse) off are concentrated in the riskier (resp., safer) parts of the city. The histogram in Figure 5 shows the distribution of risk across hexagons, separating those that are better off from those that are worse off after the counterfactual change. Risk is measured as the log return period, or recurrence. The return period is the inverse of the annual burn probability, and, through a log transformation, allows seeing in more detail what is going on at low levels of risk. Overall, wildfire risk harms the owners of the land in risky places, but benefits those that own land in the safer places of the city.

Migration in and out of the San Diego metropolitan area moderates the welfare costs of wildfires. As shown in section D of the appendix, removing risk in a model where I do not allow the choice of living in or out of the San Diego metropolitan area increases rents by 1.76% and increases welfare by \$19.2 billion. Wages fall by 0.07%, compared to a 0.39% fall in the open city case. The total welfare cost of wildfires in a closed city is \$19.2 billion, 1.25 times the cost in an open city.

In contrast with the open city case, welfare costs in a closed city are not spread evenly between landowners and workers: \$16.3 billion come from workers, and \$2.9 billion, from landowners. In

a closed city, removing risk increases the welfare of both workers and landowners. But opening the city to migration means that the increase in workers' welfare attracts more people to the city, which depresses wages and increases rents further, washing out some of the average welfare gains for workers. For landowners, the increase in population translates to a higher demand for housing and therefore a larger welfare change.

Figure 5: Risk distribution of landowners that are better off or worse off without wildfire risk



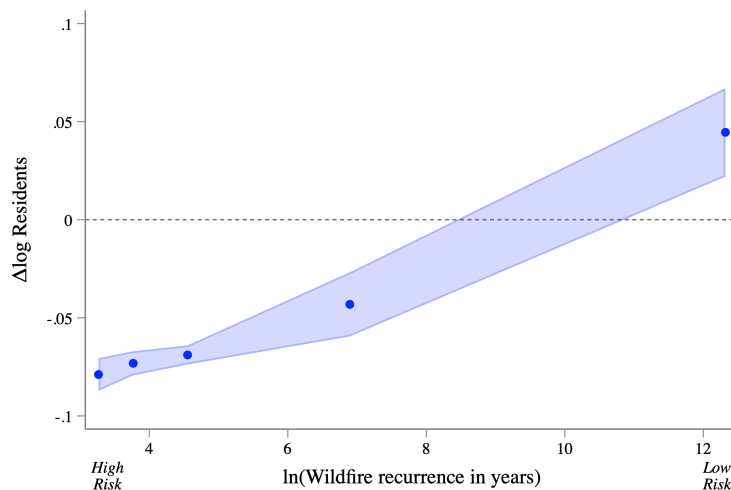
Notes: Two histograms of the distribution of initial risk. The samples are split by whether landowners in the hexagon are better off or worse off after wildfire risk is removed.

VII.B The Effects of Land-use Restrictions

To quantify the effects of housing supply regulations, I consider a counterfactual deregulation experiment that has two parts. First, I lift all density limits; thus, in the model, I set $\bar{H}_i \rightarrow \infty$ in every hexagon i . Second, I rezone the areas close to downtown from single-family to multi-family residential use. I implement this rezoning in my model by setting the fraction of multi-family land to 1 in every residential area within 8 miles of downtown San Diego. In this scenario, as in the counterfactual where risk is removed, the welfare cost of regulations is the welfare change from a baseline equilibrium with regulations to a new equilibrium without regulations: $\mathcal{W}(\text{No Regul}, 0)$.

Land-use deregulation leads to a reallocation of people away from natural hazard-prone areas, as illustrated in Figure 6. It presents a binned scatter plot of the log changes in the number of residents due to deregulation (y-axis) against wildfire risk (x-axis). As before, I measure wildfire risk as the log of the return period, or recurrence, of wildfires. A low return period means higher risk, so the plot shows that the riskiest places shrink and the safest places grow in this scenario. The absolute value of the negative numbers in the plot can be interpreted as the fraction of the current population in hazard-prone areas that would not live here absent housing supply restrictions. Therefore, a value of about -0.7 in the hexagons with a log recurrence of 5 or less means that around 7% of the population living in the areas with a wildfire every 150 years would not be living there if land-use regulations were removed.

Figure 6: The effect of land-use deregulation on wildfire risk exposure



Notes: Binned scatter plots and 95% confidence intervals (Cattaneo et al., 2019). Standard errors are clustered by tract.

The number of people living in areas with zero to moderate wildfire risk (i.e., the areas with a 3% cumulative likelihood of being in a wildfire over 30 years) increases by 12.8%, from 2.63 million to 2.97 million. Moreover, the population in areas with a moderate to major wildfire risk (i.e., 3–14% likelihood of being in a wildfire over 30 years) falls by 4%, from 157,000 to 151,000. Finally,

the population in areas with a severe to extreme wildfire risk (i.e., higher than 14% likelihood of being in a wildfire over 30 years) falls by 6.9%, from 195,000 to 181,000; therefore, 13,474 fewer people would be exposed to at least severe wildfire risk. To put this result into perspective, a mandated relocation out of 4.9% of the riskiest residential land (5% of populated hexagons) would be needed to achieve the same 6.9% reduction in severe to extreme risk exposure.

If the San Diego metropolitan is closed to migration, the count of people at risk falls even more. Figure A.9 in the appendix is the same as Figure 6 but using the counterfactual changes from a model where moving in or out of San Diego is not an option. The population at risk falls less when regulations in an open city are removed, because the ensuing drop in rents makes the city more attractive overall to workers. Therefore, more people choose to live in San Diego and some move into risky areas. For that reason, in principle, land-use deregulation in an open city could even lead to more people living in at-risk areas.

Land-use deregulation leads to a net welfare increase because the improvements in the well-being of workers are larger than the losses of landowners. Deregulation reduces rents by 28% and wages by 3.3%, and leads to an increase of 10.7% in the number of people in the San Diego metropolitan area. As a result, welfare increases by \$791 million per year, as shown in the first row of Table 3. The equivalent variation from deregulation for workers is of \$2.5 billion per year, or \$2,365 per worker per year (i.e., 2.7% of average annual income). Finally, the total certainty equivalent profits of landowners falls by 20.9%, or \$1.7 billion per year.

Land-use deregulation decreases equilibrium insurance premiums, especially in the standard market. Premiums in the standard market and in the FAIR plan implied by the model are \$3.94 and \$30, respectively, per \$1,000 of coverage. The city-wide coverage-weighted mean premium is \$9.48 per \$1,000 of coverage. On average, premiums are 62% of landowners' own expected payouts. In hexagons served by the standard market premiums are 56% of expected payouts, and the FAIR Plan premiums are 83% of expected payouts. Deregulation reduces premiums 0.74% on average, and they fall 0.91% in the standard market and 0.08% in the FAIR Plan hexagons. Premiums as a ratio of expected payouts also fall, but by a very small amount.²⁰

These results suggest that landowners have strong incentives to keep the current regulations. In the deregulation counterfactual, landowners' 20.9% reduction in total welfare is driven by the plunging profits of landowners close to downtown. This can be seen by plotting the distribution of changes in certainty equivalent profits by deregulation status (Figure A.8), or by mapping the changes in expected profits (Figure A.4). Moreover, profits fall more in hexagons with less slack between allowed and built units in the initial equilibrium. I show this with regressions of the counterfactual changes in profits on spatial lags of the fraction initially built (Figure A.7). While the number of residents in those hexagons increases, both rents and net profits fall. The pattern is qualitatively the same if I use the closed city version of the model.

²⁰Wagner (2019) documents that, throughout high-risk flood zones in the eastern U.S., the mean price of flood insurance is about two-thirds of homeowners' own expected payouts. She finds willingness to pay for flood insurance between \$141 to \$165 per \$1,000 of coverage. While the premiums implied by my simple model are significantly lower, conceptually the coverage only includes property damages, not any other risk such as health risks.

The maps in Figure A.4 also show that some owners of peripheral land are better off in the scenario with land-use deregulation. These landowners lose residual demand to the now deregulated central areas. Consequently, rents increase and population falls. However, because rents rise more than the demand falls, the landowners enjoy higher profits. This result implies that they face a downward sloping and inelastic demand, and that the initial rents are below what a hexagon-level monopolist would set.

These welfare costs can also be interpreted either as a lower bound on the unobserved value of regulations or as the minimum Pareto weights on landowners that would make the policy optimal. First, the interpretation as a lower bound on the unobserved value of regulations would result from a planner who maximizes worker surplus, landowner surplus, and some unobserved (positive) value of the regulations. Second, the results imply that housing supply regulations would be neutral if landowners' welfare was weighed at 1.47 times the welfare of (incumbent) workers, or, equivalently, a 59.5% weight was placed on landowner welfare and a 40.5% weight on worker welfare.

Migration in and out of the metropolitan area mitigates the cost that regulations impose on workers and the benefit they bring landowners. Carrying out the same deregulation experiment but with a closed city yields an equivalent variation that is 1.9 times the one with an open city, and causes certainty equivalent profits to fall 1.58 times compared to those in the open city case. The benefits of deregulation in terms of risk exposure are larger if workers are not allowed to leave the city: the number of people living in areas with moderate to major wildfire risk falls by 11.8%, and the number of people living in areas with severe or extreme wildfire risk falls by 13.9%. By migrating, workers can avoid some of the amenity cost of wildfire risk, so the benefits of deregulation are smaller.

VII.C The Contribution of Land-use Regulations to the Cost of Wildfire Risk

In the previous sections I looked separately at the total welfare cost of wildfire risk and at the degree to which risk exposure is driven by housing supply regulations. In this section, I go one step further and quantify what fraction of the welfare cost of wildfire risk is accounted for by the current land-use regulations. My model allows doing this by netting out the welfare cost of regulations that would arise in a counterfactual city without wildfire risk.

The fraction of the welfare cost of wildfire risk due to land-use regulations is

$$\frac{\mathcal{W}(\text{No Regul}, 0) - \mathcal{W}(\text{No Regul \& No Risk}, \text{No Risk})}{\mathcal{W}(\text{No Risk}, 0)}. \quad (17)$$

The first term on the numerator is the gain in welfare from the change to an equilibrium without land-use regulations. The second term, subtracted from the first, is the gain in welfare from the change to an equilibrium without land-use regulations but where there is no risk both in the initial equilibrium and in the new equilibrium. Intuitively, if the current land-use regulations contribute to the welfare costs of wildfire, then the gains from land-use deregulation in a city where risk is in-existent must be smaller than the gains from deregulation in a risky city. The numerator can also be thought of as the estimator in a difference-in-differences setup to estimate the interaction

between land-use regulations and wildfire risk. In such a setup, we compare two cities that differ only in wildfire risk exposure and observe two periods between which both cities undergo land-use deregulation. Of course, in making this comparison, we need the model to know three of the four equilibrium values needed.

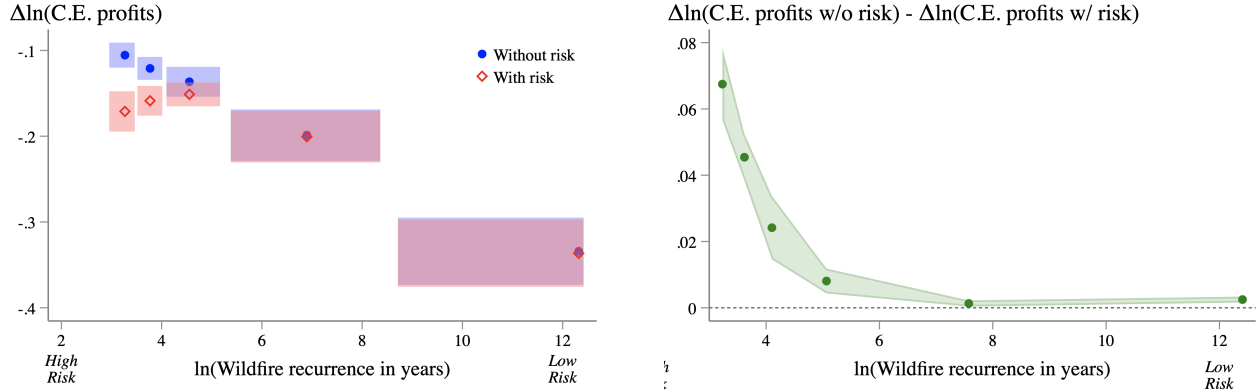
This welfare exercise has the attractive feature of holding some of the potential unobserved benefits from land-use regulations fixed and focusing only on the costs. As in a difference-in-differences setup, this measure holds constant every effect of regulations that is common across risk profiles. These unobserved benefits include any direct preferences of landowners for land-use regulations. This setup does not, however, help to account for workers' preferences for regulations because workers are mobile, so their preferences would affect the equilibrium allocation.

I find that wildfire risk magnifies the welfare costs for workers and the benefits for the owners of land in central areas. Comparing the two first rows of column 2 in Table 3 shows that workers' gains from land-use deregulation are 2.47% higher in a city with wildfire risk; therefore, regulations hurt workers more if wildfire risk is present. Looking at column 3, the losses from land-use deregulation in the central parts of the city are 2.93% higher when wildfire risk is present. Wildfire risk in the periphery makes the safe central land more valuable in relative terms; that is, it operates as a positive (outwards) shift of floorspace demand through the general equilibrium linkages in the housing market. When that positive demand shock happens somewhere where the quantity limits bind, the quantity limit transfers more of the surplus to the owners of land.

Unlike the owners of land in central areas, owners of land in the periphery see a lower value in regulations when there is no wildfire risk. The reduction in their certainty equivalent profits due to deregulation is 4.30% lower in a city with wildfire risk (rows 1 and 2 of column 4 in Table 3). The difference between central and peripheral areas arises because the periphery suffers direct negative consequences of wildfire risk, since it lowers the amenity value of the land and increases insurance costs. Figure 7 explores this relationship between the effects of regulations on profits and risk, at the level of hexagons. The figure shows binned scatter plots. The left panel shows the changes in log certainty equivalent profits against wildfire risk separately for a city with and without wildfire risk. In the safer areas (right of the scale), removing risk does not lead to much different changes in profits. In contrast, the riskier areas (towards the left of the plot) show a smaller fall in certainty equivalent profits in the absence of wildfire risk. The size of the gap, as shown in the right panel of the figure, is as much as 7% on average in the areas that are most prone to wildfire risk.

The results show that land-use regulations can in effect explain part of the cost of wildfire risk. Row 4 of Table 3 shows the numerator in Equation 17, whereas row 3 shows the denominator. The last row (row 5) shows the ratio of the two. Overall, land-use regulations account for 10.1% of the total cost of wildfires. For workers, regulations account for 16.6% of the welfare cost. This number is higher, at 48.1%, for the owners of central land, and 8.82% for the owners of land in the periphery. To put these results in perspective, a 10% increase in wildfire risk probabilities results in a welfare decrease equal to 7.6% of the total cost of wildfire risk (row 3 in Table 3). For workers, the welfare decrease that results from a 10% increase in wildfire risk probabilities is 14%, for owners

Figure 7: The effect of deregulation on landowner profits



Notes: Binned scatter plots and 95% confidence intervals (Cattaneo et al., 2019). Standard errors are clustered by tract. C.E. is certainty equivalent profits.

of central land, it is 13.5%, and for owners of land in the periphery, it is 71%.

The welfare cost of risk due to land-use regulations in levels is \$1.5 billion, or \$77 million per year over 30 years discounted at 5%. Therefore, the joint presence of wildfire risk and land-use regulations generates a loss in surplus beyond the transfers between workers and landowners.

VII.D The Effects of Population Growth and Climate Change

I now explore how population growth and variation in wildfire risk driven by climate change will affect the welfare costs of wildfire risk, land-use regulations, and their interaction. To do so, I repeat the scenarios in the last three sections but starting from forecasted levels of population and wildfire risk. For the latter, I replace the current burn probabilities (δ_i) with predictions based on the estimates in Section VI.D. For the former, I use the U.S. census projections of national growth in the population aged 18 to 64 years. The projections go as far as the year 2060, and I extend them to the year 2100 by assuming population keeps growing at 1.5% per year, the average of the period 2016–2060.

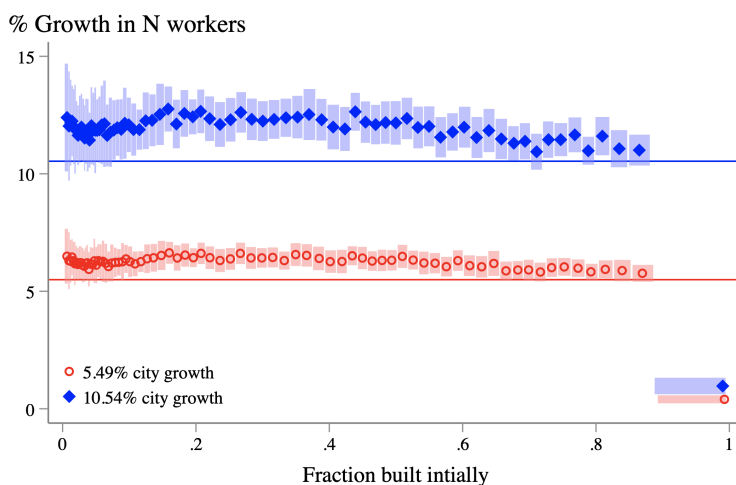
An alternative exercise (results in the appendix) is to close the city and have an exogenous increase in its population according to regional projections. However, I choose to consider an increase in the national population instead, because there is uncertainty in how much the San Diego population will grow, having slowed down in recent years, even before the large drop during the COVID-19 pandemic. One of the main drivers of this slowdown is housing affordability, widely credited to restrictive land-use regulations (Molnar, 2022). Since my model can directly speak to these forces, an exercise that increases the national population is richer and more realistic.

First, simulations show that the areas with current spare capacity grow faster, because areas close to built-out barely grow. Moreover, an increase in the national population growth rate leads to areas with spare capacity growing even faster as more places become built to capacity. In this model, I increase the national population by 14.7% (the projection for 2060) and 29.6% (the

projection for 2100) while keeping the distribution of land-use regulations fixed at current levels. The model predicts that these two national growth scenarios would translate to San Diego growing by 5.49% and 10.54%, respectively. In the appendix I show that repeating this exercise but starting without land-use regulations would lead the city to grow by 7.04% by 2060 and by 13.64% by 2100, with currently restricted places growing more than less restricted places.

For each of these growth scenarios, Figure 8 shows binned scatterplots of population growth against the fraction that is built out under current land-use regulations. The two horizontal lines depict the city-level growth, 5.49% and 10.54%. Focusing first on the 2060 horizon, the circles show that population increases more than the city average of 5.49% in the areas not currently close to being built out (the left section of the x-axis). In contrast, areas that are currently at capacity do not grow at all, and some areas that are close to being built out grow only a little. This result implies that areas in the periphery grow more than proportionally to city growth. In 2100 we see a similar pattern where areas that are currently underbuilt grow more than average, and areas that are built out or close to being built out on average see virtually no growth. Comparing the two time horizons shows that areas close to being built out or at capacity barely grow more in 2100 than they did in 2060, while areas with spare capacity grow even more over the average city growth in 2100 than they did in 2060.

Figure 8: The effect of national population growth



Notes: Binned scatter plots and 95% confidence intervals (Cattaneo et al., 2019). Standard errors are clustered by tract.

Second, I explore the effect of simultaneous increases in national population and wildfire risk to 2060 levels. In Table 4, I present the welfare changes that would result from the same scenarios discussed before but now with higher national population and future wildfire risk. The total welfare cost of wildfire risk increases by 18.7% relative to its cost today. This increase results from the equivalent variation to no wildfire risk rising by 28.5%, to \$473 per worker per year, the certainty equivalent profits to land in the center increasing by 75%, and the certainty equivalent profits to

Table 4: Welfare effects of removing wildfire risk or land-use regulations with future population and risk

Scenario	(1)	(2)	(3)	(4)	(5)
	Workers (\$/worker)	Workers (\$M)	Landowners (\$M) Center	Landowners (\$M) Periphery	Total (\$M)
1. No LUR	2,681	2,942	-1,022	-1,177	743
2. No LUR in world w/o risk	2,580	2,831	-971	-1,199	661
3. No risk	431	473	-84	517	907
4. Cost of risk due to LUR (row 1 - row 2)	101	111	-50	21	82
5. Ratio of rows 4 and 3	23.4%	23.4%	60.1%	4.15%	9.03%

Notes: The units are 2018 U.S. dollars per year, and \$M stands for million dollars. The welfare measures are equivalent variation for the workers and the change in certainty equivalent profits for the landowners. The last column is the equally weighted sum of columns 2, 3, and 4. Landowners are partitioned into two groups: hexagons within 8 miles of downtown (the center) and the remaining hexagons (the periphery). The first scenario (row 1) considers a change from the observed equilibrium (with land-use regulations and wildfire risk) to an equilibrium without land-use regulations as described in the main text. The second scenario (row 2) considers a change from an equilibrium without wildfire risk to an equilibrium with neither wildfire risk nor land-use regulations. The third scenario (row 3) considers a change from the observed equilibrium (with land-use regulations and wildfire risk) to an equilibrium without wildfire risk. LUR stands for land-use regulations.

land in the periphery increasing by 16.4%. Underlying these welfare changes is an increase in risk exposure: the number of residents exposed to at least 1% (resp., 20%) probability of their homes burning within 30 years increases by 7.4%, to 377,700 (resp., 11.8%, to 178,100).

The total welfare cost of land-use regulations, shown in the last column of row 1 of Table 4, falls by 6%, to \$743 million per year relative to today. This decrease happens because the benefits of land-use regulations to landowners increase more than do the costs to workers. The equivalent variation to land-use deregulation increases by 19%, to \$2,681 per worker per year, whereas the certainty equivalent profits of landowners in central and peripheral areas increase by 26% and 36%, respectively.

The importance of land-use regulations in driving the cost of wildfires falls overall because the increases in the importance of these regulations for workers and owners of central land are compensated by a reduction in their importance for the owners of land in the periphery. The overall fraction falls by almost 1 percentage point, to 9.03% of the net welfare costs of wildfires. For workers, the fraction increases by 6.8 percentage points, to 23.4%, and for the owners of land in the center, it increases by 12 percentage points, to 60.1%. In the periphery, the fraction of wildfires' welfare costs accounted by land-use regulations falls by 4.7 percentage points, to 4.15%.

Finally, I examine the extent to which changes in wildfire risk or changes in population contribute to these results. Tables A.7 and A.8 in the appendix present the results I obtained by

repeating the analysis but changing population size and wildfire risk one at a time. The first takeaway from this exercise is that it is the growth in population that accounts for the drop in overall welfare costs of land-use regulations. When only wildfire risk rises, the overall welfare cost of land-use regulations virtually does not change, because the higher costs to workers compensate for the higher benefits to landowners (i.e., it is a pure surplus transfer). The second takeaway is that population growth can account for about 10% of the increase in the total welfare cost of wildfires. When only the size of the population (resp., wildfire risk) is increased, the total welfare cost of wildfires increases by 2% (resp., 16%).

VII.E Mandated Relocation

This section explores the consequences of mandating the relocation out of the riskiest places in the San Diego metropolitan area. I implement the policy experiment by setting the maximum density $\bar{H}_i = 0$, effectively banning development, in the 5% riskiest hexagons.

Experts and policymakers have proposed the managed retreat of homes from hazard-prone areas to improve climate resiliency (GAO, 2020). An example is the voluntary buyout program operated by FEMA. After a natural disaster, FEMA offers to pay landowners an assessed pre-disaster fair market price and the area cannot legally be developed with permanent structures in the future. Another example is a program in Paradise, California. The town, which was devastated by the Camp Fire in 2018, aims to buy high-risk properties and create a “wildfire buffer” of fire-resistant green spaces around the city (Siegler, 2021; Smith, 2022).

As a result of the mandated relocation of the 5% riskiest hexagons, the population exposed to one fire every 150 years falls by 8.89% and the average insurance premium falls by 15.3% (Table A.9 in the appendix). Interestingly, the policy has a net positive effect on landowner profits of \$78.1 million per year. The certainty equivalent profits in the relocated hexagons are \$107.7 million per year, but the gain in profits in the rest of the city are \$107.7 million per year. That gain is 3.6 times what it would take to compensate the owners of the banned land. However, the equivalent variation to the policy for workers is a loss of \$210 per worker per year. The total welfare impact of the mandated relocation on both landowners and workers is a loss of \$141.5 million per year.

However, in reality, existing relocation programs are not mandatory. The government does not use eminent domain to take at-risk property for public benefit. My results suggest that in San Diego, the owners of at-risk land that do not reside there would be willing to sell their properties. However, getting owner-occupiers to sell their properties would prove difficult, as the amenity value of living in these risky areas is otherwise high.

VII.F A Realistic Reform of Land-use Regulations

In this section, I explore the effects of upzoning the areas within half a mile of a major transit stop in the City of San Diego. These areas are known as Transit Priority Areas (TPA). I rezone residential land in these areas to multi-family use and set the density limits \bar{H}_i equal to the value that implies at least a maximum of 10 units per lot.

In recent years, state-level policymakers in California have been active in passing laws to incentivize the building of homes. Two examples, passed in late 2021, are SB 9 and SB 10 (Sisson, 2022). The first one allows single-family lots to be split in two and permits duplexes on each of the new lots (effectively allowing for four homes where there was one). The second law, SB 10, allows local governments to rezone for developments of 10 units or fewer in urban infill or transit-adjacent parcels without additional environmental review.

I find that upzoning TPAs, a policy change similar to SB 10, can replicate 85.6% of the welfare gains of full land-use deregulation. With this policy, the net gains are of \$677 million per year, compared to \$791 million per year with full deregulation. Moreover, landowners lose \$1,677 certainty equivalent profits per year, 72.7% of the losses from full deregulation. The equivalent variation of the policy for workers is \$1,896 per worker per year, 76.8% of the \$2,365 from full deregulation.

VIII Conclusions

In this paper, I examined the extent to which land-use regulations restricting development in safer areas drive people to live in at-risk areas. This shows how institutions, such as those regulating land use, can hinder adaptation to climate change by relocating out of harm's way.

I developed a quantitative urban model that captures some of the fundamental ways in which environmental risk, in the form of natural hazards that destroy property and harm people, shapes the inner structure of a city. In the model, land-use regulations benefit landowners and reallocate the population to unregulated at-risk areas. These effects depend on estimated disamenities from wildfire risk, insurance access, and the spatial correlation between wildfire risk and location characteristics. Combining this model with detailed micro-data in the metropolitan area of San Diego, I quantified three types of welfare cost: of wildfire risk, of regulations, and of their interaction. I highlighted how welfare effects are distributed between workers and landowners, and between owners of land with different degrees of land-use regulation and wildfire risk. Overall, my results suggest that climate change will increase wildfire risk, and population growth will lead to more people living in at-risk areas.

The issues considered in this paper are relevant for other cities and other environmental threats. Housing growth in the United States is disproportionately happening in places at risk of a multitude of natural hazards, and I show that the geography of housing supply within cities matters in explaining this pattern. In particular, I show that Combined Statistical Areas in the United States with a less elastic supply of housing in safe areas saw particularly high growth in risky areas. My study of wildfire risk in the San Diego metropolitan area helps to explain how the presence of people in environmentally risky places arises from the interaction of the institutional framework, defined by land-use regulations, with individual choices, where these choices weigh risk exposure against other attractive features of a place and costly mitigation with insurance.

References

- ACOSTA, C. (2021): “The Incidence of Land Use Regulations,” *SSRN Electronic Journal*.
- ALBERT, C., P. BUSTOS, AND J. PONTICELLI (2021): “The Effects of Climate Change on Labor and Capital Reallocation,” *SSRN Electronic Journal*.
- ALEXANDRE, P., M. MOCKRIN, S. STEWART, R. HAMMER, AND V. RADELOFF (2014): “Rebuilding and new housing development after wildfire,” *International Journal of Wildland Fire*, 24.
- ALEXANDRE, P. M., S. I. STEWART, N. S. KEULER, M. K. CLAYTON, M. H. MOCKRIN, A. BARMASSADA, A. D. SYPHARD, AND V. C. RADELOFF (2016): “Factors related to building loss due to wildfires in the conterminous United States,” *Ecological Applications*, 26, 2323–2338.
- ANAGOL, S., F. V. FERREIRA, AND J. REXER (2021): “Estimating the Economic Value of Zoning Reform,” *SSRN Electronic Journal*.
- ANDELA, N., D. C. MORTON, L. GIGLIO, Y. CHEN, G. R. VAN DER WERF, P. S. KASIBHATLA, R. S. DEFRIES, G. J. COLLATZ, S. HANTSON, S. KLOSTER, D. BACHELET, M. FORREST, G. LASSLOP, F. LI, S. MANGEON, J. R. MELTON, C. YUE, AND J. T. RANDERSON (2017): “A human-driven decline in global burned area,” *Science*, 356, 1356–1362, doi: 10.1126/science.aal4108.
- ANDERSON, M. L. (2019): “As the Wind Blows: The Effects of Long-Term Exposure to Air Pollution on Mortality,” *Journal of the European Economic Association*, 18, 1886–1927.
- BALBONI, C. (2021): “In Harm’s Way? Infrastructure Investments and the Persistence of Coastal Cities,” Working paper, Department of Economics, Massachusetts Institute of Technology.
- BARRECA, A., K. CLAY, O. DESCHENES, M. GREENSTONE, AND J. S. SHAPIRO (2016): “Adapting to climate change: The remarkable decline in the US temperature-mortality relationship over the Twentieth Century,” *Journal of Political Economy*, 124.
- BARWICK, P. J., D. DONALDSON, S. LI, Y. LIN, AND D. RAO (2021): “Improved Transportation Infrastructure Facilitates Adaptation to Pollution and Temperature Extremes,” *SSRN Electronic Journal*.
- BAUM-SNOW, N. AND L. HAN (2021): “The Microgeography of Housing Supply,” Working paper.
- BAYLIS, P. AND J. BOOMHOWER (2019): “Moral Hazard, Wildfires, and the Economic Incidence of Natural Disasters,” Working paper.
- BAYLIS, P. W. AND J. BOOMHOWER (2021): “Mandated vs. Voluntary Adaptation to Natural Disasters: The Case of U.S. Wildfires,” *National Bureau of Economic Research Working Paper Series*, No. 29621.

- BLAUDIN DE THÉ, C., B. CARANTINO, AND M. LAFOURCADE (2021): “The carbon ‘carprint’ of urbanization: New evidence from French cities,” *Regional Science and Urban Economics*, 89, 103693.
- BROWN, M. R. G., V. AGYAPONG, A. J. GREENSHAW, I. CRIBBEN, P. BRETT-MACLEAN, J. DROLET, C. McDONALD-HARKER, J. OMEJE, M. MANKOWSI, S. NOBLE, D. T. KITCHING, AND P. H. SILVERSTONE (2019): “Significant PTSD and Other Mental Health Effects Present 18 Months After the Fort McMurray Wildfire: Findings From 3,070 Grades 7-12 Students,” *Frontiers in Psychiatry*, 10, 623.
- BRYAN, G. AND M. MORTEN (2019): “The aggregate productivity effects of internal migration: Evidence from Indonesia,” *Journal of Political Economy*, 127.
- BRYANT, R. A., L. GIBBS, H. C. GALLAGHER, P. PATTISON, D. LUSHER, C. MACDOUGALL, L. HARMS, K. BLOCK, V. SINNOTT, G. IRETON, J. RICHARDSON, AND D. FORBES (2018): “Longitudinal study of changing psychological outcomes following the Victorian Black Saturday bushfires,” *Australian & New Zealand Journal of Psychiatry*, 52, 542–551, PMID: 28605987.
- BURKE, M., M. L. CHILDS, B. D. LA CUESTA, M. QIU, J. LI, C. F. GOULD, S. HEFT-NEAL, AND M. WARA (2023): “Wildfire Influence on Recent US Pollution Trends,” *National Bureau of Economic Research Working Paper Series*, No. 30882, author contact info: Marshall Burke Doerr School of Sustainability Stanford University Stanford, CA 94305 E-Mail: mburke@stanford.edu Marissa Childs Center for the Environment Harvard University E-Mail: mchilds@fas.harvard.edu Brandon De la Cuesta Stanford University SIEPR, Gunn Building Stanford, CA 94305 E-Mail: brandon.delacuesta@stanford.edu Minghao Qiu E-Mail: mhqiu@stanford.edu Jessica Li 473 Via Ortega Stanford, CA 94305 USA E-Mail: jbli@stanford.edu Carlos F. Gould Department of Earth System Science Stanford University 473 Via Ortega Stanford, CA 94305 E-Mail: cf-gould@stanford.edu Sam Heft-Neal Center on Food Security and the Environment Stanford University 473 Via Ortega Stanford, CA 94305 E-Mail: sheftneal@stanford.edu Michael Wara 473 Via Ortega Stanford, CA 94305 United States E-Mail: mwara@stanford.edu.
- BURKE, M., A. DRISCOLL, J. XUE, S. HEFT-NEAL, J. BURNEY, AND M. WARA (2020): “The Changing Risk and Burden of Wildfire in the US,” Working Paper 27423, National Bureau of Economic Research.
- BURKE, M., S. HEFT-NEAL, J. LI, A. DRISCOLL, P. W. BAYLIS, M. STIGLER, J. WEILL, J. BURNEY, J. WEN, M. CHILDS, AND C. GOULD (2021): “Exposures and Behavioral Responses to Wildfire Smoke,” *National Bureau of Economic Research Working Paper Series*, No. 29380.
- CAL-ADAPT (2018): “LOCA Derived Data,” Data derived from LOCA Downscaled CMIP5 Climate Projections. Cal-Adapt website developed by University of California at Berkeley’s Geospatial Innovation Facility under contract with the California Energy Commission. Retrieved August 8, 2022 from <https://cal-adapt.org/>.

- CAMERON, P. A., B. MITRA, M. FITZGERALD, C. D. SCHEINKESTEL, A. STRIPP, C. BATEY, L. NIGGEMEYER, M. TRUESDALE, P. HOLMAN, R. MEHRA, J. WASIAK, AND H. CLELAND (2009): “Black Saturday: the immediate impact of the February 2009 bushfires in Victoria, Australia,” *Medical Journal of Australia*, 191, 11–16.
- CARLETON, T., A. JINA, M. DELGADO, M. GREENSTONE, T. HOUSER, S. HSIANG, A. HULTGREN, R. E. KOPP, K. MCCUSKER, I. NATH, J. RISING, A. RODE, H. K. SEO, A. VIAENE, J. YUAN, AND A. T. ZHANG (2021): “Valuing the Global Mortality Consequences of Climate Change Accounting for Adaptation Costs and Benefits,” *SSRN Electronic Journal*.
- CAROZZI, F. AND S. ROTH (2023): “Dirty density: Air quality and the density of American cities,” *Journal of Environmental Economics and Management*, 118, 102767.
- CART, J. (2021): “Lightning could spark more California fires as world warms,” *CalMatters*.
- CATTANEO, M. D., R. K. CRUMP, M. H. FARRELL, AND Y. FENG (2019): “On Binscatter,” .
- CIGNARALE, T., J. LAUCHER, K. ALLEN, AND L. LANDSMAN-SMITH (2017): “The Availability and Affordability of Coverage for Wildfire Loss in Residential Property Insurance in the Wildland-Urban Interface and Other High-Risk Areas of California: CDI Summary and Proposed Solutions,” .
- COLAS, M. AND J. M. MOREHOUSE (2022): “The environmental cost of land-use restrictions,” *Quantitative Economics*, 13.
- COLLINS, S. R., D. C. RADLEY, AND J. C. BAUMGARTNER (2022): “Trends in Employer Health Care Coverage, 2010–2020,” *Commonwealth Fund*.
- CORREIA, S., P. GUIMARÃES, AND T. ZYLKIN (2020): “Fast Poisson estimation with high-dimensional fixed effects,” *The Stata Journal*, 20, 95–115.
- COSTINOT, A., D. DONALDSON, AND C. SMITH (2016): “Evolving Comparative Advantage and the Impact of Climate Change in Agricultural Markets: Evidence from 1.7 Million Fields around the World,” *Journal of Political Economy*, 124, 205–248.
- COUTURE, V., C. GAUBERT, J. HANDBURY, AND E. HURST (2020): “Income Growth and the Distributional Effects of Urban Spatial Sorting,” Tech. Rep. 14350.
- CRUZ, J.-L. (2021): “Global Warming and Labor Market Reallocation,” Working paper.
- CRUZ, J.-L. AND E. ROSSI-HANSBERG (2021): “The Economic Geography of Global Warming,” Working Paper 28466, National Bureau of Economic Research.
- DERYUGINA, T., G. HEUTEL, N. H. MILLER, D. MOLITOR, AND J. REIF (2019): “The Mortality and Medical Costs of Air Pollution: Evidence from Changes in Wind Direction,” *American Economic Review*, 109, 4178–4219.

- DESMET, K., R. E. KOPP, S. A. KULP, D. K. NAGY, M. OPPENHEIMER, E. ROSSI-HANSBERG, AND B. H. STRAUSS (2021): “Evaluating the Economic Cost of Coastal Flooding,” *American Economic Journal: Macroeconomics*, 13, 444–86.
- DINGEL, J. I. AND F. TINTELOT (2021): “Spatial Economics for Granular Settings,” Tech. rep.
- FAVILUKIS, J., P. MABILLE, AND S. V. NIEUWERBURGH (2022): “Affordable Housing and City Welfare,” *The Review of Economic Studies*, rdac024.
- FINNEY, M. A., C. W. MCHUGH, I. C. GRENFELL, K. L. RILEY, AND K. C. SHORT (2011): “A simulation of probabilistic wildfire risk components for the continental United States,” *Stochastic Environmental Research and Risk Assessment*, 25, 973–1000.
- FRAP (2019): “The California Department of Forestry and Fire Protection’s Fire and Resource Assessment Program (FRAP),” Data retrieved May 28, 2020 from <https://frap.fire.ca.gov/>.
- GAO (2020): “Climate change: A climate migration pilot program could enhance the nation’s resilience and reduce federal fiscal exposure,” .
- GARNACHE, C. (2020): “Does the Salience of Risk Affect Large, Risky Asset Prices?” *SSRN Electronic Journal*.
- GELLMAN, J., M. WALLS, AND M. J. WIBBENMEYER (2021): “Wildfire, Smoke, and Outdoor Recreation in the Western United States,” Working Paper 21-22, Resources for the Future (RFF).
- GLAESER, E. L. AND M. E. KAHN (2010): “The greenness of cities: Carbon dioxide emissions and urban development,” *Journal of Urban Economics*, 67, 404–418.
- GRILICHES, Z. AND H. REGEV (1995): “Firm productivity in Israeli industry 1979-1988,” *Journal of Econometrics*, 65.
- GYOURKO, J. AND R. MOLLOY (2015): “Chapter 19 - Regulation and Housing Supply,” in *Handbook of Regional and Urban Economics*, ed. by G. Duranton, J. V. Henderson, and W. C. Strange, Elsevier, vol. 5 of *Handbook of Regional and Urban Economics*, 1289 – 1337.
- HANDEL, B., I. HENDEL, AND M. D. WHINSTON (2015): “Equilibria in Health Exchanges: Adverse Selection versus Reclassification Risk,” *Econometrica*, 83, 1261–1313.
- HEFT-NEAL, S., C. F. GOULD, M. CHILDS, M. V. KIANG, K. NADEAU, M. DUGGAN, E. BENDAVID, AND M. BURKE (2023): “Behavior Mediates the Health Effects of Extreme Wildfire Smoke Events,” *National Bureau of Economic Research Working Paper Series*, No. 30969, author contact info: Sam Heft-Neal Center on Food Security and the Environment Stanford University 473 Via Ortega Stanford, CA 94305 E-Mail: sheftneal@stanford.edu Carlos F. Gould Department of Earth System Science Stanford University 473 Via Ortega Stanford, CA 94305 E-Mail: cfgould@stanford.edu Marissa Childs Center for the Environment Harvard University E-Mail:

- mchilds@fas.harvard.edu Mathew Kiang E-Mail: mkiang@stanford.edu Kari Nadeau E-Mail: knadeau@hsph.harvard.edu Mark Duggan Stanford University Department of Economics 579 Jane Stanford Way Stanford, CA 94305-6072 E-Mail: mgduggan@stanford.edu Eran Bendavid Department of Medicine Stanford University E-Mail: ebd@stanford.edu Marshall Burke Doerr School of Sustainability Stanford University Stanford, CA 94305 E-Mail: mburke@stanford.edu.
- HEUTEL, G., N. H. MILLER, AND D. MOLITOR (2021): “Adaptation and the Mortality Effects of Temperature across U.S. Climate Regions,” *Review of Economics and Statistics*, 103.
- ISSLER, P., R. H. STANTON, C. VERGARA-ALERT, AND N. E. WALLACE (2020): “Mortgage Markets with Climate-Change Risk: Evidence from Wildfires in California,” *SSRN Electronic Journal*.
- JIA, R., X. MA, AND V. W. XIE (2022): “Expecting Floods: Firm Entry, Employment, and Aggregate Implications,” NBER Working Papers 30250, National Bureau of Economic Research, Inc.
- JOHNSTON, D. W., Y. K. ÖNDER, M. H. RAHMAN, AND M. A. ULUBAŞOĞLU (2021): “Evaluating wildfire exposure: Using wellbeing data to estimate and value the impacts of wildfire,” *Journal of Economic Behavior and Organization*, 192.
- KAHN, M. E. (2016): “The climate change adaptation literature,” *Review of Environmental Economics and Policy*, 10.
- KIM, M.-K. AND P. M. JAKUS (2019): “Wildfire, national park visitation, and changes in regional economic activity,” *Journal of Outdoor Recreation and Tourism*, 26, 34–42.
- KNITTEL, C. R., D. L. MILLER, AND N. J. SANDERS (2016): “Caution, Drivers! Children Present: Traffic, Pollution, and Infant Health,” *The Review of Economics and Statistics*, 98, 350–366.
- KNORR, W., A. ARNETH, AND L. JIANG (2016a): “Demographic controls of future global fire risk,” *Nature Climate Change*, 6, 781–785.
- KNORR, W., L. JIANG, AND A. ARNETH (2016b): “Climate, CO₂ and human population impacts on global wildfire emissions,” *Biogeosciences*, 13, 267–282.
- KNORR, W., T. KAMINSKI, A. ARNETH, AND U. WEBER (2014): “Impact of human population density on fire frequency at the global scale,” *Biogeosciences*, 11, 1085–1102.
- LEE, K. D. (2020): “Essays in Urban and Labor Economics,” Ph.D. thesis, UCLA.
- LITTELL, J. S., D. L. PETERSON, K. L. RILEY, Y. LIU, AND C. H. LUCE (2016): “A review of the relationships between drought and forest fire in the United States,” *Global Change Biology*, 22, 2353–2369.

- LTDB (2010): “Longitudinal Tract Data Base (LTDB),” Data retrieved August 1, 2020 from <http://www.s4.brown.edu/us2010/Researcher/Bridging.htm>.
- MARTYNOV, P. (2021): “Welfare Effects of Zoning: Density Restrictions and Heterogeneous Spillovers,” Job market paper, University of California, Berkeley.
- MASSETTI, E. AND R. MENDELSON (2018): “Measuring climate adaptation: Methods and evidence,” *Review of Environmental Economics and Policy*, 12.
- MCCONNELL, K., S. WHITAKER, E. FUSSELL, J. DEWAARD, K. PRICE, AND K. CURTIS (2021): “Effects of Wildfire Destruction on Migration, Consumer Credit, and Financial Distress,” *FRB of Cleveland Working Paper*.
- MCCOY, S. J. AND R. P. WALSH (2018): “Wildfire risk, salience & housing demand,” *Journal of Environmental Economics and Management*, 91, 203–228.
- MOLNAR, P. (2022): “Over the next few years, will San Diego County’s population continue to decline?” *The San Diego Union-Tribune*.
- MONKKONEN, P., M. LENS, AND M. MANVILLE (2020): “Built-out cities? How California Cities Restrict Housing Production through Prohibition and Process,” *SSRN Electronic Journal*.
- MUELLER, J., J. LOOMIS, AND A. GONZÁLEZ-CABÁN (2009): “Do repeated wildfires change homebuyers’ demand for homes in high-risk areas? A hedonic analysis of the short and long-term effects of repeated wildfires on house prices in Southern California,” *Journal of Real Estate Finance and Economics*, 38, 155–172.
- NATH, I. (2021): “The Food Problem and the Aggregate Productivity Consequences of Climate Change,” *SSRN Electronic Journal*.
- NATIONAL RESEARCH COUNCIL (2011): *Climate Stabilization Targets: Emissions, Concentrations, and Impacts over Decades to Millennia*, Washington, DC: The National Academies Press.
- PARISIEN, M.-A., S. SNETSINGER, J. A. GREENBERG, C. R. NELSON, T. SCHOENNAGEL, S. Z. DOBROWSKI, AND M. A. MORITZ (2012): “Spatial variability in wildfire probability across the western United States,” *International Journal of Wildland Fire*, 21, 313–327.
- PIERCE, D. W., J. F. KALANSKY, AND D. R. CAYAN (2018): “Climate, Drought, and Sea Level Rise Scenarios for the Fourth California Climate Assessment,” .
- PLANTINGA, A. J., R. WALSH, AND M. WIBBENMEYER (2020): “Priorities and Effectiveness in Wildfire Management: Evidence from Fire Spread in the Western United States,” Working Paper 20-21, Resources for the Future (RFF).
- PRISM (2020): “PRISM Climate Group, Oregon State University,” Data retrieved August 3, 2022 from <https://prism.oregonstate.edu>.

- PSARROS, C., C. THELERITIS, M. ECONOMOU, C. TZAVARA, K. T. KIOULOS, L. MANTONAKIS, C. R. SOLDATOS, AND J.-D. BERGIANNAKI (2017): “Insomnia and PTSD one month after wildfires: evidence for an independent role of the “fear of imminent death”,” *International Journal of Psychiatry in Clinical Practice*, 21, 137–141, pMID: 28084115.
- RADELOFF, V. C., D. P. HELMERS, H. A. KRAMER, M. H. MOCKRIN, P. M. ALEXANDRE, A. BAR-MASSADA, V. BUTSIC, T. J. HAWBAKER, S. MARTINUZZI, A. D. SYPHARD, AND S. I. STEWART (2018): “Rapid growth of the US wildland-urban interface raises wildfire risk,” *Proceedings of the National Academy of Sciences*, 115, 3314–3319.
- RICHARDSON, L. A., P. A. CHAMP, AND J. B. LOOMIS (2012): “The hidden cost of wildfires: Economic valuation of health effects of wildfire smoke exposure in Southern California,” *Journal of Forest Economics*, 18, 14–35.
- ROMPS, D. M., J. T. SEELEY, D. VOLLARO, AND J. MOLINARI (2014): “Projected increase in lightning strikes in the United States due to global warming,” *Science*, 346, 851–854.
- SAIZ, A. (2010): “The Geographic Determinants of Housing Supply*,” *The Quarterly Journal of Economics*, 125, 1253–1296.
- SANDAG (2019): “Housing in the San Diego Region: Building permits, cost, and vacancies,” .
- SCOTT, J. H., J. W. GILBERTSON-DAY, C. MORAN, G. K. DILLON, K. C. SHORT, AND K. C. VOGLER (2020): “Wildfire Risk to Communities: Spatial datasets of landscape-wide wildfire risk components for the United States,” Tech. rep., Forest Service Research Data Archive, Fort Collins, CO.
- SEVEREN, C. (2019): “Commuting, labor, and housing market effects of mass transportation: Welfare and identification,” .
- SEVEREN, C., C. COSTELLO, AND O. DESCHÊNES (2018): “A Forward-Looking Ricardian Approach: Do land markets capitalize climate change forecasts?” *Journal of Environmental Economics and Management*, 89, 235–254.
- SHARYGIN, E. (2021): “Estimating Migration Impacts of Wildfire: California’s 2017 North Bay Fires,” .
- SHORT, K. C. (2017): “Spatial wildfire occurrence data for the United States, 1992-2015 [FPA_FOD_20170508],” .
- SIEGLER, K. (2021): “In Fire Scorched California, Town Aims To Buy The Highest At-Risk Properties,” *NPR*.
- SISSON, P. (2022): “San Diego Tackles California’s Housing Crisis and Car-Centric Design,” *Planning Magazine*.

- SMITH, L. J. (2022): “Could a buffer shield Californian homes from wildfire?” *BBC*.
- STAVROS, E. N., J. ABATZOGLOU, N. K. LARKIN, D. MCKENZIE, AND E. A. STEEL (2014): “Climate and very large wildland fires in the contiguous western USA,” *International Journal of Wildland Fire*, 23, 899–914.
- SYDNOR, J. (2010): “(Over)insuring Modest Risks,” *American Economic Journal: Applied Economics*, 2, 177–199.
- TSIVANIDIS, N. (2019): “Evaluating the impact of urban transit infrastructure: Evidence from bogota’s transmilenio,” *Unpublished manuscript*.
- U.S. EPA (2019): *Integrated science assessment (ISA) for particulate matter*, EPA/600/R-19/188, Center for Public Health and Environmental Assessment, U.S. Environmental Protection Agency.
- VALENTINYI, A. AND B. HERRENDORF (2008): “Measuring factor income shares at the sectoral level,” *Review of Economic Dynamics*, 11, 820 – 835.
- WAGNER, K. (2019): “Adaptation and Adverse Selection in Markets for Natural Disaster Insurance,” *SSRN Electronic Journal*.
- WEHNER, M. F., J. R. ARNOLD, T. KNUTSON, K. E. KUNKEL, AND A. N. LEGRANDE (2017): “Droughts, floods, and wildfires,” in *Climate Science Special Report: Fourth National Climate Assessment, Volume I*, ed. by D. J. Wuebbles, D. W. Fahey, K. A. Hibbard, D. J. Dokken, B. C. Stewart, and T. K. Maycock, Washington, DC, USA: U.S. Global Change Research Program, 231–256.
- WESTERLING, A. L. (2016): “Increasing western US forest wildfire activity: sensitivity to changes in the timing of spring,” *Philosophical Transactions of the Royal Society B: Biological Sciences*, 371, 20150178.
- WIBBENMEYER, M., S. E. ANDERSON, AND A. J. PLANTINGA (2019): “Salience and the Government Provision of Public Goods,” *Economic Inquiry*, 57.
- WINKLER, R. L. AND M. D. ROULEAU (2021): “Amenities or disamenities? Estimating the impacts of extreme heat and wildfire on domestic US migration,” *Population and Environment*, 42, 622–648.
- XU, R., P. YU, M. J. ABRAMSON, F. H. JOHNSTON, J. M. SAMET, M. L. BELL, A. HAINES, K. L. EBI, S. LI, AND Y. GUO (2020): “Wildfires, Global Climate Change, and Human Health,” *N Engl J Med*, 383, 2173–2181.
- ZHENG, S., R. WANG, E. L. GLAESER, AND M. E. KAHN (2011): “The greenness of China: Household carbon dioxide emissions and urban development,” *Journal of Economic Geography*, 11.

ZHOU, X., K. JOSEY, L. KAMAREDDINE, M. C. CAINE, T. LIU, L. J. MICKLEY, M. COOPER, AND F. DOMINICI (2021): “Excess of COVID-19 cases and deaths due to fine particulate matter exposure during the 2020 wildfires in the United States,” *Science Advances*, 7, eabi8789.

ZUZAK, C., E. GOODENOUGH, C. STANTON, M. MOWRER, N. RANALLI, D. KEALEY, AND J. ROZELLE (2021): “National Risk Index Technical Documentation,” Tech. rep., Federal Emergency Management Agency, Washington, DC.

Urban Policy and Spatial Exposure to Environmental Risk

Appendices for Online Publication

Augusto Ospital

A Data Appendix

This section presents the details of the parcel data that I use to estimate and calibrate the model.

Download the parcel dataset for San Diego County. To begin, I downloaded the parcel dataset for San Diego County from the SanGIS/SANDAG GIS Data Warehouse, which I retrieved on January 26, 2020. The reference date for the information is December 28, 2019. This dataset includes the parcel polygons and associated parcel information provided by the San Diego County Assessor/Recorder/County Clerk (ARCC) in their Master Property Record (MPR file) and Parcel Assessment Record (PAR file). SanGIS also adds situs address information, if provided by the addressing authority.

Process the parcel data. First, I filtered out parcels owned by public agencies to exclude all public land such as Navy housing. Second, I recoded parcels with units but no floorspace, or vice versa, by setting the unit count to zero and the assessed value to missing. Third, I did not count commercial units (mostly hotels and hospitals), institutional units (e.g., dorms, religious buildings), industrial units, or government and recreational units as housing units. Fourth, I excluded from the sample plots under 300 square feet and parcels with assessed values under \$50 per square feet or over \$1,500 per square feet.¹ Finally, I created a broad zoning identifier by classifying the zoning codes in the data into single-family residential, multi-family residential, commercial, and agriculture.

Collect land-use regulations and development standards. I collected land-use regulations and development standards for the 19 different jurisdictions in San Diego County. Table A.1 shows the total housing units, plot area, and assessed value by jurisdiction. Each jurisdiction has its specific zoning designations and development regulations. There are 18 incorporated cities plus all unincorporated areas. Zoning in unincorporated areas falls under the county's jurisdiction. I obtained land-use zoning designations maps from relevant city and county planning departments, and then collected the associated development regulations from municipal codes for each jurisdiction. Jurisdictions can be divided into two groups based on data availability: those where zoning shapefiles are available and those where they are not. The last column of table A.1 indicates what jurisdictions belong to each group. The first group includes 10 of the largest and most populated

¹For reference, the 5 most expensive homes for sale in San Diego on Zillow on September 9, 2022 had prices per square feet of \$1,684, \$2,140, \$2,718, \$3,660, and \$6,584. The 5 least expensive homes for sale had prices per square feet of \$94, \$104, \$134, \$138, and \$182.

jurisdictions, accounting for 85% of all units, 77% of all plot areas, 85% of all built area, and 85% of all assessed value.

In jurisdictions where zoning shapefiles are available, I assigned each parcel's centroid to the zone polygon over it. Then I merged the zones to the development standards (minimum lot size, maximum units per lot, maximum units per lot acre) extracted from the municipal code. For jurisdictions where zoning shapefiles are not available, I substituted them with the broader zoning classification available in the parcel data from SANDAG. Then, I hand-matched these zones to the zoning designations and standards in the municipal code. The reference dates for the zoning information is in most cases between August 2019 and February 2020. The exceptions are La Mesa and Escondido (June and September, 2021) and Encinitas (September 2023). Table A.2 presents summary statistics of the data.

Impute missing land-use regulations. If the development standards were missing for a parcel, I imputed them as follows. I imputed the median value of other parcels with the same municipality-specific zoning, if any were available. As a result, the number of parcels with housing units and maximum density information increased from 358,878 to 440,654, and those with minimum lot size information increased from 510,681 to 512,582. If the data was still missing, I imputed the median value of other parcels with the same broad zoning in the county. As a result, the number of parcels with housing units and maximum density information increased from 440,654 to 603,227, and those with minimum lot size information increased from 512,582 to 603,395.

Aggregate to a hexagonal grid. I defined a regular hexagonal grid using Uber's H3 hierarchical geospatial indexing system. H3 supports 16 resolutions, where each finer resolution has cells with one-seventh of the area of the coarser resolution. I aggregated the parcel-level data to resolution-9 hexagons, which in my sample have an average side length of 215 meters (705 feet) and an area of 0.12 square kilometers (29 acres). The radius of the smallest circle that contains a regular hexagon of side 215 meters (circumcircle radius) is 215 meters as well. The radius of the largest circle contained within the hexagon (incircle radius) is 186 meters (611 feet).

To assign parcels to hexagons I performed a spatial intersection between the parcel polygons from SANDAG and the hexagonal grid. I first aggregated to hexagons by municipality-specific zones, weighing parcels by intersecting area. Using the aggregated plot area, I computed the maximum number of units allowed and the maximum number of lots allowed. I then aggregated to the level of hexagons by broad zones.

Address inconsistencies between zoning codes and observed developments. There are reasons beyond data errors for such discrepancies. Two such reasons are: (1) some developments may have been constructed before stricter zoning codes were adopted, and (2) developers may petition for exceptions or "variances" to build taller or at a higher density than allowed. To handle these cases, I assumed that the less strict potential restriction applies. Specifically, I replaced the maximum number of units allowed by the observed number of units when the latter exceeds the former. This step was carried out after aggregating to hexagons by municipality-specific zones but before aggregating to hexagons by broad zones.

Table A.1: Aggregates of the residential parcel data by jurisdiction

Jurisdiction	Units	Plot area (sf.)	Building area (sf.)	Assessed value (\$)	Shapefile?
City of San Diego	337,084	19,776,623,354	466,961,423	120,039,963,014	Yes
County of San Diego	94,906	21,413,471,435	187,807,379	43,380,472,104	Yes
Chula Vista	59,212	4,627,814,995	99,702,762	20,363,015,362	Yes
Oceanside	51,560	5,950,456,088	77,516,140	16,523,317,845	No
Escondido	36,627	4,144,146,687	53,946,273	10,889,636,583	Yes
Carlsbad	33,436	4,413,370,558	71,560,877	19,712,218,624	Yes
Vista	26,932	1,814,172,069	36,771,618	7,486,836,911	Yes
El Cajon	24,644	1,168,852,600	31,410,522	5,768,851,779	Yes
San Marcos	20,457	6,232,240,744	37,179,890	8,475,741,791	No
Encinitas	20,186	1,368,184,548	39,598,937	12,823,568,697	Yes
La Mesa	19,115	645,406,485	24,201,838	5,030,467,888	Yes
Poway	13,763	1,784,518,062	29,970,563	7,643,029,753	Yes
Santee	13,494	4,431,233,108	19,841,756	4,076,818,578	No
National City	9,785	271,346,638	10,035,070	1,643,584,624	No
Lemon Grove	7,748	119,829,556	9,623,986	1,718,350,175	No
Imperial Beach	6,325	83,062,490	7,013,767	1,353,365,859	No
Coronado	5,265	409,594,770	9,749,031	4,594,297,152	No
Solana Beach	3,936	607,442,353	7,870,477	2,892,064,771	No
Del Mar	1,572	67,001,825	3,352,075	1,804,628,023	No

Notes: Aggregates of residential parcels in San Diego County. The last column indicates if zoning shapefiles were procured or not. See the main text for details.

Table A.2: Summary statistics of the residential parcel and zoning data

	count	mean	std	min	50%	max
Plot area (sf.)	891,518	88,982	360,840	1.000	7,800	24.2M
Building area (sf.)	560,669	2,183	3,659	3.000	1,770	99,999
Units	560,669	1.402	6.172	1.000	1.000	549.0
Assessed value (\$)	535,283	553,390	1.3M	10,718	416,988	145.3M
Assessed value (\$ per sf.)	535,283	251.1	142.3	50.00	226.4	1,500
Bedrooms	857,616	3.167	10.42	0.000	3.000	999.0
Baths	857,765	2.179	1.502	0.000	2.000	99.90
Owner-occ. dummy	842,054	0.548	0.498	0.000	1.000	1.000
View dummy	623,276	0.330	0.470	0.000	0.000	1.000
Max. units per lot	519,159	1.017	0.151	1.000	1.000	8.000
Min. lot size (sf.)	891,518	9,342	13,861	2,500	6,000	435,600
Max. units per acre	891,518	10.82	11.11	0.125	8.000	108.9
Max. lot coverage (frac.)	575,737	0.528	0.177	0.200	0.500	0.987
Single-fam. zone dummy	891,518	0.818	0.386	0.000	1.000	1.000

Notes: Summary statistics of residential parcels in San Diego County. The average is computed conditional on being non-zero in the following rows: building area and units.

B List of parameters and quantification strategies

Table A.3: List of parameters and quantification strategies

Parameter	Definition	Value	Source
ε^B	hexagon preferences homogeneity	1.725	Martynov (2021) for NYC
ε^E	tract preferences homogeneity	4.65	Lee (2020) for LA
ε^C	city preferences homogeneity	2.7	Bryan and Morten (2019)
σ	risk aversion	5×10^{-4}	Handel et al. (2015)
α	labor's share in production	0.80	Valentinyi and Herrendorf (2008)
μ	non-land input share in housing	0.46	Severen (2019), highest
ψ_i	home size	-	Calibrated
φ^B	wildfires amenity damage	-	Estimated
φ^H	wildfire property damage	0.10	Calibrated from building loss

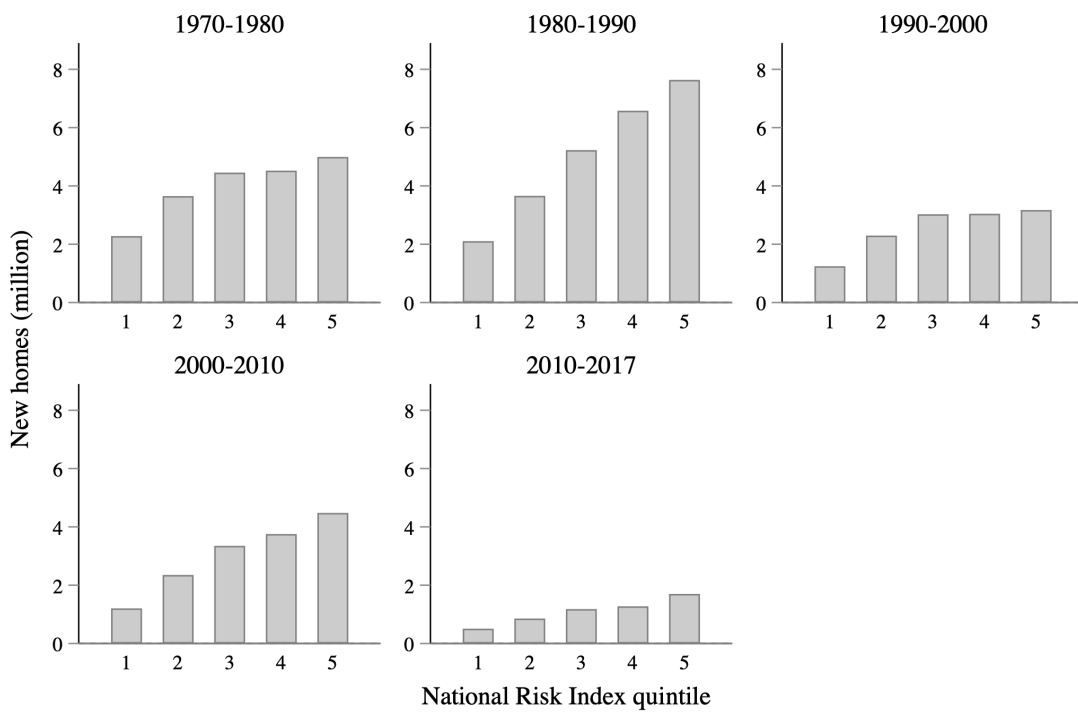
C Additional Figures And Tables

Table A.4: The relation between maximum temperatures and wildfire risk

	(1)	(2)	(3)	(4)
	Fire	Fire	Fire	Fire
ln(Summer Max. Temp.)	10.177*** (1.957)	8.123*** (2.520)	4.216*** (0.690)	2.433*** (0.464)
Constant	-37.581*** (6.641)	-30.503*** (8.549)	-18.068*** (2.360)	-11.884*** (1.573)
Year FE	No	Yes	No	Yes
Hex FE	Yes	Yes	No	No
Res-5 hex FE	No	No	Yes	Yes
Observations	754,728	754,728	2,131,740	2,131,740
Log pseudolikelihood	-117,773	-114,597	-138,374	-134,454

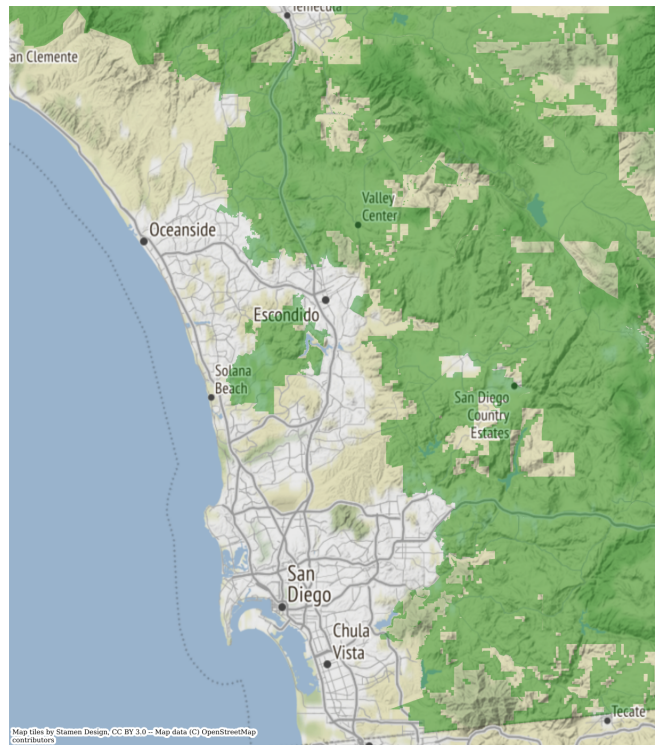
Notes: Poisson pseudo-maximum likelihood regressions (Correia et al., 2020). The units of observation are Uber H3 hexagons at resolution 7. The variable *Fire* is a dummy that indicates the hexagon burned that year. The summer maximum temperatures are the June–August average temperature in degrees Celsius. The wildfire occurrences are constructed from CAL FIRE data (FRAP, 2019). The temperature data is from PRISM (2020). The standard errors are one-way clustered at the level of resolution-5 hexagons by year and shown in parentheses. Asterisks indicate 10% (*), 5% (**), and 1% (***) significance.

Figure A.1: Decadal housing growth and natural hazard risks (FEMA) since 1970



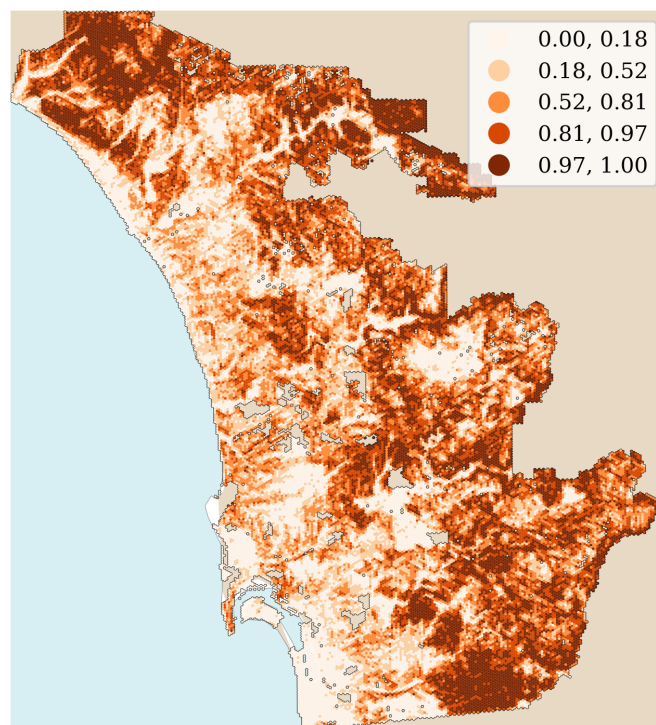
Notes: The number of homes is the housing unit count from the Longitudinal Tract Data Base (LTDB). The risk quintiles are computed over FEMA's 2020 National Risk Index of natural hazard risk, where 1 means lowest risk and 5 means highest risk.

Figure A.2: The San Diego metropolitan area



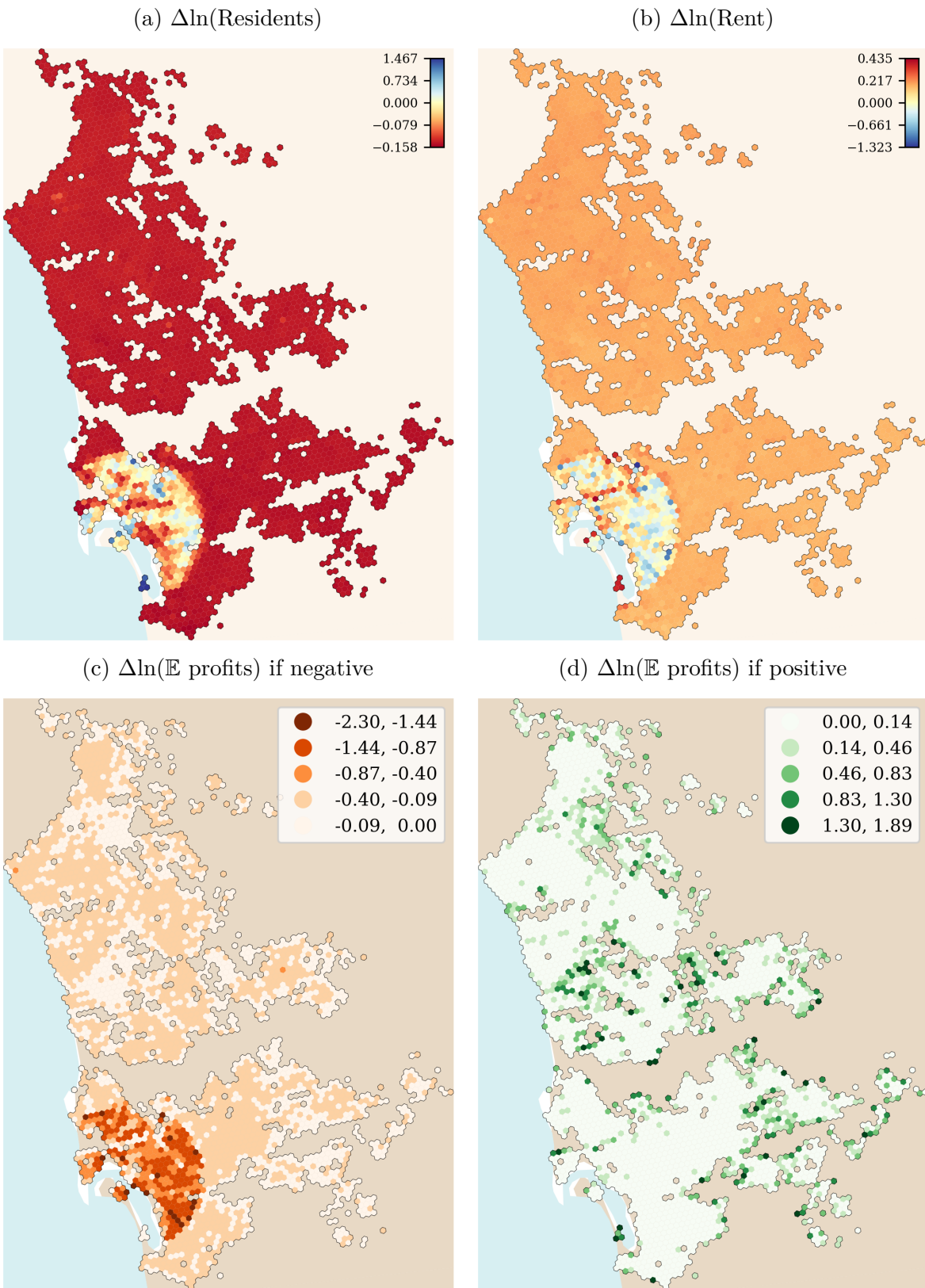
Notes: The areas shaded in green are protected land owned by the State of California or the federal government. The San Diego metropolitan area is contained in the county of San Diego, located in the southwestern corner of California. As of the 2020 census, its population of 3.3 million makes it the second most populous county in California and the fifth most populous in the country. To the south, the metropolitan area is limited by the U.S.–Mexico border, and to the northwest, north of Oceanside, by land owned by the U.S. military. From east to west, the San Diego metropolitan area stretches from the Pacific Ocean to the Peninsular Ranges, beyond which is the Colorado Desert.

Figure A.3: Fraction of area of steep slope (greater than 15%)



Notes: Choropleth maps of the fraction of resolution-9 regular hexagons that have slopes over 15%. The source of the slope map is the LUEG-GIS Service, Planning & Development Services, County of San Diego.

Figure A.4: Effects of deregulation on population and rents - Open city



Note: Choropleth maps of the change in population, rents, and expected profits due to the deregulation counterfactual experiment.

Figure A.5: Fraction of dwelling policies from the FAIR plan

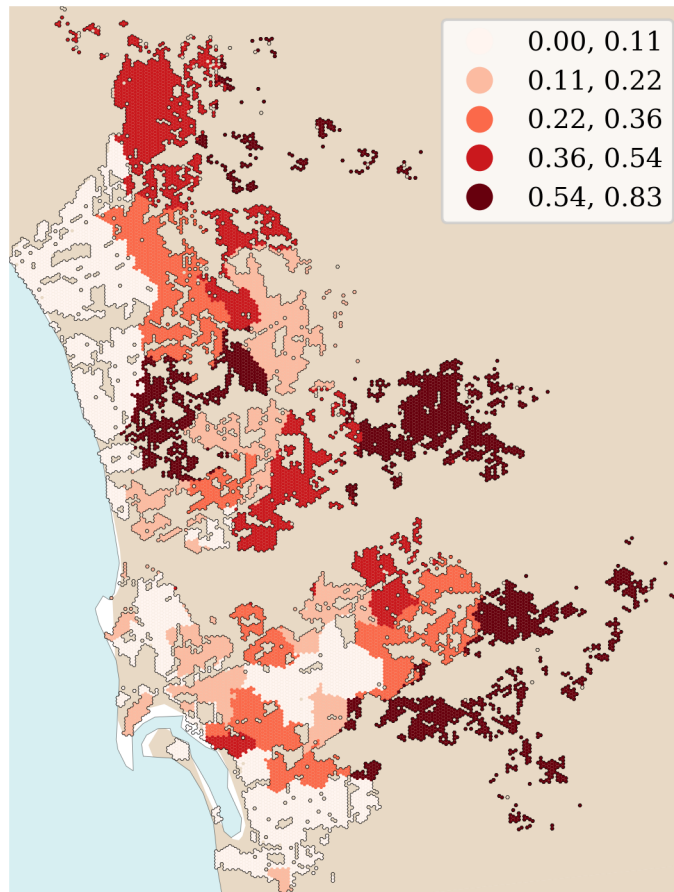


Figure A.6: Setting the cutoff to be in the admitted market

FAIR Plan policies as fraction of dwelling policies

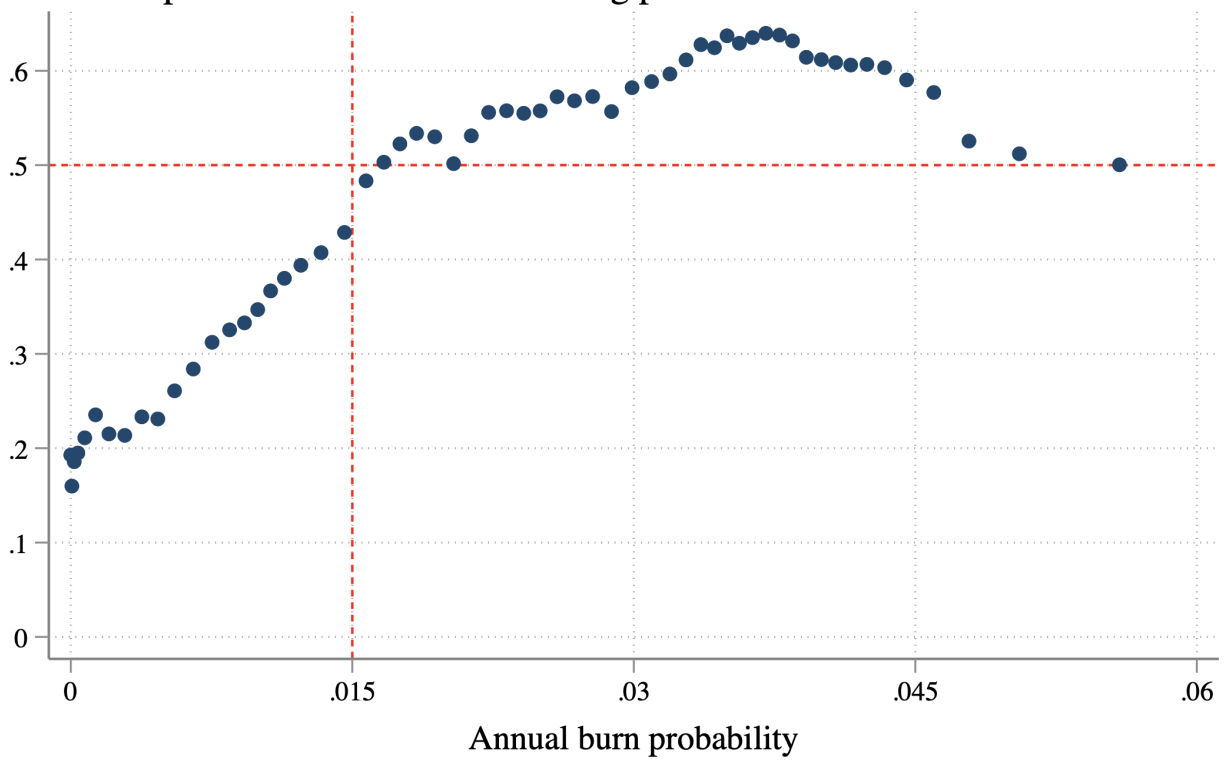
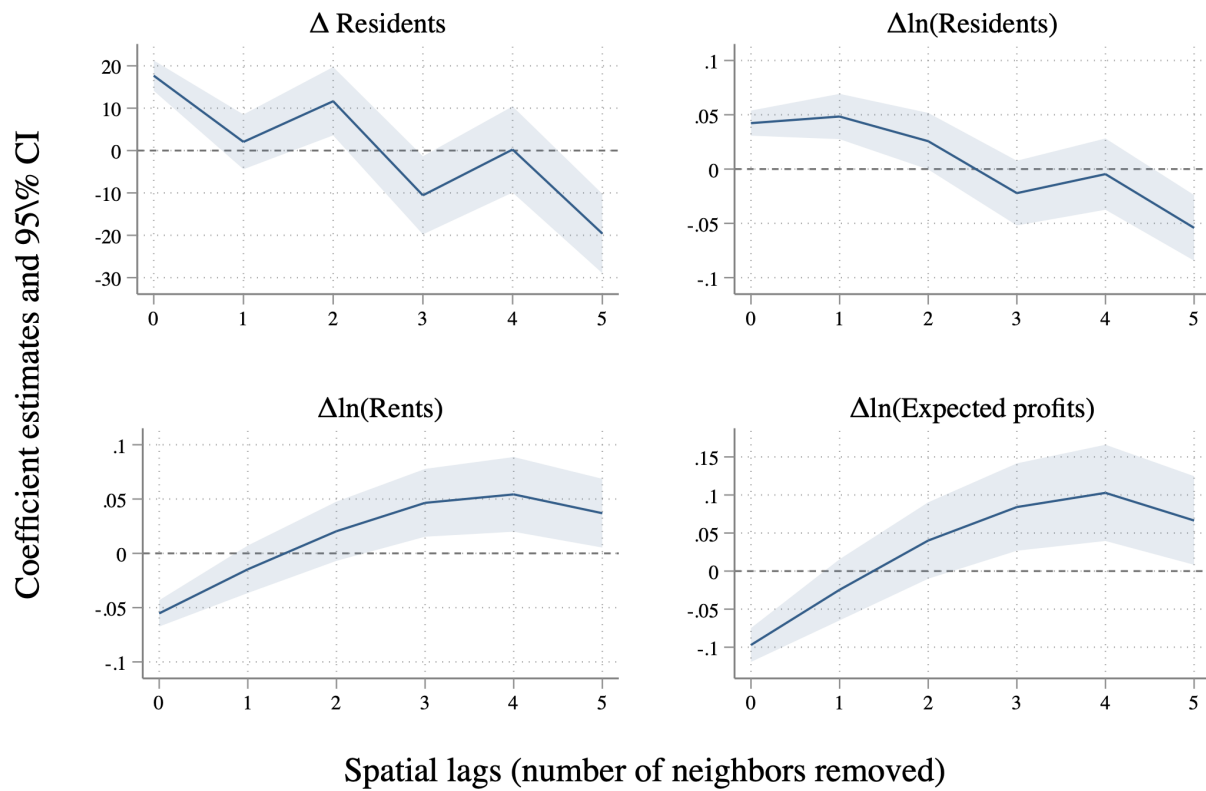


Figure A.7: Effect of deregulation by initial regulation slack



Notes: regressions with counterfactual changes due to deregulation on the left-hand side, and spatial lags of the fraction initially built of the maximum allowed on the right-hand side. Standard errors clustered by resolution 6 parent hexagon.

Figure A.8: Distribution of changes in profits due to deregulation

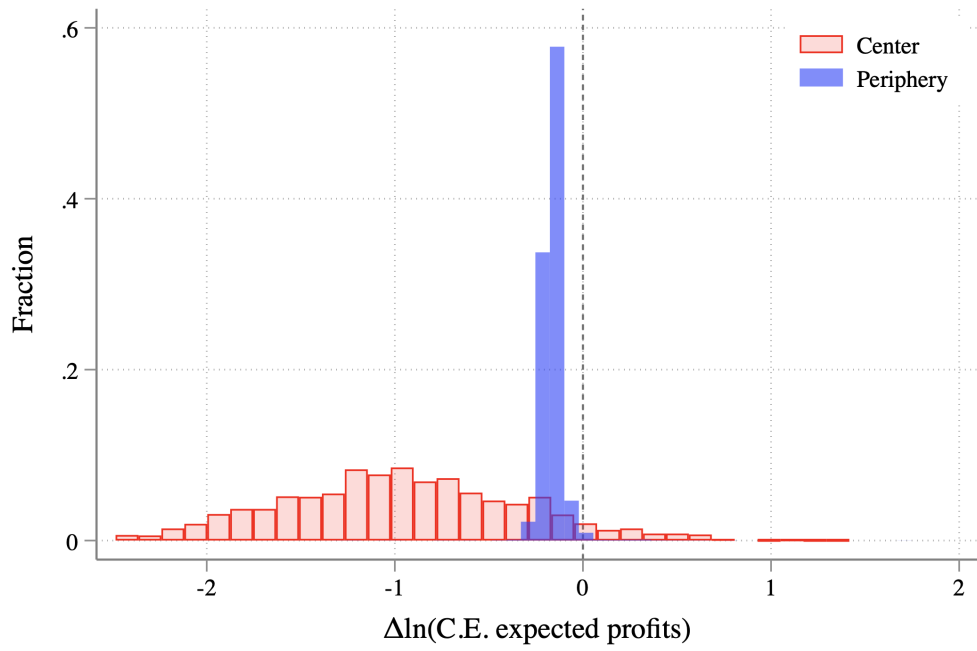
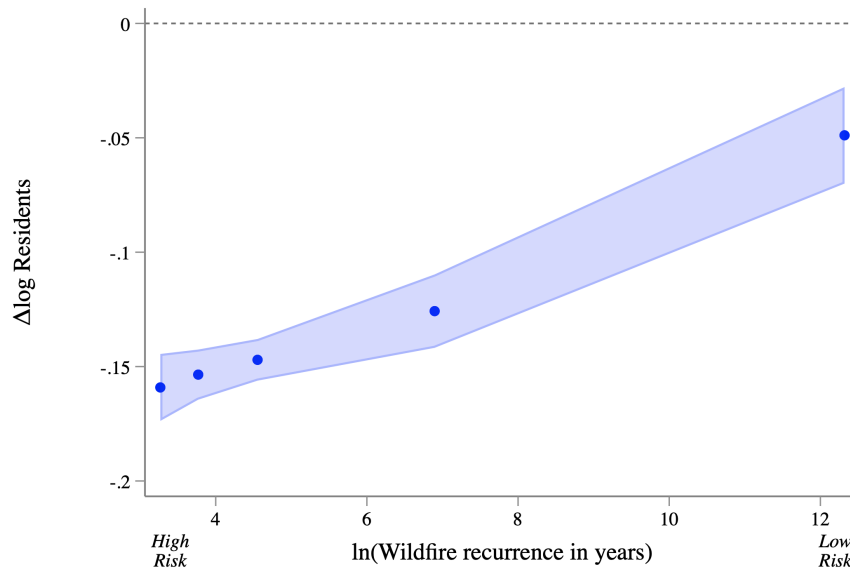
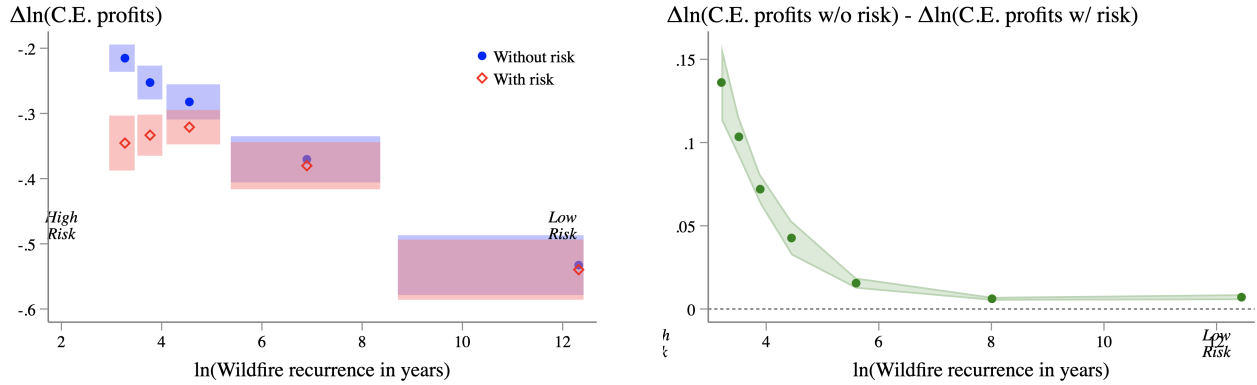


Figure A.9: The effect of deregulation on wildfire risk exposure in a closed city



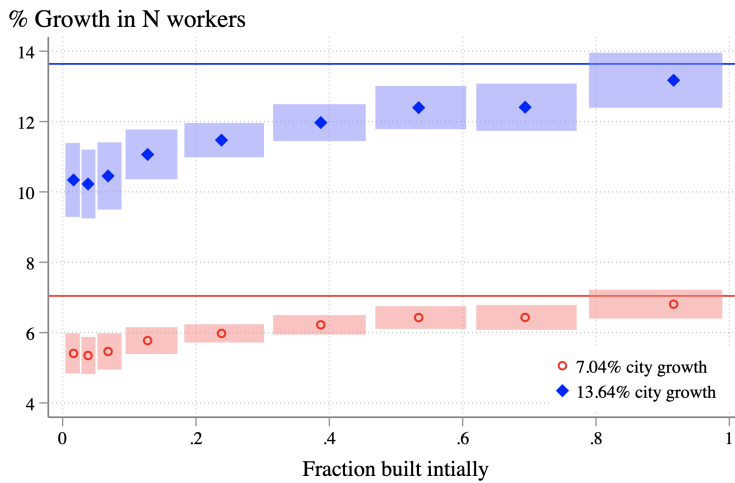
Notes: Binned scatter plots and 95% confidence intervals (Cattaneo et al., 2019). Standard errors are clustered by tract.

Figure A.10: The effect of deregulation on landowner profits in a closed city



Notes: Binned scatter plots and 95% confidence intervals (Cattaneo et al., 2019). Standard errors are clustered by tract.

Figure A.11: The effect of national population growth in a deregulated city



Notes: Binned scatter plots and 95% confidence intervals (Cattaneo et al., 2019). Standard errors are clustered by tract. The fraction built in the horizontal axis is in the data. The initial equilibrium in the simulation already has no regulations.

Table A.5: Instrumental variable estimates of the amenity effects of wildfire risk

	lnE[B_i]		
	(0)	(1)	(2)
δ_i	-2.695*** (0.263)	-4.104** (1.305)	-6.576** (2.191)
Topo., Weather, Dist. controls	Yes	Yes	Yes
Hex-7 fixed effects	Yes	Yes	Yes
Estimator	OLS	IV	IV
Observations	13,925	13,925	13,925
F-stat (CD)		91.20	24.16
F-stat (KP)		30.24	6.88

Notes: The units are the percentage change due to 1 standard deviation increase in burn probability (δ_i). Standard errors clustered by resolution-7 hexagon in parentheses. Asterisks indicate 10% (*), 5% (**), and 1% (***) significance. The Cragg-Donald (CD) and Kleibergen-Paap (KP) statistics correspond to non-robust and heteroskedasticity-robust multivariate analogues to the first-stage F stats. Instrument (1): interaction of hex-level topo and weather (X_i^B) with 1km-resolution non-anthropogenic burn probability (Parisien et al., 2012). Instrument (2): interaction of X_i^B with the leave-out pre-2010 cumulative burn history in the resolution-7 hex.

Table A.6: Changes in risk exposure when removing regulations

RiskFactor	Chance of burning	W/ regulations	W/o regulations	Difference
1	0%	2,399,885 (80.4%)	2,708,974 (82.0%)	309,089 (1.6 p.p.) [12.9%]
2	0-1%	232,453 (7.8%)	261,178 (7.9%)	28,725 (0.1 p.p.) [12.4%]
3	1-3%	57,983 (1.9%)	59,060 (1.8%)	1,077 (-0.2 p.p.) [1.9%]
4	3-6%	36,169 (1.2%)	33,539 (1.0%)	-2,630 (-0.2 p.p.) [-7.3%]
5	6-9%	23,600 (0.8%)	21,830 (0.7%)	-1,770 (-0.1 p.p.) [-7.5%]
6	9-14%	39,191 (1.3%)	36,217 (1.1%)	-2,974 (-0.2 p.p.) [-7.6%]
7	14-19%	29,257 (1.0%)	27,174 (0.8%)	-2,083 (-0.2 p.p.) [-7.1%]
8	19-26%	37,208 (1.2%)	34,593 (1.0%)	-2,615 (-0.2 p.p.) [-7.0%]
9	26-36%	28,072 (0.9%)	26,664 (0.8%)	-1,408 (-0.1 p.p.) [-5.0%]
10	+36%	100,212 (3.4%)	92,844 (2.8%)	-7,367 (-0.5 p.p.) [-7.4%]

Notes: The chance of burning is cumulative over 30 years. That is, if δ is the annual probability, the cumulative probability is $1 - (1 - \delta)^{30}$. The main figures are population counts. The numbers between parentheses are percentages over the total population, or percentile point differences in the last column. The numbers between brackets in the last column are the percentage change in population count going from the equilibrium with regulations to the one without regulations.

Table A.7: Welfare effects of removing risk or regulations with future population

Scenario	(1)	(2)	(3)	(4)	(5)
	Workers (\$/worker)	Workers (\$M)	Landowners (\$M) Center	Landowners (\$M) Periphery	Total (\$M)
1. No LUR	2,665	2,933	-1,013	-1,181	739
2. No LUR in world w/o risk	2,581	2,841	-971	-1,199	671
3. No risk	360	397	-70	452	779
4. Cost of risk due to LUR (row 1 - row 2)	83	92	-42	18	68
5. Ratio of rows 4 and 3	23.2%	23.2%	60.1%	4.0%	8.74%

Notes: The units are 2018 US dollars per year, and \$M stands for million dollars. The welfare measures are equivalent variation for the workers and the change in certainty equivalent profits for the landowners. The last column is the equally weighted sum of columns (2), (3) and (4). Landowners are partitioned into two groups: hexagons within 8 miles of downtown (the Center) and the remaining hexagons (the Periphery). The first scenario (row 1) considers a change from the observed equilibrium (with regulations and risk) to an equilibrium without regulations as described in the body of the text. The second scenario (row 2) considers a change from an equilibrium without risk to an equilibrium with neither risk nor regulations. The third scenario considers a change from the observed equilibrium (with regulations and risk) to an equilibrium without wildfire risk.

Table A.8: Welfare effects of removing risk or regulations with future risk

Scenario	(1)	(2)	(3)	(4)	(5)
	Workers (\$/worker)	Workers (\$M)	Landowners (\$M) Center	Landowners (\$M) Periphery	Total (\$M)
1. No LUR	2,384	2,479	-818	-870	791
2. No LUR in world w/o risk	2,305	2,398	-786	-907	705
3. No risk	429	446	-62	499	883
4. Cost of risk due to LUR (row 1 - row 2)	79	82	-32	37	86
5. Ratio of rows 4 and 3	18.3%	18.3%	51.9%	7.41%	9.77%

Notes: The units are 2018 US dollars per year, and \$M stands for million dollars. The welfare measures are equivalent variation for the workers and the change in certainty equivalent profits for the landowners. The last column is the equally weighted sum of columns (2), (3) and (4). Landowners are partitioned into two groups: hexagons within 8 miles of downtown (the Center) and the remaining hexagons (the Periphery). The first scenario (row 1) considers a change from the observed equilibrium (with regulations and risk) to an equilibrium without regulations as described in the body of the text. The second scenario (row 2) considers a change from an equilibrium without risk to an equilibrium with neither risk nor regulations. The third scenario considers a change from the observed equilibrium (with regulations and risk) to an equilibrium without wildfire risk.

Table A.9: Welfare effects of removing risk or upzoning Transit Priority Areas in the City of San Diego

Scenario	(1)	(2)	(3)	(4)	(5)
	Workers (\$/worker)	Workers (\$M)	Landowners (\$M) Center	Landowners (\$M) Periphery	Total (\$M)
1. No LUR	1,817	1,896	-414	-805	677
2. No LUR in world w/o risk	1,769	1,845	-400	-827	618
3. No risk	353	368	-48	444	764
4. Cost of risk due to LUR (row 1 - row 2)	49	51	-14	22	59
5. Ratio of rows 4 and 3	13.8%	13.8%	28.2%	4.94%	7.74%

Notes: The units are 2018 US dollars per year, and \$M stands for million dollars. The welfare measures are equivalent variation for the workers and the change in certainty equivalent profits for the landowners. The last column is the equally weighted sum of columns (2), (3) and (4). Landowners are partitioned into two groups: hexagons within 8 miles of downtown (the Center) and the remaining hexagons (the Periphery). The first scenario (row 1) considers a change from the observed equilibrium (with regulations and risk) to an equilibrium without regulations as described in the body of the text. The second scenario (row 2) considers a change from an equilibrium without risk to an equilibrium with neither risk nor regulations. The third scenario considers a change from the observed equilibrium (with regulations and risk) to an equilibrium without wildfire risk.

D Counterfactual scenarios in a closed city

Table A.10: Counterfactual prices and allocations in a closed city

	(1)	(2)	(3)	(4)
	Baseline	No LUR	No risk	No LUR & No risk
Population	2.984M	2.984M	2.984M	2.984M
Workers	1.043M	1.043M	1.043M	1.043M
Workers (Center)	301.432K	408.444K	292.840K	395.417K
Workers (Periphery)	741.936K	634.923K	750.527K	647.951K
C.E. rent profits	8.040B	5.386B	8.191B	5.603B
C.E. rent profits (Center)	1.928B	900.829M	1.817B	854.244M
C.E. rent profits (Periphery)	6.112B	4.485B	6.374B	4.749B
£ property damage	10.859M	7.880M	0.000	0.000
Wages	89.217K	88.447K	89.154K	88.480K
Rents	14.200K	9.560K	14.450K	9.945K
Rents (Center)	11.738K	4.084K	11.410K	4.001K
Rents (Periphery)	15.201K	13.083K	15.636K	13.572K
Premiums	9.529	9.425	-	-

Notes: C.E. stands for certainty equivalent; LUR stands for land-use regulation. The unit M means million, and B means billion. Wages and rents are population-weighted averages. Premiums are coverage-weighted averages.

Table A.11: Changes in risk exposure when removing regulations in a closed city

RiskFactor	Chance of burning	W/ regulations	W/o regulations	Difference
1	0%	2,399,885 (80.4%)	2,440,742 (81.8%)	40,856 (1.4 p.p.) [1.7%]
2	0-1%	232,453 (7.8%)	237,277 (8.0%)	4,824 (0.2 p.p.) [2.1%]
3	1-3%	57,983 (1.9%)	53,940 (1.8%)	-4,043 (-0.1 p.p.) [-7.0%]
4	3-6%	36,169 (1.2%)	30,953 (1.0%)	-5,216 (-0.2 p.p.) [-14.4%]
5	6-9%	23,600 (0.8%)	20,087 (0.7%)	-3,514 (-0.1 p.p.) [-14.9%]
6	9-14%	39,191 (1.3%)	33,403 (1.1%)	-5,788 (-0.2 p.p.) [-14.8%]
7	14-19%	29,257 (1.0%)	25,218 (0.8%)	-4,039 (-0.1 p.p.) [-13.8%]
8	19-26%	37,208 (1.2%)	31,932 (1.1%)	-5,276 (-0.2 p.p.) [-14.2%]
9	26-36%	28,072 (0.9%)	24,663 (0.8%)	-3,408 (-0.1 p.p.) [-12.1%]
10	+36%	100,212 (3.4%)	85,815 (2.9%)	-14,396 (-0.5 p.p.) [-14.4%]

Notes: The chance of burning is cumulative over 30 years. That is, if δ is the annual probability, the cumulative probability is $1 - (1 - \delta)^{30}$. The main figures are population counts. The numbers between parentheses are percentages over the total population, or percentile point differences in the last column. The numbers between brackets in the last column are the percentage change in population count going from the equilibrium with regulations to the one without regulations.

Table A.12: Welfare effects of removing risk or regulations in a closed city

Scenario	(1)	(2)	(3)	(4)	(5)
	Workers (\$/worker)	Workers (\$M)	Landowners (\$M) Center	Landowners (\$M) Periphery	Total (\$M)
1. No LUR	4,589	4,788	-1,027	-1,627	2,133
2. No LUR in world w/o risk	4,372	4,561	-963	-1,625	1,973
3. No risk	808	843	-111	262	993
4. Cost of risk due to LUR (row 1 - row 2)	217	227	-65	-2	160
5. Ratio of rows 4 and 3	26.9%	26.9%	58.1%	-0.71%	16.1%

Notes: The units are 2018 US dollars per year, and \$M stands for million dollars. The welfare measures are equivalent variation for the workers and the change in certainty equivalent profits for the landowners. The last column is the equally weighted sum of columns (2), (3) and (4). Landowners are partitioned into two groups: hexagons within 8 miles of downtown (the Center) and the remaining hexagons (the Periphery). The first scenario (row 1) considers a change from the observed equilibrium (with regulations and risk) to an equilibrium without regulations as described in the body of the text. The second scenario (row 2) considers a change from an equilibrium without risk to an equilibrium with neither risk nor regulations. The third scenario considers a change from the observed equilibrium (with regulations and risk) to an equilibrium without wildfire risk.

E Housing growth in risky places within and between cities

The recent growth into risky places is both due to more homes being built in risky cities and to more homes being build in the riskier parts of the city. Moreover, if we go back in time to 1970 a significant component of the growth into risky areas was due to the expansion of the cities into risky places. I make that two points with exact decompositions of the changes in the fraction of homes at risk.

Let Y_{ct}^r be the stock of homes in tracts at risk r in city (CSA) c at time t . Neither risk rating nor city limits change over time. The total housing stock at risk r is $Y_t^r = \sum_c Y_{ct}^r$ and the national stock of housing is $Y_t = \sum_r \sum_c Y_{ct}^r$. Furthermore, define the national fraction of homes at risk r as $S_t^r \equiv Y_t^r / Y_t$, the city fraction at risk $s_{ct}^r \equiv Y_{ct}^r / Y_{ct}$, and the city share of national housing $y_{ct} = Y_{ct} / Y_t$. Then we can write the national fraction of homes at risk r as

$$S_t^r = \sum_c y_{ct} \cdot s_{ct}^r.$$

If all the city areas at risk r in time t had at least one home in time $t-1$, $Y_{ct-1}^r \neq 0$ for all c and r , then the change in the national fraction of homes at risk r can be decomposed into the contribution of changes in the distribution of homes within cities and the contribution of the relative growth between cities as follows:

$$\Delta S_t^r = \underbrace{\sum_c \bar{y}_c \cdot \Delta s_{ct}^r}_{\text{within cities}} + \underbrace{\sum_c \Delta y_{ct} \cdot \bar{s}_c^r}_{\text{between cities}} \quad (18)$$

where the averages are defined between the two periods: $\bar{x} = (x_t + x_{t-1})/2$ for any variable x . This is the formula used in [Griliches and Regev \(1995\)](#). The right panel of figure 2 shows the results of decomposing the change between 2000 and 2017 in the fraction of housing units over quintiles of FEMA's 2020 National Risk Index. The black outline bars depict the total change in the housing share (the left hand side of equation 18) and the dark bars show the contribution of within-city growth (the first term on the right hand side of equation 18). The figure shows that riskier places around the country received a higher share of total housing, and this happened both because there are more homes in riskier cities (the between-cities component of the decomposition) and more homes in the riskier parts of the city (the within-city component).

If we go further back in time and consider changes from 1970 to 2017, it is not longer true that all the city areas with homes in 2017 had at least one home in 1970. Therefore we can extend the decomposition formula as follows:

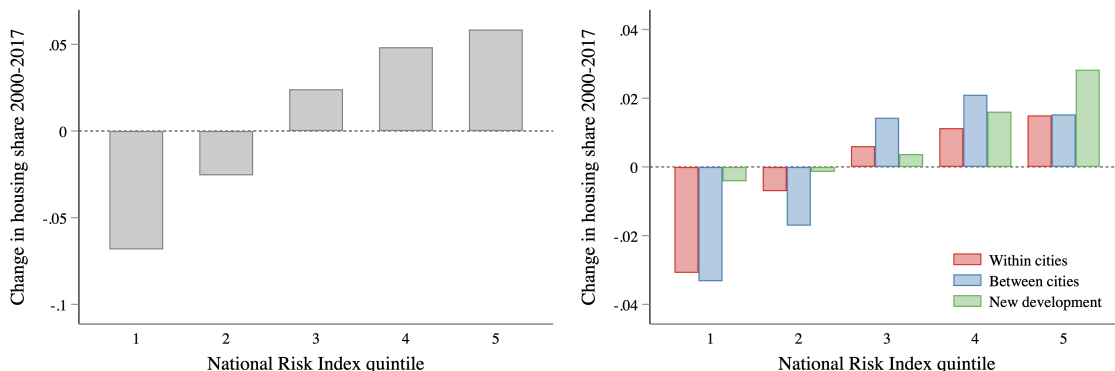
$$\Delta S_t^r = \underbrace{\sum_{c : s_{ct-1}^r \neq 0} \bar{y}_c \cdot \Delta s_{ct}^r}_{\text{within cities}} + \underbrace{\sum_{c : s_{ct-1}^r \neq 0} \Delta y_{ct} \cdot (\bar{s}_c^r - \bar{S}_t^r)}_{\text{between cities}} + \underbrace{\sum_{c : s_{ct-1}^r = 0} y_{ct} \cdot (s_{ct}^r - \bar{S}_t^r)}_{\text{new development}} \quad (19)$$

where the third (and new) term captures the change due to the placement of housing in previously empty tracts.² Note that I normalize by subtracting the mean national fraction between the two periods, \bar{S}_t^r .

Figure A.12 presents the results. The left panel shows the total change in the housing share (the left hand side of equation 19) and the right panel shows the decomposition (the terms on the right hand side of equation 19). The takeaway from the figure is that within-city patterns of growth had a significant contribution to risk exposure.

²Strictly speaking it is the case that some developed tracts in 2017 were empty in 2000, but if we apply the full decomposition in equation 19 to 2000–2017 changes the last term is virtually zero.

Figure A.12: Decomposition of changes in the national fraction of housing at risk from 1970 to 2017



Notes: The number of homes is the housing unit count from the Longitudinal Tract Data Base (LTDB). The risk quintiles are computed over FEMA’s 2020 National Risk Index of natural hazard risk.

F Housing Supply in the Safest Parts Of Cities with Different Risk Cutoffs

The growth into risky areas was higher in cities where safe areas had less elastic housing supply. I show this by combining the relative natural hazard risk measure from FEMA with tract-level estimates of housing supply elasticities from [Baum-Snow and Han \(2021\)](#).

Let i be a Census tract in city c and $R_i \in [0, 100]$ the relative natural hazard risk ranking of tract i within city c , where $R_i = 100$ is the most risky. I define cities as Combined Statistical Areas (CSA). I then estimate

$$\Delta \log(Y_i)_{2017-2000} = \mu_c + \alpha \underbrace{\mathbb{1}\{R_i > r\}}_{\text{risky area}} + \beta \underbrace{\mathbb{1}\{R_i > r\}}_{\text{risky area}} \times \underbrace{(\bar{\gamma}_c^r - \bar{\gamma}^r)}_{\text{safe area elast.}} + \text{error}_i. \quad (20)$$

The left hand side of the equation is the tract-level log change in housing stock between 2000 and 2017. On the right hand side, μ_c is a CSA fixed effect and r is a risk cutoff such that $r \in (0, 100)$. I construct the relative risk rating R_i from FEMA’s 2020 National Risk Index. The variable $\bar{\gamma}_c^r$ is the mean housing supply elasticity among “safe” tracts of city c , where safety is defined according to cutoff r ,

$$\bar{\gamma}_c^r \equiv \frac{\sum_{j \in c} \mathbb{1}\{R_j \leq r\} \gamma_j}{\sum_{j \in c} \mathbb{1}\{R_j \leq r\}},$$

and $\bar{\gamma}^r$ is the average $\bar{\gamma}_c^r$ across cities. The tract-level housing supply elasticities γ_j are the estimates in [Baum-Snow and Han \(2021\)](#) for the year 2000.³ The coefficient α measures the growth in risky places relative to safe places within a city with the mean housing supply elasticity in safe areas. The coefficient β measures how that growth changes if we increase the supply elasticity above the one in the average city.

The estimates of Equation 20 show that there is growth into risky areas ($\alpha > 0$) but that growth is lower for cities where the housing supply is more elastic in safe areas ($\beta < 0$). Table A.13 makes the point for a range of cutoffs $r \in \{10, 30, 60, 90\}$. For example, the interpretation of Column 5 is that, in a city at the

³I use their quadratic finite mixture model (FMM) estimates.

mean level of supply elasticity in safe tracts (0.33), the tracts in the top 10% riskier places grew 4.55 log points (4.7%) more than the rest. However, there are significant differences between cities: in a city with a housing supply in safe areas among the 5% more elastic (0.33+0.14) risky areas grew only 1.59 log points (1.6%) more. Instead in a city among the 5% with less elastic housing supply (0.33-0.12) the riskier areas grew 7.09 log points (7.3%) more.

Table A.13: Housing supply elasticity in safe areas and growth in risky areas

	$\Delta \log(\text{Homes})$ 2000–2017				
	(1)	(2)	(3)	(4)	(5)
$\mathbb{1}\{Risk > r\}$	-0.0152 (0.054)	-0.0521 (0.044)	-0.0889* (0.052)	0.0035 (0.097)	0.3538 (0.320)
$\mathbb{1}\{Risk > r\} \times \bar{\gamma}^{Risk \leq r}$	-0.3122* (0.175)	-0.4077** (0.137)	-0.5326** (0.169)	-0.2497 (0.314)	0.8112 (0.986)
$\mathbb{1}\{Risk > r\} \times \bar{\gamma}$	0.1387 (0.151)	0.2394* (0.130)	0.3574** (0.158)	0.0770 (0.295)	-0.9556 (0.973)
γ	0.4064*** (0.032)	0.4013*** (0.028)	0.4004*** (0.026)	0.4037*** (0.029)	0.4071*** (0.032)
Cutoff r	10	30	50	70	90
CSA FE	Yes	Yes	Yes	Yes	Yes
Observations	48,231	48,291	48,291	48,291	48,291
Average $\bar{\gamma}$	0.31	0.31	0.31	0.32	0.33
5% of $\bar{\gamma}$	0.20	0.20	0.20	0.20	0.21
95% of $\bar{\gamma}$	0.46	0.43	0.45	0.46	0.47

Notes: The number of homes is the housing unit count from the Longitudinal Tract Data Base (LTDB). The relative risk ratings are computed over FEMA’s 2020 National Risk Index of natural hazard risk. The tract-level housing supply elasticities (γ ’s) are from [Baum-Snow and Han \(2021\)](#). The standard errors shown in parentheses are one-way clustered at the level of CSA by the risky-place indicator. Asterisks indicate 10% (*), 5% (**), and 1% (***) significance.

These results hold if we restrict our attention to wildfire risk, the focus of the rest of the paper. Table [A.14](#) estimates Equation 1 again but only for the 11 Western continental U.S. states and only for wildfire risk. I construct the relative wildfire risk rating from FEMA’s 2020 Wildfire Risk Index. The patterns are the same as with the all-hazard risk index, with a positive and significant coefficient on the risky-place dummy and a negative and significant coefficient on the interaction with the mean safe-area supply elasticity. While interesting, I leave the analysis of heterogeneity across other natural hazards for future work.

Table A.14: Wildfire risk in Western U.S.: housing supply elasticity in safe areas and growth in risky areas

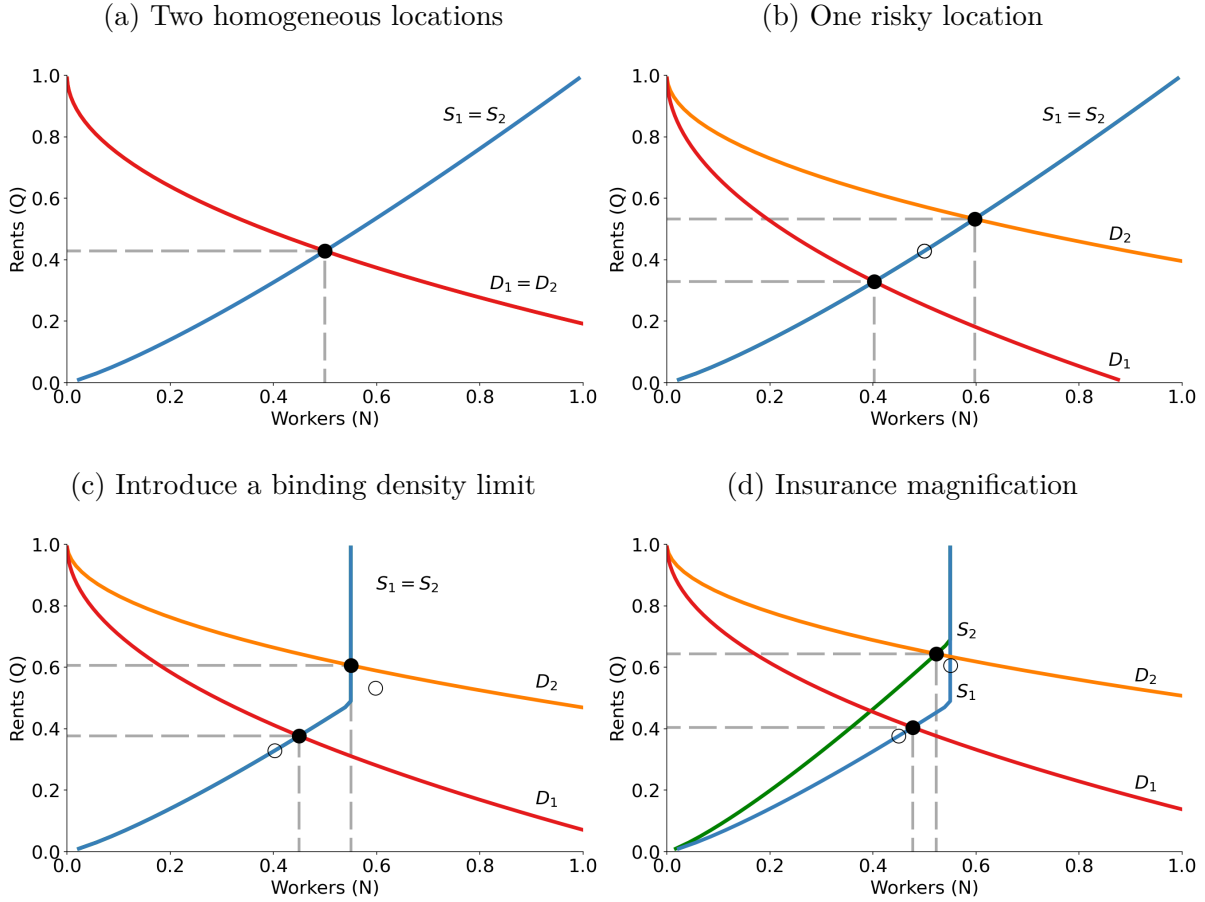
	$\Delta\log(\text{Homes})$ 2000–2017				
	(1)	(2)	(3)	(4)	(5)
$\mathbb{1}\{Risk > r\}$	-0.0565* (0.032)	-0.0607** (0.024)	-0.0809** (0.029)	-0.1317** (0.041)	-0.2606*** (0.069)
$\mathbb{1}\{Risk > r\} \times \bar{\gamma}^{Risk \leq r}$	-0.2801*** (0.067)	-0.2582*** (0.046)	-0.2920*** (0.058)	-0.4526*** (0.089)	-0.6992** (0.216)
$\mathbb{1}\{Risk > r\} \times \bar{\gamma}$	0.2035** (0.095)	0.2109** (0.071)	0.2594** (0.083)	0.3959** (0.121)	0.7639*** (0.200)
γ	0.3167*** (0.036)	0.3069*** (0.031)	0.3071*** (0.031)	0.3106*** (0.034)	0.3201*** (0.039)
Cutoff r	10	30	50	70	90
CSA FE	Yes	Yes	Yes	Yes	Yes
Observations	14,025	14,066	14,069	14,069	14,069
Average $\bar{\gamma}$	0.46	0.47	0.48	0.49	0.50
5% of $\bar{\gamma}$	0.22	0.23	0.26	0.29	0.33
95% of $\bar{\gamma}$	0.69	0.69	0.69	0.68	0.68

Notes: The number of homes is the housing unit count from the Longitudinal Tract Data Base (LTDB). The relative risk ratings are computed over FEMA’s 2020 National Risk Index of wildfire risk. The tract-level housing supply elasticities (γ ’s) are from [Baum-Snow and Han \(2021\)](#). The standard errors shown in parentheses are one-way clustered at the level of CSA by the risky-place indicator. Asterisks indicate 10% (*), 5% (**), and 1% (***) significance.

G Theory Appendix

G.1 Example of the main mechanisms in the model

Figure A.13: Examples of the equilibrium in a simplified version of the model



Note: The plots display the spatial equilibrium of a simple version of the model with only two locations indexed by 1 and 2, a closed city, and a workforce with a mass of 1. Panel (a) graphs the equilibrium with two homogeneous locations and no wildfire risk. The landowner's choices aggregate to supply functions S_1 and S_2 , while the worker's choices aggregate to demand functions D_1 and D_2 . The equilibrium population shares N_1 and N_2 , and the rent prices Q_1 and Q_2 are determined at the intersection of the supply and demand functions in each location. Panel (b) shows how the equilibrium changes if we assume that location 1 is exposed to natural hazard risk. For simplicity, we assume that risk exposure only affects demand. The new equilibria are indicated by black filled dots, while the old equilibria (from panel a) are indicated with an empty dot. Risk exposure shifts D_1 downwards and, through equilibrium forces, shifts D_2 upwards. Panel (c) imposes a density limit of 0.55 to the same setting as panel (b). The new equilibria are indicated by filled dots, and the old ones (from panel b) are indicated with empty dots. Finally, panel (d) illustrates the role of insurance distortions. The cross-subsidization effectively behaves as an increase in construction costs in the safe location 2, so the supply function S_2 shifts to the left.

G.2 Decomposition of the welfare effects of natural hazard risk

A simple decomposition can help illustrate how the covariance between housing affordability and safety shapes the welfare costs of natural hazard risk.

For the remaining part of this section, we assume there is no commuting (so there is a single mobility parameter $\varepsilon^B = \varepsilon^E = \varepsilon$), and that all locations are homogeneous except for natural

hazard risk. Moreover, there are no supply effects of natural hazards, and the amenity damages are given by function $\varphi(\delta_i) \geq 0$, with $\varphi(0) = 1$ and $\varphi'(\delta_i) > 0$, where, as before, δ_i is “risk” exposure understood as the probability of a natural hazard occurring in location i .

Under these simplifying assumptions, the expected indirect utility of living in the city is

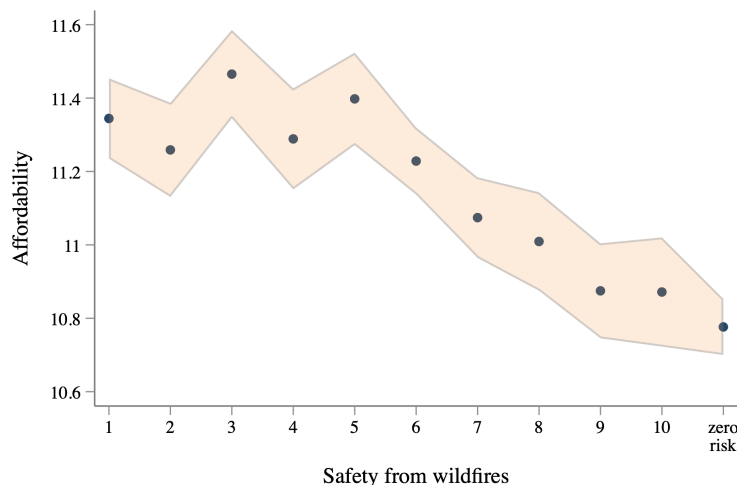
$$\mathcal{V} = \left(\sum_{i=1}^{\mathcal{I}} \left[\frac{W_i - Q_i}{\varphi(\delta_i)} \right]^\varepsilon \right)^{1/\varepsilon} = \left(\sum_{\text{Locations}} \left[\frac{\text{Income} - \text{Housing}}{\text{Safety}} \right]^{\text{Mobility}} \right)^{1/\text{Mobility}},$$

where Q_i is housing rent, so $W_i - Q_i$ is consumption or housing affordability. We can then decompose the expected indirect utility as follows:

$$\mathcal{V}^\varepsilon = \underbrace{\left[\sum_i (W_i - Q_i)^\varepsilon \right]}_{\mathcal{V}^\varepsilon \text{ with no risk}} \underbrace{\left[\frac{1}{\mathcal{I}} \sum_i \varphi(\delta_i)^{-\varepsilon} \right]}_{\text{mean safety}} + \text{Cov} \left[\underbrace{(W_i - Q_i)^\varepsilon}_{\text{affordability}}, \underbrace{\mathcal{I} \varphi(\delta_i)^{-\varepsilon}}_{\text{safety}} \right].$$

The first term is the indirect utility absent natural hazards scaled by a measure of mean safety in the city. To the extent that affordability and safety are negatively correlated within the city, the second term will be negative, and welfare will be lower. In the case of wildfires in San Diego, we see that the covariance between disposable income $W_i - Q_i$ and an inverse of the probability of burning δ_i is negative, as shown in Figure A.14 below.

Figure A.14: Covariance between affordability and safety from wildfire risk



Notes: Tract-level binned scatter plot and 95% CIs (Cattaneo et al., 2019). Y-axis: log disposable income after housing costs (ACS). X-axis: deciles of fire return period (recurrence) plus a bin with all locations with zero risk.

G.3 Landowner's certainty equivalent profits

The maximized expected utility of a landowner is given by

$$\mathbb{E}[u_i^*] = (1 - \delta_i)u\left(\Pi_i - p_i d_i - \frac{p_i}{\sigma} \ln \mathcal{O}_i\right) + \delta_i u\left(\Pi_i - p_i d_i + \frac{1 - p_i}{\sigma} \ln \mathcal{O}_i\right)$$

where $\mathcal{O}_i \equiv \frac{\delta_i}{1 - \delta_i} \frac{1 - p_i}{p_i}$ is the ratio of the odds of wildfire relative to insurance premiums. Using the assumed utility function and after some manipulation this expression becomes

$$\mathbb{E}[u_i^*] = 1 - \exp[-\sigma(\Pi_i - p_i d_i)] [(1 - \delta_i)\mathcal{O}_i^{p_i - 1} + \delta_i \mathcal{O}_i^{p_i}].$$

The certainty equivalent \mathcal{C}_i of a landowner in hexagon i is implicitly defined as

$$u(\mathcal{C}_i) = \mathbb{E}[u_i^*].$$

We then solve for \mathcal{C}_i to obtain

$$\mathcal{C}_i = \Pi_i - p_i d_i - \frac{1}{\sigma} \ln [(1 - \delta_i)\mathcal{O}_i^{p_i - 1} + \delta_i \mathcal{O}_i^{p_i}].$$

The first term is the profits without wildfires. The second term is the cost of full insurance under fair pricing. And the third term is an adjustment due to risk aversion and distortions in insurance markets. If landowners are more risk averse then σ is larger and the last term is smaller, making the certainty equivalent higher because being insured becomes more valuable. If the insurer prices fairly in every location, $p_i = \delta_i$, then $\mathcal{O}_i = 1$ so the certainty equivalent equals $\mathcal{C}_i = \Pi_i - p_i d_i$, the full insurance value without distortions.

Replacing the equilibrium prices Q_i and total floorspace in hexagon i , H_i , the certainty equivalent profits per unit of land in hexagon i are

$$\mathcal{C}_i = \left[Q_i - \varphi_i^H p_i - \mu \left(\frac{H_i}{\chi D_i L_i^h} \right)^{\frac{1 - \mu}{\mu}} \right] \frac{H_i}{L_i^h} - \frac{1}{\sigma} \ln [(1 - \delta_i)\mathcal{O}_i^{p_i - 1} + \delta_i \mathcal{O}_i^{p_i}].$$